Doctoral Thesis

Study on DNA polymorphism and biological polysaccharides in plant resources

Surina Borjihan

September 2013

Study on DNA polymorphism and biological polysaccharides in plant resources

（植物資源中の DNA 多様性と生理活性糖鎖に関する研究）

A thesis submitted to Graduate School of Engineering
in partial fulfillment of the requirements
for the degree of

Doctor of Engineering

Surina Borjihan

Department of Bio and Environmental Chemistry
Kitami Institute of Technology, Japan

September 2013

Contents

General abstract

In this doctoral thesis, the DNA analysis, structure of the carbohydrate and biological activities of polysaccharide in natural plants were studied.

Lacquer (urushi), originally produced in Asia, is the only natural paint that is polymerized by an enzyme, laccase, to give a beautiful coating surface. *Rhus verniciflua* that produces lacquer sap is both traditional and important industrial trees for an environment friendly paint of the next generation. Morphological, anatomical, and chemical characters of lacquer tree have been employed to delimit the lacquer plants, because, the genetic information is very limited.

Recently, valuable studies on the phylogeny of lacquer plants have been reported based on the chloroplast *trn*L (310bp) and *trn*L-F (470bp) and PS-ID gene sequences (plastid sub-type identity). However there are no reports on the analysis of ITS (internal transcribed spacer) and ETS (external transcribes spacer) regions of the nuclear DNA and 5S, *rbc*L (Large subunit of ribulose-1,5-bisphosphate carboxylase) and *mat*k regions of the chloroplast DNA. We have analyzed the DNA sequences of lacquer trees in Abashiri A, B, and C areas to reveal the relationship between DNA sequences and geographical distance. In this study, we describe the sequence analysis of lacquer tree

(*Rhus verniciflua*) in Hokkaido and the sequences were compared to those in Iwate and Fukushima prefectures, which are famous lacquer-growing districts at present and in the past in Japan. From the phylogenetic results of an intra-species genetic diversity in the length and GC content in the ITS region, we found for the first time polymorphism in lacquer tree cultivars. The lacquer trees in Abashiri C area were adapted to the cold environment from the point of sap production.

Lacquer laccase is a copper containing glycoprotein consisted of 533 amino acids and carbohydrates have 45% of the weight. For the analysis of carbohydrate structure and glycosylation sites of laccase glycoprotein, glycoprotein 1mg was digested with enzymes by trypsin and PNGase A and the digested sample was analyzed by using LC/MS/MS and MALDI-TOF/MS. The lacquer laccase is relatively heavily glycosylated glycopreotein. From MS/MS spectra, we found that twelve of the potential fifteen Asn-X-Thr/Ser sites were determined to be sites of *N*-linked glycosylation. Asn 5, 14, 28, 124, 180, 194, 233, 274, 284, 347, 381, and 398 were found to be bound carbohydrates in this study. Each *N*-glycan composition was elucidated and the possible structures were deduced.

In the last part, we studied on the natural polysaccharide, Konjac glucomannan which is a naturally occurring polysaccharide and difficult to dissolve in water and DMSO

because of having high molecular weights. Before sulfation, hydrolysis by diluted sulfuric acid was carried out to decrease molecular weights to $\overline{M}_n$=19.2x10^4-0.2x10^4. Sulfation with piperidine-*N*-sulfonic acid or SO_3-pyridine complex gave sulfated konjac glucomannan with the molecular weights of $\overline{M}_n$=1.0x 10^4-0.4x10^4 and degree of sulfation of DS = 1.3-1.4. It was found that the sulfated konjac glucomannans had potent anti-HIV activity of the 50% effective concentration of EC_{50}=1.2-1.3 μg/ml, which activity was almost the same as that of an AIDS drug, ddC, EC_{50}=3.2 μg/ml, and medium blood anticoagulant activity, AA =0.8-22.7 units/mg, which activities were almost the same activities as those of standard sulfated polysaccharides, curdlan (10 unit/mg) and dextran (22.7 unit/mg) sulfates. Structural analysis of sulfated konjac glucomannans was performed by a high resolution NMR measurement and the interaction between polylysine as a model compound of proteins and peptides was calculated preliminary from a surface plasmon resonance (SPR) measurement, suggesting that sulfated konjac glucomannans had a high binding stability on poly-L-lysine as a model compound of proteins and peptides.

Chapter 1

General Introduction

1.1 Lacquer plants

Lacquer plants belong to the genus *Rhus*, a member of the family Anacardiaceae and Dicotyledonae tribe [1] [2]. *Anacardiaceae* is an economically important plant family of approximately 750 species including cashew, mango, pistachio and poison ivy. *Anacadiaceae*, it is mostly distributed in tropical Africa, Asia with small numbers in subtropical and temperature areas [3] [4].

Lacquer is a natural polymer that has been used in Asian countries for thousands of years [5] [6]. There are three kinds of lacquer trees growing in Asia, *Rhus vernicifera* mainly contains urushiol in China, Japan,and Korea, *R. succedanea* that mainly contains laccol in Vietnam and Taiwan, and Melanorrhoea usitata that the main component is Thitsiol in Burma and Thailand. The constituents and properties of the lacquers vary not only by species but also by the age of the tree, location, and season of collection [7][8].

Lacquer, originally produced in Asia, is the only natural product, which is polymerized by an enzyme, laccase, to give a beautiful coating surface [9]. In the sap of lacquer tree, there are three major

components such as urushiols (60-70%) (3- or 4-alkenyl catechol derivatives)[10-13], enzyme laccase (1.5-2%) [14], and polysaccharides (3-5%) [15]. And It also contains 20-30% water and 4-10% plant gum.

There are six kinds of species of *Rhus* genus and *toxicodendron* genus in Japan, *Toxicodendron vernicifluum* (called urushi in Japan), *Toxicodendron tricocarpum* (Yama-urushi), *Toxicodendron orientale* (Tsuta-urushi), *toxicodendron succedaneum* (Haze-noki), *toxicodendron sylvestre* (Yama-haze), *Rhus javanica var. roxburghii* (Nurude), respectively [16].

"*Urushi"* is *Rhus Toxicodendron*, or *Poison oak* is a creeping shrub from 1 to 3 feet high, with long cord-like shoots, emitting strong lateral fibers; the stems are either erect or decumbent. It is distributed at Kyushu, Miyazaki to Honshu and a part of Hokkaido in Japan in cultivation. The bark is brownish-gray. The leaves are ternate, on long, semi-cylindrical petioles; the leaflets are broadly oval or rhomboidal, 2 to 6 inches long, 2/3 as wide, petiolate, acuminate, smooth and shining above, slightly downy beneath, especially on the veins; The flowers are small, greenish-white, dioecious, and grow in axillary, subsessile, racemose panicles on the sides of the new shoots. The fruit is a roundish, smooth, dry berry, of a pale-green color, approaching to white, and contains a solitary bony seed

"*Tsuta-urushi*" is a deciduous woody vine that is native to all over

Japan, the Kuril Islands, Sakhalin and China. This vine grows in montane beech forests and climbs up adjacent trees by the aerial roots. The leaves are tri-lobed compound and turn red in fall. The panicles are borne in the axiles and the yellowish-green flowers bloom from May to June. It is dioecious. This vine can give you a skin irritation if you touch it accidentally.

"*Nurude*" is a semi-tall deciduous tree that is distributed through Japan, the Korean Peninsula, China and Taiwan. Leaves look like Lacquer tree, though it is differ from winged rachis. Pale yellowish white flowers in panicles come from August to September. Some aphids are parasitic on the leaves and form the galls which include tannin. The gall may be rarely caused a skin irritation.

"*Haze-noki*" is a tall deciduous tree that is distributed widely westward from Kanto district of Honshu to Shikoku, Kyushu of Japan and Southeast Asia. This tree grows in mountains and fields and can reach 7-10 m in height. There odd- pinnate compound with 4-8 pairs of broad-lanceolate leaflets. It is dioecious. The panicles are borne and the small yellowish green flowers bloom from May to June. The fruits are drupes and ripen pale brown in fall. The wax is obtained from the inner endocarps, and used as raw material of Japanese candle. This tree may be rarely caused a skin irritation.

"*Yama-urushi*" is a semi-tall deciduous tree that is distributed throughout Japan, also the Korean Peninsula and China. This tree

grows commonly in mountains and can reach 3-8 m in height. It is dioecious. The leaves are odd-pinnate compound with 4-8 pairs of ovate or elliptic leaflets. The rachis and petioles are often tinged reddish. The panicles are borne on the axiles and the small yellowish-green flowers bloom from May to June. This tree resembles wax tree, though it is defined by grayish-white barks, heavyset leaves with concave veins and fruits with stinging hairs. The leaves and stems can give you a skin irritation if you touch them accidentally.

"*Yama-haze*" is a semi-tall deciduous tree that is distributed westward from Tokai district of Honshu to Shokoku, Kyushu of Japan, also Taiwan, the Korean Peninsula and China. This tree grows in hill forest edges and can reach 5-6 m in height. The leaves are odd-pinnate compound with 5-15 ovate leaflets. It resembles to the Wax tree (Rhus succedanea), though it is defined by the rough hairs on veins and rachis. The yellowish green, conservative flowers bloom from May to June. The fruits are flat and glabrous [17].

In Asian countries, lacquer and lacquer wares have a long history more than 9000 years. The sap is mainly collected from *Rhus vernicifuum* for the coating material of lacquer ware and glue for lumber. The another useful species in lacquer plants is Rhus Succedaneum that the wax extracted from the seed was used the candle making and the hair oil for sumo from the Edo period

(1603-1868 CE)[18]. Even now, it is widely applied to industries such as medical supplies, cosmetic and stationary.

When urushi exudates from lacquer trees are dried, they produce tough and brilliant film and have been used as naturally occurring coating materials. Because of these characteristics, lacquer ware has been in important folk art in Japan, China, and the south-east Asia over the past 5000-7000 years.

Lacquer has been used in Japan and China for as not only a coating material but also a traditional medicine based on experiences. We have reported the biological activities of lacquer polysaccharides such as anti-HIV and blood coagulant acceleration activities [19].

In addition, the use of urushi exudates as the coating materials is an environmentally friendly process, since it does not involve any organic solvents [20-23].The production of lacquer in Asia is getting decrease due to the environmental changes and economic situations. The lacquer that is the only natural plant that product with polymerizability by the enzyme, laccase, would be playing vital role in the next generation.

1.2. Phylogenetic analysis technology

Traditionally, biological specimens have been identified using morphological features, such as habit, leaf and flower shape, size and color, etc. In morphologically and ergo taxonomically difficult groups, it sometime requires an experienced professional taxonomist years to deal with species identification [24].

Molecular techniques are being used increasingly in plant systematic. Besides restriction site analysis of cpDNA, the use of nucleotide sequences has become an even more powerful approach. Informative marker genes include, besides others, the chloroplast genes *rbc*L (coding for the large subunit of rubisco) and nuclear genes, such as rDNA genes [25].

The nuclear rDNA units, separated by intergenic spacers, consist of the 18S, 5.8s and 26S coding regions in the plants. The 5.8S coding region, flanked by the internal transcribed spacers 1 and 2 (ITS1 and ITS2), is located between the 18S and 26S coding regions. One of the advantages of the rDNA as a phylogenetic tool is that the repeat unit consisted of the several regions that have different rates of sequence change. Therefore, different regions of the molecular can be used to examine lineages with different levels of divergence [26] [27]. The 18S and 26S coding regions have been used to address phylogenetic questions at the family level or higher taxonomic levels in plants. On the other hand, the ITS region appear too useful for

the phylogenetic studies at the intra special level. This gene family undertakes rapid concerted evolution. In the mean while, the ITS sequences appear to be useful for assessing relationship between lower taxonomic levels such as among genera and species because the sequence change of the spacer region evolve more rapidly than that of the coded region[28]. But, these two spacers often have too few variable nucleotide sites to provide robust inferences at all nodes. The external transcribed spacer (ETS) has been shown to be useful to supplement ITS data for plant phylogenetic studies [29].

Structure of 18S-26sS rDNA unit

The 5S DNA is an alternative sequence region with high numbers of copies. The repeated units are several hundreds of base pairs in length containing the 5S rRNA gene (approximately 120bp) and the nontranscribed spacer (NTS). The 5S rRNA gene sequence is very well-conserved between plants species while the spacer is species-specific and the sequence has been used for phylogenetic studies and species identification [30-33].

The structure of 5S region

5' ---5s rRNA—NTS—5s rRNA—NTS—5s rRNA—NTS—5s rRNA—NTS--- 3'

The gene for the large subunit of the ribulose-bisphosphate carboxylase (*rbc*L) located on the chloroplast genome, is an appropriate choice for inference of phylogenetic relationships at higher taxonomic levels [34]. Because of its slow synonymous nucleotide substitution rate in comparison with nuclear genes and its functional constraint that reduces the evolutionary rate of nonsynonymous substitutions. *rbc*L provides all the catalytically essential residues of RuBisCO, the critical enzyme for both the reductive and oxidative photosynthetic carbon cycles. The activity of RuBisCO is thought to be limited by environmental stress. The holoenzyme consists of eight large catalytic subunits (*rbc*Ls) and eight small subunits (*rbc*Ss). The sequence of rbcL has great phylogenetic utility because of its conserved nature [35].

The *mat*K gene is an approximately 1.5kb protein-coding rengion between two highly conserved exons of the *trn*k gene. The *mat*K region has both conserved and variable segments, a quality that aids in DNA amplification and resolution of relationships. Also of interest is a comparison of molecular data with other classifications based on floral morphology, seedings and morphology and cytology [36].

1.3 DNA analysis of lacquer plants

Rhus verniciflua that produce lacquer sap is important industrial trees, and morphological, anatomical, and chemistry characters have been employed to delimit the lacquer plants [37]. But its genetic information is very limited. The main component of lacquer sap, Urushiol, its synthesis way is not yet unclear and the completely phylogenetic relationships of lacquer plants in Japan and Asian such as china, Vietnam are unknown. Recently, valuable studies on the phylogeny of the Lacquer plants have been reported based on the chloroplast *trn*L (310bp) and *trn*L-F(470bp) and PS-ID gene sequences(plastid sub-type identity)[38] [39]. But there are no reports on the analysis of ITS (internal transcribed spacer) and ETS (external transcribes spacer) regions of the nuclear DNA and 5S, rbcL (Large subunit of ribulose-1,5-bisphosphate carboxylase) and matk regions of the chloroplast DNA.

1.4 *N*-glycan in plants

In plants, as in other eukaryotes, *N*-glycan is covalently linked to specific Asn residues constitutive of *N*-glycosylation sites of the protein. The *N*-glycosylation sites are the tripeptide Asn-X-Ser/Thr where X can be any amino acid except proline and aspartic acid. All *N*-glycan share a common minimal structure $Man_3GlcNAc_2$

constituted of a N, N'-diacetyl chitobiose unit, a β -mannose residue linked to the chitobiose and two α-mannose residues linked to hydroxyl 3 and 6 of the β-mannose. According to the substitutions of this core, plant *N*-glycan has so far been classified into two categories: the high-mannose- type and complex-type *N*-glycan [40].

High mannose-type *N*-glycan

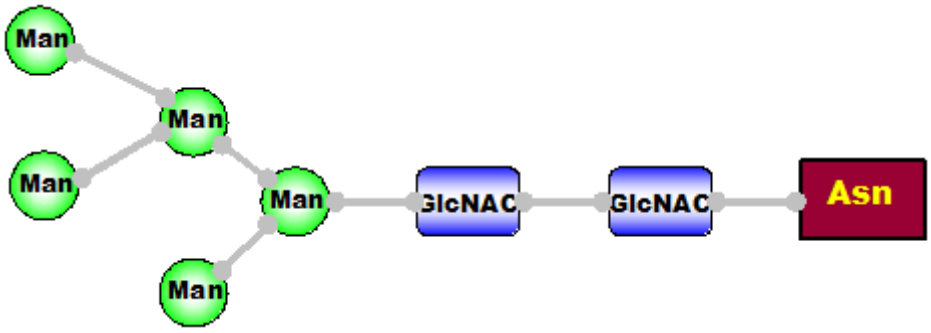

Complex-type *N*-glycan

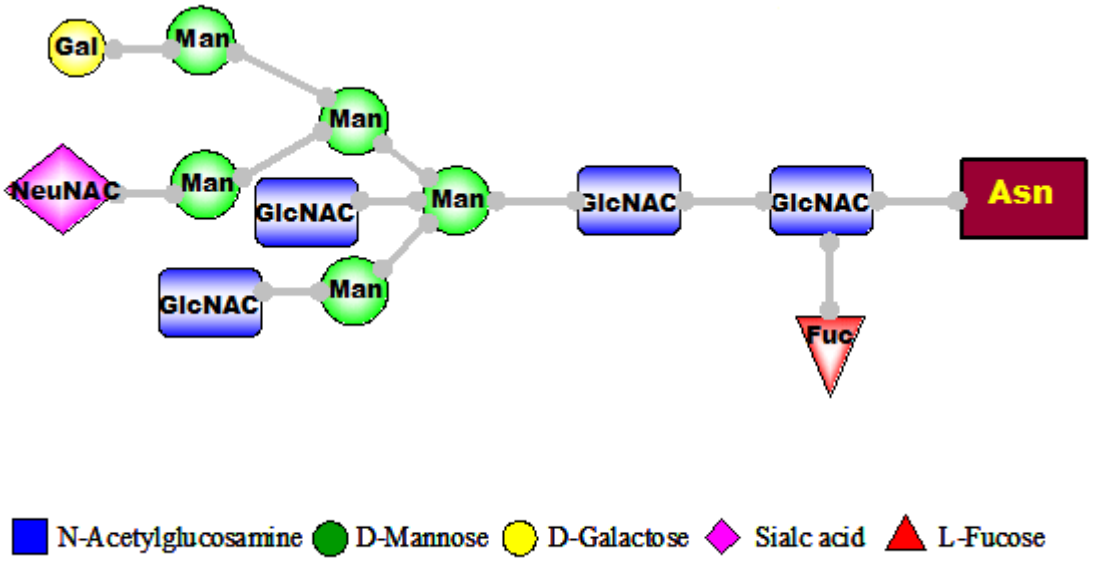

In eukaryotes, *N*-linked glycans have numerous roles. Some of

them, such as a prevention of proteolytic degradation or induction of the correct folding of the protein, often directly depend on the large dimension of oligosaccharides covering the protein backbone in an umbrella-like manner. *N*-linked oligosaccharides may also contain targeting information, or may be directly involved in protein recognition or cell-cell adhesion processes. In plants, the roles of *N*-glycans have been studied using different approaches, such as the use of *N*-glycosylation and N-glycan-processing inhibitors, site-directed mutagenesis of *N*-glycosylation sites or the study of mutants affected in the maturation of *N*-glycans. In these three strategies, either the *N*-glycosylation is completely suppressed or only the processing to complex-type *N*-glycans is inhibited. In both cases, the analysis of the effects of these alterations has provided some information concerning the roles of the *N*-glycosylation and of the *N*-glycan processing in plants [41]. *N*-glycosylation plays an essential role in the biological activity, stability, and folding of glycoproteins [42]. Because late *N*-glycan modification in plants differs from that in mammals, recombinant proteins produced in transgenic plants will not be identical to mammalian glycoproteins [43,44]. Plant complex *N*-glycan contains β-1,2-xylose, core α-1,3-fucose, and Lewis a epitope (Fucα-1-4[Galβ1-3]GlcNAc-R) instead of β-1,4-galactose modified with sialic acid commonly found in mammals. Moreover, these plant-specific *N*-glycans are

potentially immunogenic or allergenic [45, 46].

Current protocols for the preparation of plant *N*-linked glycans for analysis by HPLC, LC/MS/MS or MALDI-TOF MS have several drawbacks. Peptide-Nglycosidase F (PNGasse F), the enzyme used to deglycosylate mammalian protein, does not cleave oligosaccharides containing a α-1, 3-linked Fuc from proteins, and therefore cannot be used to yield plant *N*-glycans [47]. PNGase A (peptide-N-glycosidase A) is used to set free plant glycans instead, but requires digestion of proteins with protease (trpsin et. al) prior to glycosidase treatment for efficient deglycosylation [48].

The picture of six species lacquer plants in Japan. (described at the next page)

1: Tsuta-urushi, in Hokkaido; 2: Nurude, in Tyoko;

3: Yama-urushi, in Nagano; 4: Yama-haze, in Gunma;

5: Haze-noki, in Okinawa; 6: Urushi, in Hokkaido.

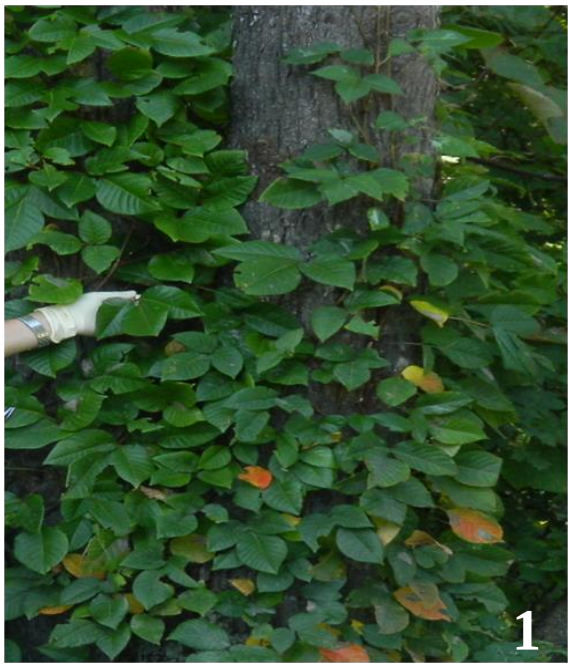
1


2


3


4


5


6

Reference

[1]McNair J.B., 1925, the geographical distribution in North America of poison ivy (Rhus toxicodendron) and allies. American Journal of Botany, 12: 338–350.

[2]Nahashe K., Miyakoshi T., 1998, a guide to urushi chemistry 2. Tosotoryo 1998, No. 574, 30-41 (in Japanese); Chem. Abstr, 128: 231-625.

[3]Pell S.K., 2004, Molecular Systematics of the cashew family (Anacardiaceae). Baton Rouge: Louisiana State University.

[4]Pell S.K., Mitchell J.D,, Lowry P.P,, Randrianasolo A., Urbatsch L.E.,2008, Phylogenetic split of Malagasy and African taxa of Protorhus and Rhus (Anacardiaceae) based on cpDNA trnL-trnFand nrDNA ETS and ITS sequence data. Systematic Botany, 33: 375–383.

[5]Kidder E.J., 1959, Ancient Peoples and Places, Thames & Hudson, Japan.

[6]Kuraku Y., Brommelle N.S., Smith P. (Eds.), 1988, Getty Conservation Institute,California, p. 45.

[7] Kumanotani J., 1995, Prog. Org. Coat., 26: 163.

[8] Vogl O., Bartus J., Qin M., Mitchell J.D., in: K.P. Ghiggino (Ed.) , 1994,Progress in Pacific Polymer Science, vol. 3, Springer-Verlag, Berlin,p. 423.

[9]Kumanotani J., 1995, Progress in Organic Coatings, 26: 163–195.

[10]Bartus J., Simonic W., Garner C., Nishiura T., Kitayama T., Hatada K.,& Vogl O., 1994, Polymer Journal, 26: 67–78.

[11]Du Y., Oshima R., Iwatsuki H., Kumanotani J., 1984a, Journal of Chromatography, 295: 179–186.

[12]Du Y., Oshima R., Kumanotani J.,1984b, Journal of Chromatography, 284: 463–473.

[13] Du Y., Oshima R., Kumanotani, J., 1985, Journal of Chromatography, 318: 378–385.

[14] Reinhammar B., 1970, Biochimica et Biophyisica Acta, 205: 35–47. Taylor, R. L., Corrad, H. E. (1972). Biochemistry, 11:1383–1388.

[15] Oshima R., Kumanotani J., 1984, Carbohydrate Research, 127: 43–57.

[16] Suzuki S., 2010, Archaeological botany of Japanese lacquer plants, The environmental development and human activity,3: 200-204.

[18] Lu R., Ono M., Suzuki. Miyakoshi, 2006, Study on the newly designed natural lacquer, Mater. Chem. Phys., 100: 158-161.

[19] Yoshida T., 2001, Synthesis of polysaccharides having specific biological activities. Prog Polym Sci, 26: 379-441.

[20] Lu R., Hariyayama, S., Ishimura T., Nagase K., Miyakoshi T.,2004, Development of a fast drying lacquer based on raw lacquer sap, prog. Org. coat., 51: 238-243.

[21]Lu R., Ishimura T., Suda K., Honda T., Miyakoshi T., 2005, Development of a fast drying hydride lacquer in low relative humidity environment based on kurome lacquer sap, polym. J. 37: 309-315

[22]Lu R., Honda T., Ishimura T., Miyakoshi T., 2005, Study on a natural drying lacquer hybridized with organic silane, J. Appl. Polym. Sci, 98: 1055-1061.

[23]Lu R., Ono M., Suzuki. Miyakoshi, 2006, Study on the newly designed natural lacquer, Mater. Chem. Phys., 100: 158-161.

[24]China Plant BOL Group, 2011, Comparative analysis of a large dataset indicates that ITS should be incorporated into the core barcode for seed plants. Proceedings of the National Academy of Sciences of the United States of America, 108, 19641–19646.

[25]Soltis P.S., Soltis D.E. and Doyle J.J., 1992, Molecular systematis of plants. Chapman and Hall, New York.

[26]Zimmer E.A., Hamby R. K., Arnold M. L., Leblanc D.A., and Theriot E. C., 1989, Ribosomal RNA phylogenies and flowering plant evolution. In B. Fernholm, K. Bremer, and H. Jornvall [eds], The hierarchy of life, 205-214.

[27]Hamby, and Zimmer E.A., 1991, Ribosomal RNA as a phylogenetic tool in plant systematics, Molecular systematics of plants, 50-91.

[28]Baldwin B.G., 1992, Phylogenetic utility of the internal

transcribed spacers of nuclear ribosomal DNA in plants: an example from the Compositae, Molecular Phylogenetics and evolution, 1: 3-16.

[29]Bruce G. Baldwin and Staci Markos, 1998, phylogenetic utility of the external transcribed spacer (ETS) of 18S-26S rDNA : congruence of ETS and ITS trees of calycadenia (compositae), molecular phylogenetics and evolution, 449-463.

[30]Barciszewska M.Z., Mashkova T.D., Kisselev L.L., Barciszewska J., 1987, The nucleotide sequences of 5S ribosomal RNAs from two plants: rape and white beet. Nucleic Acids Res.15: 363.

[31]Yang Y.W., Tseng P. F., Tai P. Y., Chang C.J., 1998, Phylogenetic position of Raphanus in relation to Brassica species based on 5S rRNA spacer sequence data. Bot. Bull. Acad. Sin. 39: 153-160.

[32]Matya´sˇek, R., Fulneo¨ek, J., Lim K.Y., Leitch A.R., Kovao˜ı´k A., 2002, Evolution of 5S rDNA unit arrays in the plant genus Nicotiana (Solanaceae). Genome, 45: 556-562.

[33]Liu Z.L., Zhang D., Wang X.Q., Ma X.F., Wang X.R., 2003, Intragenomic and interspecific 5s rDNA sequence variation in five Asian pines. Am. J. Bot. 90: 17-24.

[34]Chase M.W., Soltis D.E.,et al., 1993, Phylogenetics of seed plants: an analysis of nucleotide sequences from the plastid gene rbcL1, Ann. Mo. Bot. 80: 528-580.

[35]Wolfe K.H., Li W.H., and Sharp P.M., 1987, Rates of nucleotide substitution vary greatly among plant mitochondrial, chloroplast, and nuclear DNAs, proc. natl. acad. sci. USA, 84: 9054-9058.

[36]Dykes, W.R.,1913, The genus Iris. Dove publication, New York.

[37]China Plant BOL Group 2011, Comparative analysis of a large dataset indicates that ITS should be incorporated into the core barcode for seed plants. Proceedings of the National Academy of Sciences of the United States of America, 108, 19641–19646.

[38]Satu Y-I., ISHIKAWA R., 2004, 〈Sannai-Maruyama site〉 the world of plants, Shokabo publishing, 62-71.

[39]田中孝尚・小林和貴・能城修一・鈴木三男（2010）ウルシの分類学と分子系統学. 漆サミット2010, 明治大学, 1月15-17日.

[40]Kornfeld R., Kornfeld S., 1985, Assembly of asparagine-linked oligosaccharides. Annu Rev Biochem, 54: 631–664.

[41] Brooks S. A., 2009, Strategies for analysis of the glycosylation of proteins: current status and future perspectives. Mol. Biotechnol. 43: 76-88.[42]Wasley L.C., Timony G., Murtha P., Stoudemire J., Dorner A.J., Caro J., et al., 1991, Theimportance of N- and O-linked oligosaccharides for the biosynthesis and invitro and in vivo biologic activities of erythropoietin. Blood ,77:2624-32.

[43]Gomord V.,Chamberlain P.,Jefferis R.,Faye L.,2005,

Biopharmaceutical production in plants: problems, solutions and opportunities. Trends Biotechnol, 23:559-65.

[44]Cabanes-Macheteau M., Fitchette-Laine A.C., Loutelier-Bourhis C., Lange C., Vine N.D., Ma J.K., et al., 1999, N-glycosylation of a mouse IgG expressed in transgenic tobacco plants. Glycobiology, 9:365-72.

[45]Altmann F. , 2007, The role of protein glycosylation in allergy. Int Arch Allergy Immunol, 142:99-115.

[46] Van Ree R., Cabanes-Macheteau M., Akkerdaas J., Milazzo J.P., Loutelier-Bourhis C., Rayon C., et al., 2000, β-(1,2)-xylose and α-(1,3)-fucose residues have a strong contribution in IgE binding to plant glycoallergens. J Biol Chem,275:11451-8.

[47]Tretter V., Altmann F., Ma ¨ rz L., 1991, Peptide -N4 -(N- acetyl -b- glucosaminyl) asparagines amidase-F cannot release glycans with fucose attached a-1-3 to the asparaginelinked N-acetylglucosamine residue, Eur. J. Biochem. 199: 647-652.

[48]Takahashi N., Nishibe H., 1981, Almond glycopeptidase acting on aspartlyglycosylamine linkages. Multiplicity and substrate specificity, Biochim. Biophys. Acta, 657: 457-467.

Chapter 2

Polymorphism of DNA sequences in Japanese lacquer tree cultivars

---

ABSTRACT

The oriental lacquer tree *Rhus verniciflua* species is an important because not only it produces a natural paint, but also it is used in oriental medicine. Lacquer tree cultivars have decreased due to forest decline and climate change. Few analyses and evaluations of lacquer DNA sequences have been reported. To reveal the relationship between DNA sequences and geographical distance, six DNA regions of lacquer trees in Hokkaido, Iwate, and Fukushima prefectures, ITS1, ITS2, ETS in nuclear ribosomal DNA (nrDNA), and *rbc*L, 5S, and *mat*K in chloroplast DNA (cpDNA), were analyzed. We found for the first time that lacquer tree cultivars had polymorphism. Among the DNA regions, ITS1 and ITS2 were found to have large differences of the sequences. The length ranged from 255 to 287 bps for ITS1 and from 277 to 283 bps for ITS2, and the maximum sequence divergences in ITS1 and ITS2 between Abashiri C area (Hokkaido) and Iwate were 22.1% and 15.2%, respectively. A

long insertion in the ITS1 region in Abashiri C and Fukushima lacquer trees appeared. The GC content increased to 68% and 63% from 55%, respectively. These results suggest that lacquer trees had polymorphism among cultivars.

2.1 Introduction

The Oriental lacquer tree is an important because it not only produces a natural paint, urushi, but also because it is used in oriental medicine [1]. The lacquer tree is widely distributed in the temperate zone of Asian countries, and six species grow in Japan. Oriental lacquer is expected to an environment-friendly natural polymer material for the next generation because lacquer sap is polymerized by the enzyme laccase at near room temperature to produce beautiful and durable surfaces on wares and interiors of buildings without any toxic organic solvent. The major components of lacquer sap are urushiol, the enzyme laccase, and polysaccharides. Many studies of lacquer have focused on the properties of lacquer as a natural paint including its use in cultural treasures, the polymerization mechanism of urushiol, and the enzyme [2].

We previously worked on the structural analysis and elucidation of specific biological activities of polysaccharides [3]. NMR

measurements have revealed that lacquer polysaccharides have a 1, 3-β-galactopyranosidic main chain and glucuronic acid in the side chains with a β-linkage, and L-arabinose and L-rhamnose in the terminal of branches with a α-linkage [4]. In addition, we found that Chinese lacquer polysaccharides had specific biological activities such as blood coagulation-promoting and antitumor activities [5]. Sulfated lacquer polysaccharides had potent anti-HIV activity on MT-4 cells at 0.5 μg/ml as the 50% effective concentration (EC_{50}) (standard curdlan sulfate EC_{50} = 0.13 □g/ml, which is one of the highest anti-HIV activities of polysaccharides, and lower blood anticoagulant activity, 9-17 unit/mg, than a standard dextran sulfate, 22.7 unit/mg (curdlan sulfate, around 10 unit/mg).

Lacquer trees in Iwate prefecture, in the Tohoku area, Japan, were transplanted to Abashiri City in Hokkaido prefecture and planted in three parts in Abashiri A and B areas in 1992 and C area in 1994. The temperature of Abashiri City in winter falls below -10°C and the snow lays deep; however, lacquer trees in Abashiri C area have grown and produced sap, suggesting that the lacquer trees are adapted well to cold environments. On the other hand, few analyses and evaluations of lacquer DNA sequences have been reported [6]. Therefore, we analyzed DNA sequences of lacquer trees in Abashiri A, B, and C areas to reveal the relationship between DNA sequences and geographical distance. In this paper, we

describe the sequence analysis of lacquer tree Rhus verniciflua in Hokkaido and compared it to those in Iwate and Fukushima prefectures, which are famous lacquer-growing districts at present and in the past in Japan. We selected five DNA regions, ITS (internal transcribed spacer) and ETS (external transcribed spacer) of nrDNA, and *rbc*L (large subunit of ribulose-1, 5- bisphosphate carboxylase), 5S, and *mat*K in cpDNA, regions that are used generally to identify plants and species. Phylogenetic analysis of the five regions afforded information about genetic divergence of sequences and environmental adaptation.

2.2 Material and methods

2.2.1 Measurement and lacquer samples

Genomic DNA was identified using an Advance Mupid-exU submarine electrophoresis system. Amplification of DNA regions (PCR) was carried out using Bio-Rad Mycycler and MJ Research Peltier PTC-200 thermal cyclers, and the purity of the DNA regions were measured by a Thermo Scientific Nanodrop 1000 spectrophotometer. Electrophoresis of the PCR product was performed using a Shimadzu MCE-202 MultiNA spectrophotometer. The sequence analysis of the DNA regions was recorded using an Applied Biosystems AB 3130 genetic analyzer with a 36 cm capillary column.

The young lacquer trees of 1 year-growth were transplanted from Iwate-Johoji area (Iwate prefecture, Japan) to Abashiri A and B areas (Hokkaido prefecture, Japan) in 1992 and to Abashiri C area in 1994, respectively. Abashiri City in winter falls below -10°C and the snow lays deep. Twenty-three lacquer trees of the species Rhus verniciflua, randomly selected five from Abashiri A area from two hundred lacquer trees, six from Abashiri B area from two hundred lacquer trees, and seven from Abashiri C area from four hundred lacquer trees, and one each from Abashiri South Park, Iwate-Johoji, Fukushima-Aizu, and Okinawa-Naha, were used for the phylogenetic analysis. The leaves were collected in summer of 2010 and 2011.

The diameter of Lacquer trees of the ABC zones in Abashiri, Japan. (cm)

No. / Area	1	2	3	4	5	6	7	8	9	10	n
A area	6	12	20	20	12	10	10	5			11.1
B area	9	20	15	20	20	15	13				16.6
C area	30	6	15	28	25	30	15	25	28	15	22.6

The picture of lacquer plant in Abshiri, Hokkaido, Japan.

A: Abashiri A area

B: Abashiri B area

C: Abashiri C area (Lacquer tapping)

D: Abashiri south park

2.2.2 Genomic DNA extraction

A fresh or dried lacquer tree leaf was ground under liquid nitrogen by using a mortar and pestle to destroy the cell wall, and then the ground leaf was stored in a freezer at -80 °C until extraction. The genomic DNA was extracted from the ground material (25-100 mg) using a DNeasy plant mini kit (Qiagen) according to the manufacturer's protocol. During the isolation procedures, contaminating RNA was removed by enzymatic hydrolysis using RNase. The cells, detergents, proteins, and polysaccharides were also removed by the precipitation buffer AP2.

The genomic DNA extracted from the ground leaf was confirmed by pulsed-field gel electrophoresis through an agarose gel. A loading buffer was added to the extracted sample, and then the solution was loaded onto 1% agarose gel in 1xTAE electrophoresis buffer in a Mupid-exU submarine electrophoresis system. A molecular maker was used in the first lane. The gel running time on the gel was 25 min. After it was run, the gel was kept in the ethyl bromide (EB) solution for 30min to develop the band of the genomic DNA.

The concentration and purity of the extracted genomic DNA were determined by comparison of absorbance at 260 nm (A260) and 280 nm (A280) using a Nanodrop 1000 spectrophotometer (Thermo Scientific). The AE elution buffer was used as a blank to remove the background.

2.2.3 Determination of yield and purity

The concentration and purity of the extracted genomic DNA were determined by the comparison to the absorbance at 260 nm (A260) and 280 nm (A280) by a spectrophotometer. In our study, we have used a Nanodrop 1000 spectrophotometer (Thermo scientific). For the measurement of absorbance, we have used the Elution buffer AE as a standard for disappearing of the background.

The DNA sample from plant tissue often contained co-purified polysaccharides and other metabolites, which interfere with OD readings. Therefore, the absorbance should measure with special attention paid to the contaminations. Absorbance scans should show a symmetric peak at 260 nm and have an overall smooth shape. Purity is determined by calculating the ratio of absorbance at 260 nm to absorbance at 280nm. Pure DNA has an A260/A280 ratio of 1.7 - 1.9.

2.2.4 PCR amplification of DNA region

A typical procedure for the PCR of the ITS region is as follows. Amplification reactions were carried out in 25 μL containing 1.5 mmol MgCL2, 0.2mmol each dNTP, 0.5μmol of each primer (N-nc18S10 and C26A as shown in Table1), 0.05U/μL Taq polymerase, and approximately 50ng DNA template. The PCR was performed in a Peltier thermal cycler PTC-200 (MJ Research) or

Mycycler (Bio-Rad). PCR conditions for the ITS region were heating at 95°C for 5 min as an initial denaturation step before performing 35 cycles consisting of 30 sec at 95°C for denaturation, 30 sec at 56°C for annealing, and 2 min at 72°C for elongation. A final extension step of 10 min at 72 °C was performed at the last cycle. The length of the PCR product was confirmed by electrophoresis (MultiNA MCE-202, Shimadzu) using DNA 1000 or 2500 kits and markers (Φx174 DNA/Hae Ⅲor pGEM® DNA). The band due to the whole ITS region appeared at around the 700 bps, and ITS-1 and -2 regions also appeared clearly at around 300 and 400 bps, respectively.

The PCR for other regions, ETS, 5s, rbcL, and matK, was performed using almost the same procedures as above.

2.2.5 Purification of amplified PCR product

(1) Magnetic beads method

The Agencourt AMPure XP system uses magnetic beads. The PCR product is adsorbed on the magnetic beads in a 70% ethanol solution. The magnetic beads are centrifuged and washed with 1xTE buffer to remove the adsorbed PCR product. This system has a high recovery of amplicons larger than 100 bps and unincorporated dNTPs, primers, primer dimers, salts, and other contaminants are efficiently removed.

(2) Gel extraction method

A Qiaex II kit was used. This protocol is designed for the extraction of 40–50 kbps DNA fragments from 0.3–2% standard or low-melting point agarose gels in a tris acetate EDTA (TAE) and tris EDTA boric acid (TEB) buffers. The DNA band on the agarose gel after electrophoresis was excised with a clean sharp scalpel. The separated DNA was extracted using extraction buffers according to their protocols.

(3) Column separation method

A Suprec-02 (Takara) filter cartridge designed for rapid purification and concentration of DNA samples after PCR was used for buffer exchange. 1xTE buffer was added to the PCR solution and the solution was transferred to the ultrafiltration cassette column of the Suprec-02 filter cartridge. The purified DNA solution was obtained by centrifugation and analyzed by electrophoresis.

2.2.6 Sequencing of purified PCR product

The sequence reaction was carried out using a BigDye Terminator v3.1 cycle sequencing kit and BigDye XTerminator purification kit according to the manufacturer's instructions. The DNA sequence of each region was determined on the AB 3130 genetic analyzer with a

36 cm capillary column (ABI). POP-7 polymer and 10xGenetic analyzer buffer with EDTA were used in sequence analysis.

2.2.7 Sequence alignment and construction of phylogenetic tree

The sequence alignment was carried out with the Clustal W program. The phylogenetic tree was constructed by the MEGA program (http: //evolgen.biol. metro-u.ac.jp/MEGA/).

2.3 Results and Discussion

2.3.1Extraction and purification of genomic DNA of lacquer tree

Fig. 1 shows the sampling place of the cultivar lacquer trees in Japan, in which, Abashiri A, B and C areas in Hokkaido prefecture were close each other. The temperatures of Abashiri City were below -10°C and the snow lies deep in winter and below 25°C in summer, respectively. In general, the lacquer trees were widely cultivated in the temperate regions. Sap can be collected after ten-year growing. The young lacquer trees of 1 year-growth were transplanted from Iwate- Johoji area (Iwate prefecture), which is one of the famous lacquer tree cultivar area in Japan, to Abashiri A and B areas in 1992 and to Abashiri C areas in 1994, respectively, and then grown in a cold environment. In the three cultivar areas (A, B, and C) in Abashiri City, and lacquer trees in the C (Abashiri C) area were planted on the southern slope of a small mountain, whereas in the A

and B areas were placed at the base of the mountain. After ten years, sap was collected only in the lacquer trees in Abashiri C area, suggesting that the lacquer trees in Abashiri C area were adapted to the cold temperatures. Therefore, several DNA regions were phylogenetically analyzed and the DNA sequences were compared to those of Iwate-Johoji lacquer trees that are the origin of Abashiri lacquer trees to determine the relationship between DNA sequences and geographical distance.

Twenty-three lacquer samples were used for phylogenetic analysis. Genomic DNA was extracted from lacquer tree leaves using a commercially available DNeasy mini kit (Qiagen). The purity of the purified genomic DNA was determined by calculating the ratio of absorbance at 260 nm to that at 280 nm, indicating that the A260/A280 ratio after purification was 1.85 and the concentration was 124.4 ng/ml; in general, pure DNA has an A260/A280 ratio between 1.7 and 1.9. These results indicate that the genomic DNA solution had high purity and contained sufficient genomic DNA for the next step.

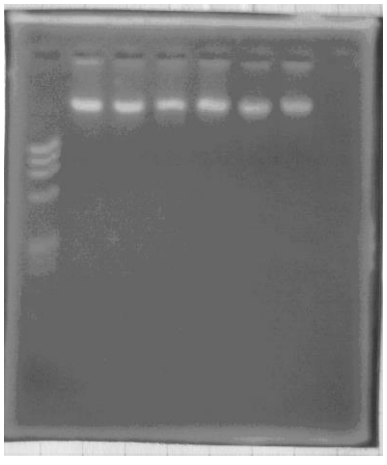

Figure2. Gel electrophoresis of Genomic DNA.

Sample: Lacquer tree at Abashiri area in Hokkaido.

Lane 1: Reference maker.

Lanes 2-7: Genomic DNA extracted in Abashiri Lacquer tree.

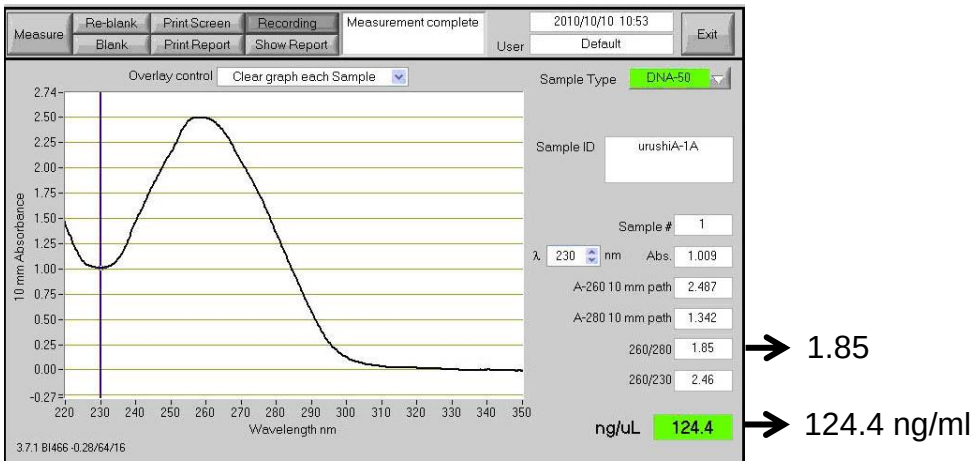

Figure3. UV profile of DNA extract in Abashiri lacquer
(Nanodrop 1000 spectrophotometer)

2.3.2 Amplification and sequence analysis of DNA regions

After extraction and purification of genomic DNA, polymerase chain reaction (PCR) amplification was performed on five DNA regions, the ITS and ETS regions of nrDNA, and the rbcL, 5S, and the matk regions of cpDNA.

The ITS region is a spacer region and useful for phylogenetic studies at the intra-species level because the DNA sequence of the spacer region evolves more rapidly than that of the coded genetic region [7]. The 5S region with several hundred base pairs in length is composed of 5S rRNA (approximately 120 bps) and non-transcribed spacer regions [8]. The 5S DNA is an alternative sequence region with high numbers of copies. The 5S rRNA gene sequence is very well-conserved between plants species, while the spacer is species-specific, and it has been used for phylogenetic

studies and species identification. The gene for the large subunit of ribulose-bisphosphate carboxylase (*rbc*L), located on the chloroplast genome, is an appropriate choice for inference of phylogenetic relationships at higher taxonomic levels, because of its slow synonymous nucleotide substitution rate in comparison with nuclear genes and its functional constraints, which reduce the evolutionary rate of non-synonymous substitutions [9]. The matK DNA is a gene of approximately 1500bp in the chloroplast genome and encodes the enzyme maturase. The matK gene has high rates of base substitutions making it useful for phylogenetic analysis at the species and genus levels [10].

The primers used in this work are shown in Table 1. Primer pairs of ITS-4 and -5 are usually used for amplification of the ITS region [11], but, in this study the primers were not suitable for the PCR amplification and sequence analysis of the lacquer genomic DNA of Rhus verniciflua and Rhus succedanea species. The combination of ITS-5 and -2 primers was not suitable for the amplification of the ITS1 region either. When other primers, a combination of N-nc18S10 and C26A [12] were used amplification of the ITS region was successful and appeared as a single band of approximately 700 bps due to the whole ITS region on the profile of electrophoresis after purification. The sequences of the ITS1 region were determined by the whole ITS and 5.8S -ITS2 sequences. Other DNA regions were amplified by using the primers as listed in Table

1 [13]-[17].

Figure3. The Multina electrophoresis for five DNA regions.

M1: marker (1000bp), 1: ITS region (about 700bp), 2: ITS2 region (350bp, including a part of 5.8S), 3: ETS region (350bp), 4: ITS1 region (300bp, including a part of 5.8s), 5: 5S region, M2: marker (2500bp), 6: *rbc*L region (1400bp), 7~9: parts of *rbc*L regions, 10: *mat*K region (2000bp).

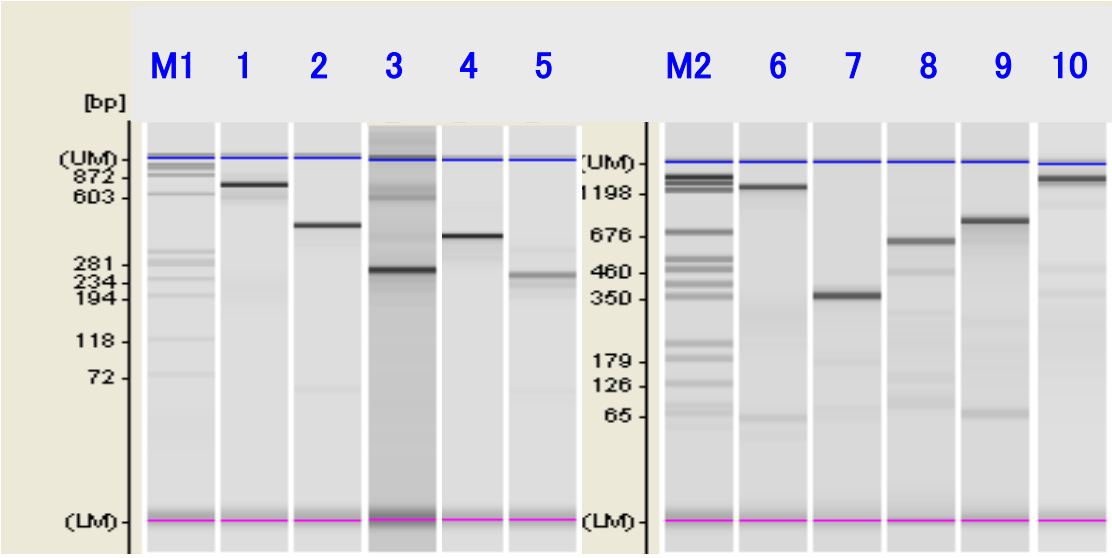

Table 2 shows the lengths and GC contents of the five DNA regions. The length of the ITS regions varied from 695 to 731 bps. The ITS1 region was extended about 30 bps in Abashiri C lacquer trees, which produce sap. No variation in the length of the sequence of ETS, 5S, rbcL, and matK regions was observed. The ITS region in Abashiri C lacquer trees provided a large variation both in length and sequence as demonstrated in Fig. 2, while other regions had almost the same length, as shown in Table 2. In particular, the GC content in ITS1, ITS2, and the whole ITS regions of Abashiri C lacquer trees (68%, 63%, and 63%, respectively) were higher than that of lacquer trees

in Abashiri A, B, and Iwate-Johoji. In general, a high GC content contributes to the stability of DNA and plays an important role in adaptation to temperatures due to an increase in stacking interactions of DNA [18]. The ITS region is a spacer region in the DNA, so the substitution rate of nucleotides is faster than that of the gene-coded regions. Although the DNA sequence of the ITS region of some trees in Abashiri A and B was different than that of Iwate-Johoji, sap was collected mainly from Abashiri C lacquer trees. We consider that large sequence divergences and increases of GC content among cultivars are probably due to the presence of polymorphism in Rhus verniciflua lacquer trees and lacquer tree cultivars in Abashiri C area have been adapted to the growth environments.

2.3.3 Construction of sequence alignment and phylogenetic tree

After sequencing, the final step was to perform a sequence alignment and construct a phylogenetic tree. The results of multiple sequence alignments can demonstrate sequence homology. We used the Clustal W program [19] for aligning sequences, as shown in Figure 2, in which the sequence indicated that the ITS1 region was 255 bps for lacquer trees outside Abashiri C and some Abashiri A and B lacquer trees. Several differences in the alignments appeared even though the lacquer trees in Abashiri C and Iwate-Johoji are the same species. In particular, a long insertion appeared in the

ITS1 region from 104 to 139 bps of Abashiri C lacquer trees and some Abashiri A, B, and Fukushima-Aizu lacquer trees. In addition, the lacquer trees in Abashiri C and some Abashiri A, B, and Fukushima-Aizu trees were high GC contents in the ITS1 region, as shown in Table 2. In general, the thermal stability of DNA increases with increasing GC content [18]. Table 3 shows the nuclear divergences of the ITS and 5S regions with large changes of sequence, which divergences were calculated by the Kimura-2 parameter model [20]. Maximum of sequence divergences in ITS 1, ITS2, and the whole ITS region were 22.1%, 15.2%, and 14.3%, respectively, indicating that the ITS region gave the largest change of sequence and was suitable to investigate genetic distance in the species. The genetic distance between Abashiri C0, A0, B0, and Iwate-Johoji was 19.5%, and Abashiri SP and Okinawa-Naha was 16.8%. The divergences between Iwate-Johoji and Abashiri A, B, SP, and Okinawa-Naha were small. These results suggest the presence of a polymorphism in lacquer cultivars with cold-resistant property.

Fig. 3 shows phylogenetic analyses of lacquer trees in the Abashiri area by neighbor-joining (NJ) and maximum parsimony (MP) phenograms based on the ITS region. Both phylogenetic trees characterized the genetic positions of lacquer trees in Abashiri into two main groups. The first genetic group contained mainly Abashiri C lacquer trees, whose sequence was greatly changed and the GC content also increased. The second genetic group contained Abashiri

A, B, and SP lacquer trees, whose sequences were similar to those of Iwate-Johoji and were not changed much. However, sap was not collected from Abashiri A and B lacquer tree cultivars. It was found that the phylogenetic tree branching was dependent on both cultivated areas and growth environments. Other phylogenetic trees of the ETS, 5S, rbcL, and matK regions were similar to each other, and no large differences were observed except the Fukushima-Aizu tree, indicating that the evolution rate of the gene-coding regions was slow. Only the Fukushima-Aizu lacquer tree was found to have a genetic distance in these areas.

Although the species of the Fukushima-Aizu lacquer tree cultivar is the same as the Iwate-Johoji trees, a large genetic distance was shown in all DNA regions used in this work. The 5S sequence alignment of Abashiri C0, Fukushima-Aizu, and Iwate-Johoji lacquer trees and phylogenetic tree are provided in Figs. 4 and 5, respectively. The lengths of the ITS1 and 5S regions were extended to 283 and 353 bps from 255 and 266 bps, respectively, of the Iwate-Johoji lacquer tree, and divergence was 22.1% and 40.5%. Long insertions appeared in both ITS1 and 5S regions, and many nucleotide substitutions occurred. The GC content in whole ITS and 5S regions increased slightly to 59%and 48%, as shown in Table 2. The sequences of the other DNA regions were also different from Iwate-Johoji lacquer trees. The Fukushima-Aizu lacquer tree produced another group in the

phylogenetic tree and had a genetic distance, as represented in Table 2 and Figures 3 and 5. The details are being investigated.

In conclusion, from the phylogenetic results of lacquer tree cultivars revealed an intra-species genetic diversity in the length and GC content in the ITS region, we found for the first time polymorphism in lacquer tree cultivars. The lacquer trees in Abashiri C area were adapted to the cold environment from the point of sap production. Polymorphism among lacquer tree cultivars was originally present in Rhus verniciflua species, because lacquer trees in Abashiri areas were transplanted from Iwate prefecture. In addition, we also found that the length and variation of sequences of Fukushima-Aizu lacquer trees are different from those of Iwate-Johoji and Abashiri lacquer trees even though these lacquer trees are the same cultivar Rhus verniciflua species. Although lacquer trees were once cultivated widely in Japan and Asian countries, the cultivation area is much smaller at present in consequence of forest decline, climate, environment, and economic changes. For the protection and conservation of the growth environment of this Asian lacquer resource, we will continue to analyze and investigate the DNA sequences and biological activities of lacquer components as a natural resource for the next generation. Further investigations on the genetics analysis of lacquer tree cultivars and relationship between polymorphism and growth environments in wide areas in Japan and Asian countries are now

in progress.

Acknowledgments

This research was partially supported by a Grant-in-Aid for Scientific Research 2009-2011 (No. 21550199) from the Japan Society for the Promotion of Science (JSPS) and the SVBL research program of Kitami Institute of Technology 2009-2011.

References

[1]Kumanotani J (1995) Urushi (oriental lacquer)-a natural aesthetic durable and future- promising coating. Prog Org Coat 26: 163-195

[2]Kobayashi S, Uyama H, Ikeda R (2001) Artificial urushi. Chem Eur J 7: 4754-4760

[3]Yoshida T (2001) Synthesis of polysaccharides having specific biological activities. Prog Polym Sci 26: 379-441.

[4]Lu R, Hattori K, Xia Z, Yoshida T, Yang J, Du Y, Miyakoshi T, Uryu T (1999) Structural analysis of polysaccharide in Chinese Lacquer by NMR spectroscopy. Sen'i-Gakkai Shi 55: 47–56

[5]Lu R, Yoshida T, Nakashima H, Premanathan M, Aragaki (2000) Specific biological activities of Chinese lacquer polysaccharides. Carbohydr Polym 43: 47–54

[6]Lee WK, Kim M, Heo K (2004) Phylogeny of Korea Rhus spp. Based ITS and rbcL sequences. Korean J Medicinal Crop Sci 12: 60-66

[7]Alvarez I, Wendel JF (2003) Ribosomal ITS sequences and plant phylogenetic inference.Mol Phyl Evol 29: 417-434

[8]Sastri DC, Hilt KRE, Appels LS, Playford J (1992) An overview of evolution in plant 5S DNA. Plant Syst Evol 183: 169-181

[9]Mark WC, Douglas ES, Richard GOl, David M, Donald HL (1993),

Phylogenetics of seed plants: an analysis of nucleotide sequences from the plastid gene rbcL. Ann Mol Bot Gard 80: 528-580

[10]Hilu K, Liang H (1997) The matK gene: sequence variation and application in plant systematic. Am J Botany 84: 830-839

[11]White B, Taylor L (1990) Amplification and direct sequencing of fungal ribosomal RNA genes for phylogenetics in "PCR protocols: a guide to methods and applications". Academic Press Inc., pp.315-322

[12]Wen J, Zimmer EA (1996) Phylogeny and biogeography of panax L. (the ginseng genus, Arslianceae): inference from IIS sequences of nuclear ribosomal DNA. Mol Phyl Evol 6:167-177

[13]Weeks A, Simpson BB (2004) Molecular genetic evidence for interspecific hybridization among endemic Hispaniolan Bursera (Burseraceae). Am J Botany 91: 976-984

[14]Baldwin B G, Markos S (1998) Phylogenetic utility of the external transcribed spacer (ETS) of 18S-26S rDNA: congruence of ETS and ITS trees of Calycadenia (Compositae). Mol Phylog Evol 10: 449-463

[15]Doveri S, Lee D (2007) Development of sensitive crop-specific polymerase chain reaction assays using 5S DNA: applications in food traceability. J Agr Food Chem 55: 4640-4644

[16]Kaufmann M, Wink M (1994) Molecular systematic of the

Nepetoideae (family Labiatae): phylogenetic implications from rbcL gene sequences. Z Naturforsch C 49c: 635-645

[17]Johnson LA, Soltis E (1994) MatK DNA sequences and phylogenetic reconstruction in Saxifragaceae s. s. System Botany 19: 143-156

[18]Zheng H, Wu H (2010) Gene-centric association analysis for the correlation between the guanine- cytosine content levels and temperature range conditions of prokaryotic species. BMC Bioinformatics 11(S7): 1-10

[19]Tamura K, Dudley J, Nei M, Kumar S (2007) MEGA4: Molecular Evolutionary Genetics Analysis (MEGA) software version 4.0. Mol Biol Evol 24: 1596-1599

[20]Kimura M (1980) A simple method for estimating evolutionary rate of base substitution through comparative studies of nucleotide sequences. J Mol Evol 16: 111-120

Legend to Figures

Figure1.Sampling place of lacquer tree cultivars in Japan.

Figure2.Sequence alignment of ITS1 region in lacquer trees.

Figure3.Sequence alignment of 5S region in lacquer trees.

Figure4.Phylogenetic tree of 5S region in Rhus verniciflua constructed by (A) neighbor-joining and (B) maximum parsimony methods, respectively. Both trees were similar each other, indicating high reliability.

Figure5.Phylogenetic tree of ITS region in Rhus verniciflua constructed by (A) neighbor-joining and (B) maximum parsimony methods, respectively. Values showed above branches indicate bootstrap values for 100 replicates supporting the respective cluster. Both trees were similar each other, indicating high reliability.

Table1. Primer sequence used in this study

Region	Primer	5'-Sequence-3'	Reference
ITS	N-nc18S10	AGGAGAAGTCGTAACAAG	[21]
	C26A	GTTTCTTTTCCTCCGCT	
ITS1	ITS-5	GGAAGTAAAAGTCGTAACAAGG	[22]
	ITS-2	GCTGCGTTCTTCATCGATGC	
ITS2	ITS3	GCATCGATGAAGAACGCAGC	[22]
	ITS4	TCCTCCGCTTATTGATATGC	
ETS	ETS1F	TTCGGTATCCTGTGTTGCTTAC	[23][24]
	18S-IGS	GAGACAAGCATATGACTACTGGCAGGATCAACCAG	
5S	5SDNAF	CTGGGAAGTCCTCGTGTTG	[25]
	5SDNAR	TTAGTGCTGTGGTATGATCGCA	
*rbc*L	*rbc*L-N	ATGTCACCACAAACAGAAACTAAAGC	[26]
	*rbc*L-NR2	TTACCCACAATGGAAGTAAACATG	
	*rbc*L-2F2	GCGCTCTACGTCTAGAGGATC	
	*rbc*L-1R	GGGTGCCCTAAAGTTCCTCC	
	*rbc*L-RF	TATTTCACTCAGGATTGGG	
	*rbc*L-R	TATCCATTGCTGGGAATTCAAATTTG	
matK	*trn*k-3F	AGTYGGGTCKAGTRAATAAA	[27]
	matK-4R	GAKAAGATTGGKTRCGGAG	
	matK-5F	AAGAGCGATKRKATTGAA	
	matK-10R	CGCTGTGATAATGAGAAAGA	
	matK-6F	TCTSCGTAASCAATCTTCTC	
	matK-7R	TGAADACRCAGYTGATC	

Table 2. Length and GC content of five DNA regions

Lacquer (*Rhus verniciflua*)	DNA region																	
	Length (bp)								GC content (%)									
	ITS	(ITS1	5.8S	ITS2)	ETS	5S	*rbc*L	*mat*K	ITS	(ITS1	5.8S	ITS2)	ETS	5S	*rbc*L	*mat*K
Abashiri-A0	695	255	161	279	341	266	1375	2160	55	55	54	55	62	46	44	34
Abashiri-A1	731	287	161	283	341	266	1375	2160	63	68	54	63	62	46	44	34
Abashiri-A2	728	287	161	283	341	266	1375	2160	62	66	54	61	62	46	44	34
Abashiri-A3	695	255	161	279	341	266	1375	2160	55	55	54	55	62	46	44	34
Abashiri-A4	731	287	161	283	341	266	1375	2160	63	68	54	63	62	46	44	34
Abashiri-A5	695	255	161	279	341	266	1375	2160	55	55	54	55	62	46	44	34
Abashiri-B0	695	255	161	279	341	266	1375	2160	55	55	54	55	62	48	44	34
Abashiri-B1	695	255	161	279	341	266	1375	2160	55	55	54	55	62	48	44	34
Abashiri-B2	695	255	161	279	341	266	1375	2160	55	55	54	55	62	48	44	34
Abashiri-B3	695	255	161	279	341	266	1375	2160	55	55	54	55	62	48	44	34
Abashiri-B4	695	255	161	279	341	266	1375	2160	55	55	54	55	62	48	44	34
Abashiri-B5	728	286	161	281	341	266	1375	2160	62	66	54	61	62	48	44	34
Abashiri-C0	731	287	161	283	341	266	1375	2160	63	68	54	63	62	46	44	34
Abashiri-C1	731	287	161	283	341	266	1375	2160	63	68	54	63	62	46	44	34
Abashiri-C2	731	287	161	283	341	266	1375	2160	63	68	54	63	62	46	44	34
Abashiri-C3	731	287	161	283	341	266	1375	2160	63	68	54	63	62	46	44	34
Abashiri-C4	728	286	161	281	341	266	1375	2160	62	66	54	63	62	48	44	34
Abashiri-C5	728	286	161	281	341	266	1375	2160	62	66	54	63	62	48	44	34
Abashiri-C6	728	286	161	281	341	266	1375	2160	62	66	54	63	62	48	44	34
Abashiri-SP	695	255	161	279	341	266	1375	2160	55	55	54	55	62	46	44	34
Iwate-Johoji	695	255	161	279	341	266	1375	2160	55	55	54	55	62	46	44	34
Okinawa-Naha	695	255	161	279	341	266	1375	2160	55	55	54	55	62	46	44	34
Fukushima-Aizu	721	283	161	277	341	353	1376	2160	59	61	54	59	59	48	44	34

Table 3. Nuclear divergence values of ITS (lower) and 5S (upper) regions in lacquer trees calculated by using Kimura-2 parameter model.

	Lacquer	1	2	3	4	5	6	7	8	8	10	11	12	13	14	15	16	17	18	19	20	21	22	23
1	Abashiri A0		0.000	0.000	0.000	0.000	0.000	0.016	0.016	0.016	0.016	0.016	0.016	0.000	0.004	0.000	0.000	0.000	0.012	0.000	0.000	0.000	0.000	0.379
2	Abashiri A1	0.159		0.000	0.000	0.000	0.000	0.016	0.016	0.016	0.016	0.016	0.016	0.000	0.004	0.000	0.000	0.000	0.012	0.000	0.000	0.000	0.000	0.379
3	Abashiri A2	0.138	0.037		0.000	0.000	0.000	0.016	0.016	0.016	0.016	0.016	0.016	0.000	0.004	0.000	0.000	0.000	0.012	0.000	0.000	0.000	0.000	0.379
4	Abashiri A3	0.000	0.159	0.138		0.000	0.000	0.016	0.016	0.016	0.016	0.016	0.016	0.000	0.004	0.000	0.000	0.000	0.012	0.000	0.000	0.000	0.000	0.379
5	Abashiri A4	0.159	0.000	0.037	0.159		0.000	0.016	0.016	0.016	0.016	0.016	0.016	0.000	0.004	0.000	0.000	0.000	0.012	0.000	0.000	0.000	0.000	0.379
6	Abashiri A5	0.000	0.159	0.138	0.000	0.159		0.016	0.016	0.016	0.016	0.016	0.016	0.000	0.004	0.000	0.000	0.000	0.012	0.000	0.000	0.000	0.000	0.379
7	Abashiri B0	0.000	0.159	0.138	0.000	0.159	0.000		0.000	0.000	0.000	0.000	0.000	0.016	0.020	0.016	0.016	0.016	0.020	0.016	0.016	0.016	0.016	0.405
8	Abashiri B1	0.000	0.159	0.138	0.000	0.159	0.000	0.000		0.000	0.000	0.000	0.000	0.016	0.020	0.016	0.016	0.016	0.020	0.016	0.016	0.016	0.016	0.405
9	Abashiri B2	0.000	0.159	0.138	0.000	0.159	0.000	0.000	0.000		0.000	0.000	0.000	0.016	0.020	0.016	0.016	0.016	0.020	0.016	0.016	0.016	0.016	0.405
10	Abashiri B3	0.000	0.159	0.138	0.000	0.159	0.000	0.000	0.000	0.000		0.000	0.000	0.016	0.020	0.016	0.016	0.016	0.020	0.016	0.016	0.016	0.016	0.405
11	Abashiri B4	0.000	0.159	0.138	0.000	0.159	0.000	0.000	0.000	0.000	0.000		0.000	0.016	0.020	0.016	0.016	0.016	0.020	0.016	0.016	0.016	0.016	0.405
12	Abashiri B5	0.143	0.033	0.004	0.143	0.033	0.143	0.143	0.143	0.143	0.143	0.143		0.016	0.020	0.016	0.016	0.016	0.020	0.016	0.016	0.016	0.016	0.405
13	Abashiri C0	0.159	0.000	0.037	0.159	0.000	0.159	0.159	0.159	0.159	0.159	0.159	0.033		0.004	0.000	0.000	0.000	0.012	0.000	0.000	0.000	0.000	0.405
14	Abashiri C1	0.159	0.000	0.037	0.159	0.000	0.159	0.159	0.159	0.159	0.159	0.159	0.033	0.000		0.004	0.004	0.004	0.008	0.004	0.004	0.004	0.004	0.379
15	Abashiri C2	0.159	0.000	0.037	0.159	0.000	0.159	0.159	0.159	0.159	0.159	0.159	0.033	0.000	0.000		0.000	0.000	0.012	0.000	0.000	0.000	0.000	0.385
16	Abashiri C3	0.159	0.000	0.037	0.159	0.000	0.159	0.159	0.159	0.159	0.159	0.159	0.033	0.000	0.000	0.000		0.000	0.012	0.000	0.000	0.000	0.000	0.379
17	Abashiri C4	0.143	0.033	0.004	0.143	0.033	0.143	0.143	0.143	0.143	0.143	0.143	0.000	0.033	0.033	0.033	0.033		0.012	0.000	0.000	0.000	0.000	0.379
18	Abashiri C5	0.138	0.037	0.000	0.138	0.037	0.138	0.138	0.138	0.138	0.138	0.138	0.004	0.037	0.037	0.037	0.037	0.004		0.012	0.012	0.012	0.012	0.379
19	Abashiri C6	0.143	0.033	0.004	0.143	0.033	0.143	0.143	0.143	0.143	0.143	0.143	0.000	0.033	0.033	0.033	0.033	0.000	0.004		0.000	0.000	0.000	0.379
20	Abashiri SP	0.008	0.168	0.148	0.008	0.168	0.008	0.008	0.008	0.008	0.008	0.008	0.153	0.168	0.168	0.168	0.168	0.153	0.148	0.153		0.000	0.000	0.379
21	Iwate-Johoji	0.000	0.159	0.138	0.000	0.159	0.000	0.000	0.000	0.000	0.000	0.000	0.143	0.159	0.159	0.159	0.159	0.143	0.138	0.143	0.008		0.000	0.379
22	Okinawa-Naha	0.008	0.168	0.148	0.008	0.168	0.008	0.008	0.008	0.008	0.008	0.008	0.153	0.168	0.168	0.168	0.168	0.153	0.148	0.153	0.000	0.008		0.379
23	Fukushima-Aizu	0.221	0.133	0.127	0.221	0.133	0.221	0.221	0.221	0.221	0.221	0.221	0.123	0.133	0.133	0.133	0.133	0.123	0.127	0.123	0.211	0.221	0.211	

a) Bold character shows the largest genetic divergence between Iwate-Johoji and Abashiri C trees.

```
Abashiri A0        GTTTCCGTAGGTGAACCTGCGGAAGGTACATTGTCAAAACCTGCCCAACAGAACGACCTGGGAACTTGTCTTTTACATCGGG----CTTTGGGTGTCAG    95
Abashiri B0        GTTTCCGTAGGTGAACCTGCGGAAGGTACATTGTCAAAACCTGCCCAACAGAACGACCTGGGAACTTGTCTTTTACATCGGG----CTTTGGGTGTCAG    95
Abashiri C0        GTTTCCGTAGGTGAACCTGCGGAAGGTACATTGTCGAAACCTGCCCAGCAGAACGACCCGCGAACCTGTGTCTTACGCCGGGGGGCCTGCGGGCCTCGTG   100
Abashiri SP        GTTTCCGTAGGTGAACCTGCGGAAGGATCATTGTCAAAACCTGCCCAACAGAACGACCTGGGAACTTGTCTTTTACATCGGG ---CTTTGGGTGTCAG    95
Iwate-Johoji       GTTTCCGTAGGTGAACCTGCGGAAGGTACATTGTCAAAACCTGCCCAACAGAACGACCTGGGAACTTGTCTTTTACATCGGG ---CTTTGGGTGTCAG    95
Okinawa Naha       GTTTCCGTAGGTGAACCTGCGGAAGGATCATTGTCAAAACCTGCCCAACAGAACGACCTGGGAACTTGTCTTTTACATCGGG----CTTTGGGTGTCAGT   95
Fukushima-Aizu     GTTTCCGTAGGTGAACCTGCGGAAGGATCATTGTCGAAACCTGCCTAGCAGAACGACCCGCGAACCTGTCTTA ACATCGGGGG--CGTGCGGGACTCGT   98

Abashiri A0        -TCGTGCAC----------TCGTGCACTCGTGCCTGCATCCACCCCCTTCGTCGCACGTTAACGAACCCCGATGCGATCCA   165
Abashiri B0        -TCGTGCAC----------TCGTGCACTCGTGCCTGCATCCACCCCCTTCGTCGCACGTTAACGAACCCCGATGCGATCCA   165
Abashiri C0        CCCGTGCGCCCCCCACCCCGTGCGGCGTCGGGTGTCGGTCGCGCGCTCCTGCCCGCGTCCGCCCCCTGCGCCGCGCGTTAACGAACCCCGGCGCGATCCG   200
Abashiri SP        -TCGTGCAC----------TCGTGCACTCGTGCCTGCATCCACCCCCTTCGTCGCACGTTAACGAACCCCGATGCGATCCA   165
Iwate-Johoji       -TCGTGCAC----------TCGTGCACTCGTGCCTGCATCCACCCCCTTCGTCGCACGTTAACGAACCCCGATGCGATCCA   165
Okinawa Naha       -TCGTGCAC----------TCGTGCACTCGTGCCTGCATCCACCCCCTTCGTCGCACGTTAACGAACCCCGATGCGATCCA   165
Fukushima Aizu     CCCGTGCGCTCCCACACG--TGCTGCGCTGGGCGTCGGTCGTACGTTTCTACGTGCGTCCGCTCCC-ACGCTGCGCATTAACGAACCCCGGCGCGAATTG   195

Abashiri A0        CGCCAAGGAATTCTTAACGAGA-AGCCCGTTCCTGTATCCCCGGACACGGTGCGCGTGCGGGATGTGTGGTCTTCTTTCATTATCTAT   255
Abashiri B0        CGCCAAGGAATTCTTAACGAGA-AGCCCGTTCCTGTATCCCCGGACACGGTGCGCGTGCGGGATGTGTGGTCTTCTTTCATTATCTAT   255
Abashiri C0        CGCCAAGGAATCCTTAACGAGA-AGCCCGTTCCCGTCGCCCCGGACACGGTGCGCGTGCGGGATGCGTGGCCTTCTTTCATTATCTAT   287
Abashiri SP        CGCCAAGGAATTCTTAACGAGA-AGCCCGTTCCTGTATCCCCGGACACGGTGCGCGTGCGGGATGTGTGGTCTTCTTTCATTATCTAT   255
Iwate-Johoji       CGCCAAGGAATTCTTAACGAGA-AGCCCGTTCCTGTATCCCCGGACACGGTGCGCGTGCGGGATGTGTGGTCTTCTTTCATTATCTAT   255
Okinawa Naha       CGCCAAGGAATTCTTAACGAGA-AGCCCGTTCCTGTATCCCCGGACACGGTGCGCGTGCGGGATGTGTGGTCTTCTTTCATTATCTAT   255
Fukushima Aizu     CGCCAAGGAAATCTTAACGAGAGAGCTCGCTCCCGTCGCCCCGGACACGGTGTGCGTGCGGGATGTGTGGCCTTCTTTCATTATCTAT   283
```

Figure 1 Sequence alignment of ITS1 region in lacquer trees.

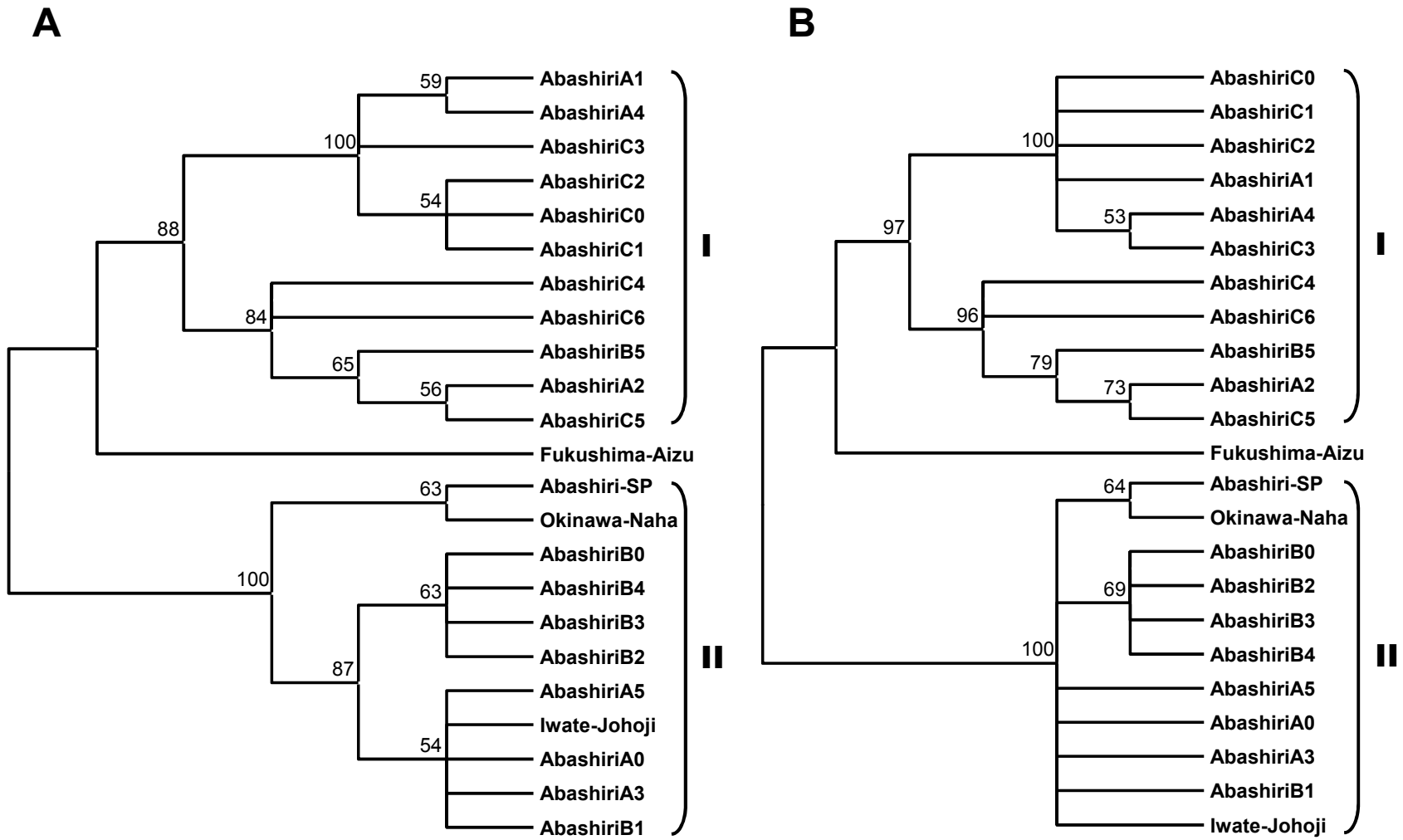

Figure 2. Phylogenetic tree of ITS region in Rhus verniciflua constructed by (A) neighbor-joining and (B) maximum parsimony methods, respectively.
Values showed above branches indicate bootstrap values for 100 replicates supporting the respective cluster. Both trees were similar each other, indicating high reliability.

```
Abashiri C0       CTGGGAAGTCCTCGTGTTGCACCCCTCATTTTTGTGACGATCCGCTTTTTTCCTTTCGTATTCATACCATCCGATTATTTTTTTCTCCGTCTCGCCTCG   99
Iwate-Johoji      CTGGGAAGTCCTCGTGTTGCACCCCTCATTTTTGTGACGATCCGCTTTTTTCCTTTCGTATTCATACCATCCGATTATTTTTTTCTCCGTCTCGCCTCG   99
Fukushima-Aizu    CTGGGAAGTCCTCGTGTTGCACCCCTCTTTTTGTCTCGATCCGCTTTTCTTTTTTTCGTATCCACCCGTTTCGTTGTTTATCGATGTTGTGTCGTGTTT   99

Abashiri C0       TTTCGTTAC-------------------------------------------------------------------------------------------  108
Iwate-Johoji      TTTCGTTAC-------------------------------------------------------------------------------------------  108
Fukushima-Aizu    CAAAGCTTCGAGCCATCACGTGTCGGCGAGCAACGGAAACGGAGAAACCGGAATCGATGCCGAGAAATTCGATTTTTTTCCCATCAGTCTCGTATAAACC  199

Abashiri C0       -------TTTGTTTATCGATGTTGTCATTTTCGGAGCTCCGGGGCATACCGGG-TGAATGTGAGACGGAATCGATGCGGTAAGCGAGAGCGTTAACGACC  200
Iwate-Johoji      -------TTTGTTTATCGATGTTGTCATTTTCGGAGCTCCGGGGCATACCGGG-TGAATGTGAGACGGAATCGATGCGGTAAGCGAGAGCGTTAACGACC  200
Fukushima-Aizu    CGTTTCGTTTGTTTATCGATGTTGTCATTTTCGGAGGTTCGAGTCATAGCGGGGTGAACGAGAGCCGGAATCGGTGTGGTGAGGGCCAG----------  288

Abashiri C0       CAGGAAGTTTGCTTAAATAAATTGATCTTGCAGTGCTTGATGGGTGCGATCATACCAGCACTAAAG  266
Iwate-Johoji      CAGGAAGTTTGCTTAAATAAATTGATCTTGCAGTGCTTGATGGGTGCGATCATACCAGCACTAAAG  266
Fukushima-Aizu    -AGGGGGTGTGCTTAAATAAATTGATTGCGCAGTGACTGATGGGTGCGATCATACCAGCACTAAAG  353
```

Figure 3. Sequence alignment of 5S region in lacquer trees

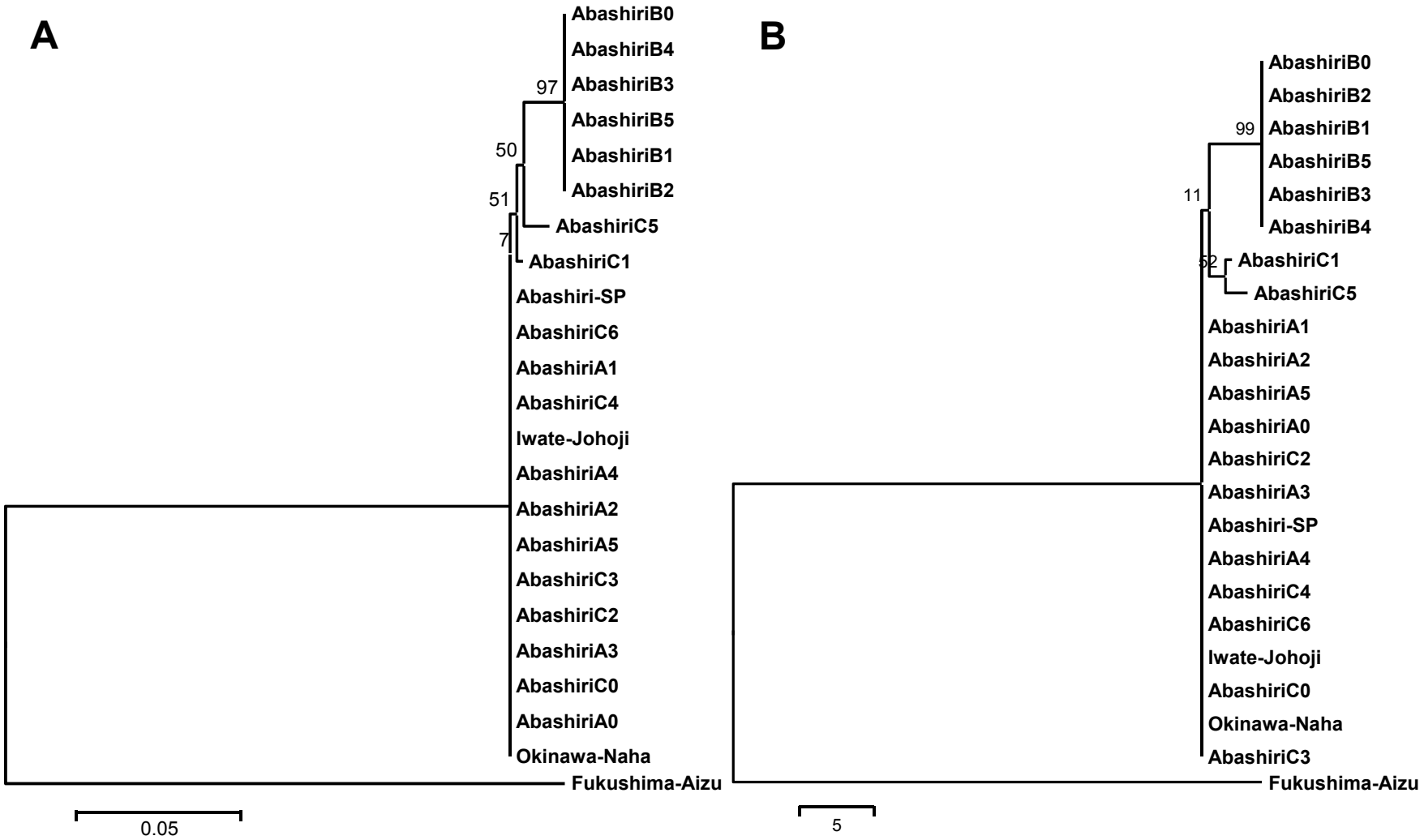

Figure 4. Phylogenetic tree of 5S region in Rhus verniciflua constructed by (A) neighbor-joining and (B) maximum parsimony methods, respectively.
Both trees were similar each other, indicating high reliability.

Chapter 3

Molecular phylogenetic analysis of Japanese lacquer plant (*Rhus verniciflua*) in Tohoku region based on nr DNA and cpDNA sequences

---

Abstract

Urushi lacquer trees have been planted in many places of Tohoku region from edo period. The sap of lacquer tree has been collected and preciously used for important fields like tableware, coating, adhersive agent and weapon. Aizuwakamtu city in Fukushima is one of famous producing area for lacquer ware in Japan from the middle of Meiji period. However, lacquer tree cultivars have decrease for climate change, forest decline and other environmental factors. Now in Japan, 90% above of lacquer sap for wares has been imported from the other Asia countries. At the mean while, the production of lacquer in Asia is getting decrease due to the environmental changes and economic situations. The lacquer that is the only natural plant that product with polymerizability by the enzyme, laccase, would be playing vital role in the next generation. For the protection and conservation of lacquer plants, we collected the lacquer samples from the three locations in

Aizuwakamatu city, Fukushima prefecture, and analysis the five regions of DNA sequence. The DNA sequences of lacquer in Aizu were compared with the sequence in Abashiri, Hokkaido and Johoji-marchi, Iwate. Analysis of five regions (ITS and ETS in nrDNA, and 5S, rbcL and matK in cpDNA) of Aizu lacquer trees revealed sequences in Aizu lacquer tree almost have similar with AbashiriC in ITS region and large divergence with Iwate-Johoji. The divergences with AbashiriC and Iwate-Johoji were 8.4% and 16.2%, respectively in ITS region.

3.1 Introduction

Lacquer tree belongs to the genus *Rhus*, a member of the family *Anacadiaceae* that contains 73 genera worldwide with approximately 600 species, including mango (Mangifera indica) and cashew (Anacardium occidentale)[1-3].

There are three kinds of lacquer trees growing in Asia, *Rhus vernicifera* mainly contains urushiol in China, Japan, and Korea, *R. succedanea* that mainly contains laccol in Vietnam and Taiwan, and Melanorrhoea usitata that the main component is Thitsiol in Burma and Thailand[4].

Oriental lacquer *(urushi)* is composed mainly of usushiols which were polymerized with laccase, i.e., an oxidation enzyme of phenols, in the presence of polysaccharides highly durable coating material

for lacquered wares and cultural assets [5].

In our previous study, we found that the lacquer polysaccharides in Myanmar and Cambodia had large amounts of arabinose and rhamnose residues. The degradation process of the polysaccharides was estimated by the GPC measurements using Aizu lacquer polysaccharides. It was found that that lacquer polysaccharides had originally one fraction having molecular weights in the tree and after collection, the molecular weight decreased gradually with the stored time of the sap [6].

As lacquer trees are sensitive to the environmental changes of the growth, and the place of the sap production is being limited and changes in DNA sequence are occurring.

In previous study, we found lacquer tree planted in the cold environment (Abashi, Hokkaido), have the change in DNA sequences compared with the original transplanted place, Johoji-march, Iwate prefecture [7].

In Japan, an urushi lacquer is precious nature paint and the lacquer tree was planted in all area of Japan for 40-50 years ago. Currently, A urushi lacquer equal or more than 90% of all over Japan is produced in Tohoku region (north-east area of Japan including six prefectures: Akita, Aomori, Fukushima, Iwate, Miyagi and Yamagata) [8].

As a famous productive area of lacquer ware in Japan, study

on Lacquer tree in Aizu-Fikushima has valuable. In this study, we aim to reveal the five regions of DNA sequences and find the divergence between Johoji-march and Abashi area.

3.2 Material and Method

3.2.1 Plant material

Twenty lacquer samples, *Rhus verniciflua,* collected from three different locations in Fukushima-Auzi in 2011 autumn.

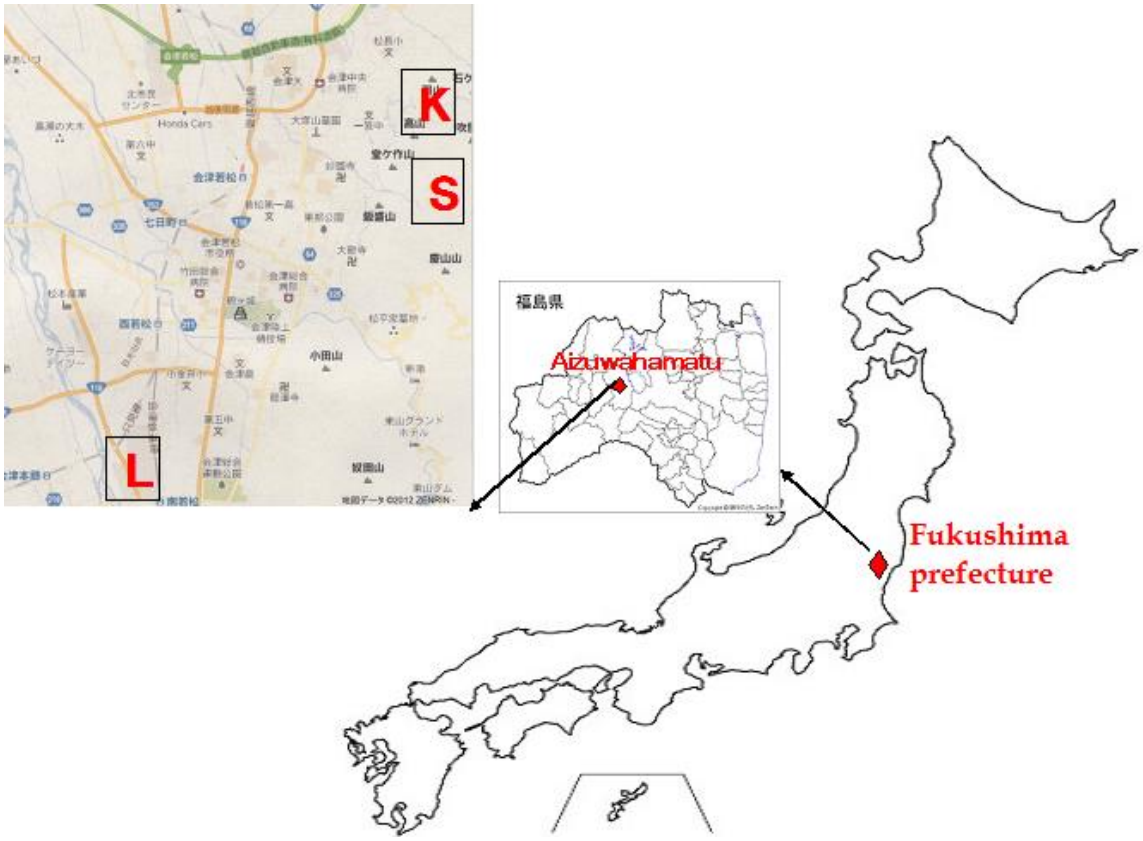

The sampling picture of lacquer plant in Aizuwakamatu, Fukushima prefecture; K: Kin-hori area; S: Syoku-san area; L: sikki-danchi area.

The sampling pictures of lacquer plant in Aizuwakamatsu, Fukushima prefecture. Left upper: Kin-hori area; left lower: Syoku-san area; Right: tapped tree in syoku-san area.

3.2.2 DNA extraction, PCR amplification and sequencing

Total genomic DNA was extracted from fresh leaf material using Dneasy plant extraction kit (Qiagen) according to the manufacture's protocol. Polymerase chain reaction (PCR) amplifications were

performed in a 25μL reaction mixture containing 1.5mmol MgCL2, 0.2mmol each dNTP mix, 0.5μmol each primers (as shown in table 1), 0.05U/μL Taq polymerase, and approximately 30-10ng DNA template. PCR were performed in a peltier thermocycler (PTC-200, MJ RESEARCH) as follows for ITS region: reaction mixtures were heated at 96℃ for 2 min as an initial denaturation step before entering 40 cycles consisting of 30s at 95℃ for denaturation, 30s at 52℃ for annealing and 1 min at 72℃ for elongation. A final extension step of 3 min at 72℃ was performed at the last cycle. For ETS region: [95℃, 10 min ;30 cycles of (94℃,1 min ; 57℃,2 min ; 72℃,2 min) ; 72℃, 16 min]. For 5S region: [95℃, 5 min; 30 cycles of (95℃,20s ; 60℃,30s ; 72℃, 30s); 72℃, 13 min]. For *rbc*L region: [94℃, 2 min ;30 cycles of (94℃, 30s ; 45℃, 30s ; 72℃,1 min); 72℃, 4 min] . For matk region:[97℃,2 min ; 30 cycles of (94℃,1.5min ; 49℃,2 min; 72℃,3 min); 72℃, 15 min]. The amplified PCR products are mainly purified by the Magnetic beads method (described in Surina Bo, 2012). Cycle sequencing reactions for all PCR products were conducted using Big Dye terminator 3.1V cycling sequencing kit with the PCR primers. 0.5μl BigDye terminator ready reaction mix, 1μl of BigDye Terminator V3.1 5X sequencing buffer, 1μl of 32pmol forward or reverse primers, 1μl of purified DNA products and the appropriate amount of sterile water for total volume of 10μl. For the *rbc*L (1400bp) and *mat*K (2000bp)

two long regions, the sequencing primers were used. Respectively, *rbc*L-1.5: 5'-GGA CCG ATG GGC TTA CCA GC-3',*rbc*L-NR2(428bp):5'-TTA CCC ACA ATG GAA GTA AAC ATG-3', *rbc*L-2F2(426bp):5'-GCG CTC TAC GTC TAG AGG ATC-3', *rbc*L-1R(1207bp):5'-GGG TGC CCT AAA GTT CCT CC-3', *rbc*L-3F(635bp)-5'-TGC GTT GGA GAG ACC GTT TC-3' for *rbc*L region and *mat*K-4R:5'-GAK AAG ATT GGK TRC GGA G-3', *mat*K-5F:5'-AAG AGC GAT KRK ATT GAA-3', *mat*K-10R:5'-CGC TGT GAT AAT GAG AAA GA-3', *mat*K-6F: 5'-TCT SCG TAA SCA ATC TTC TC-3' for *mat*K region.The cycle sequencing was performed in a Peltier thermal cycler PTC-200 (MJ Research) with the following setting: initial denaturation at 96℃ for 1min, followed by 25 cycles of 96℃ for 10s, 50℃ for 5s and 60℃ for 4min. Sequencing products were cleaned using sephadex G-100, then resolved on 10μl Hi-Di formamide and were sequenced on the AB 3130 genetic analyzer with a 36 cm capillary column (ABI).

3.2.3 Data analysis

Sequences for each region were aligned with CLUSTAL W program [9]. The genetic pairwise distance for each marker was calculated using MEGA 4.1 version and Kimura two-parameter distance model [10][11].Phylogenetic analysis of ITS was conducted with MEGA 4.0 using maximum parsimony method (MP) and the

neighbor-joining method (NJ) .In the neighbor-joining was calculated based on the kimura 2-parameter model. The percentage of replicate trees in which the associated taxa clustered together in the bootstrap test (100 replicates) is shown above the branches. Parsimony analysis was performed using a Min-mini heuristic with search and random addition sequence (100 replicate).

3.3 Result and discussion

3.3.1 PCR amplification and sequencing of ITS region

PCR reactions for Aizu samples can't be successfully amplified with the PCR reaction buffer (Takara). So we applied the 2X GC buffer I (5mM Mg2+ plus, Takara) to the PCR reactions as following: 0.25μL Taq polymerase, 2μL dNTP mix, 12.5 μL GC buffer, 0.5μL each N-nc18S10 and C26A primers and final volume is adjusted to 25μL by sterile water and successful get PCR bands of ITS region.

But even we applied the GC buffer for PCR reaction; the sequencing can't be read correctly for Auzi S1, 4, 5 and K1~5 plant samples. So we have used the pair primers of N-nc18S10 and ITS4 (5'-TCC TCC GCT TAT TGA TAT GC-3', White et al, 1990) for sequencing and get the good sequencing results.

3.3.2 The divergences of five DNA regions

In ITS region, we found the maximum divergence in ITS1 region

is between Fukushima-Aizu and Iwate-Johoji, 27.8% and ITS2 region give 11.5% and there is no divergence rate in 5.8S region in table 1. That is because of 5.8S region is genetic region and ITS1 and 2 is spacer regions.

Table 1

There are a little divergence rates in ETS, 5S and *rbc*L regions. The divergences of matK region are from 5.9~6.7%, it may be caused by *mat*K region has a little higher evolutionary rate that is faster approximately 2-3 times than *rbc*L region [10].

Table 2. The variations of five DNA regions.

DNA region	ITS1	5.8S	ITS2	ITS	ETS	5S	*rbc*L	*mat*K
Aizu-Aizu	13.9[a]	0	4.4	8.4	1.2	3	1.4	6.7
Aizu-AbashiriC	13.5	0	4.1	8.4	0.9	3	1.1	5.9
Aizu-Johoji	27.8	0	11.4	16.2	0.9	3	1.1	5.9

a %percentage, calculated from Pair distance with kimura-two-parameter.

3.3.3 The Lengths and GC contents of five regions

Table1 is shown the length and GC content for five regions.

In ITS region, we found the length is 729bp for Kin-hori area (Aizu-K), 732bp for Sikki-tanchi area (Aizu-L), and there are two type of length (729 and 732 bp) for Syoku-san area (Aizu-S). GC contents of ITS region for sample are all higher than 60% except for Iwate-Johoji. The lengths of ETS, 5S, *rbc*L and *mat*K regions also

are shown in tab.3.

Table 3

3.3.4 Phylogennetic analysis

The phylogenetic trees of ITS region were constructed by two methods, neighbor joining (NJ) and maximum parsimony (MP).

MP Phylogenetic Tree based on ITS sequences is out of 117 most parsimonious trees (length = 114) is shown. The consistency index is (0.710526), the retention index is (0.925676), and the composite index is 0.836356 (0.657717) for all sites and parsimony-informative sites (in parentheses). The percentage of replicate trees in which the associated taxa clustered together in the bootstrap test (100 replicates) is shown above the branches. The MP tree was obtained using the Close-Neighbor-Interchange algorithm with search level 3 [2, 3] in which the initial trees were obtained with the random addition of sequences (10 replicates). There were a total of 692 positions in the final dataset, out of which 24 were parsimony informative.

The neighbor-joining method was calculated based on the kimura 2-parameter model. The percentage of replicate trees in which the associated taxa clustered together in the bootstrap test (100 replicates) is shown above the branches.

Figure 1

We also constructed the trees of ITS1 and ITS2 regions using NJ method that are shown in Fig.2.

Conclusion

We collected Urushi leap samples from the three difference places from Auziwakamatu city in Fukushima province. In ITS region analysis, there have two kinds of ITS sequence detected in Auzi samples and from the phylogenetic results of lacquer tree cultivars revealed an intra-species genetic diversity in the phylogenetic tree of the ITS region, there also maybe have polymorphism in Aizu lacquer tree cultivars. We found 27.8% divergence between Aizu cultivars and Abashiri C, it can't easily explain by its rapid evolutionary rate of ITS region. So we would like to explain it from the rn DNA structure in which ITS region exists.

Acknowledgement

This research was partially supported by a Grant-in-Aid for Scientific Research 2009-2011 (No. 21550199) from the Japan Society for the Promotion of Science (JSPS) and the SVBL research program of Kitami Institute of Technology 2009-2011.

Reference

[1] Brizicky GK. (1963) Toxinomic and nomenclatural notes on the genus Rhus (Anacardiaceae), Journal of the Arnold arboretum, 44, 60-80.

[2] Croquist A. (1981), an integrated system of classification of flowering plants, New York: Columbia University press.

[3] Pell SK (2004) Molecular systematic of the cashew family (Anacardiaceae), Baton Rouge: Louisiana State University.

[4] J. Kumanotani (1999), Urushi (oriental lacquer)-a natural aesthetic durable and future-promising coating Prog. Org. Coat. , 26 163.

[5] Du, Y., Oshima, R., Iwatsuki, H., and Kumanotani, J. (1984), 'High resolution gas-liquid chromatographic analysis of urushiol of the lacquer tree, Rhus vernicifera, without derivatization', Journal of Chromatography A 295 179-186

[6] Lu R. and Yoshida T. (2003), structure and molecular weight of Asia lacquer polysaccharides, 54, 419-424.

[7] Surina Bo., Yoshida T. (2012)

[8] Kobayashi N. (2002), A study of planted urushi lacquer tree of Tohoku region and ingredient analysis of urushi lacquer, annual review of Tohoku university of art and design No. 9, 30-37. (in Japanese)

[9] Kimura M (1980) A simple method for estimating evolutionary

rate of base substitution through comparative studies of nucleotide sequences. J Mol Evol 16: 111-120

[10] Tamura K, Dudley J, Nei M, Kumar S (2007) MEGA4: Molecular Evolutionary Genetics Analysis (MEGA) software version 4.0. Mol Biol Evol 24: 1596-1599.

[11] Kimura M (1980) A simple method for estimating evolutionary rate of base substitution through comparative studies of nucleotide sequences. J Mol Evol 16: 111-120.

Table 1. Nuclear divergence values of ITS1 (lower) and IITS2 (upper) regions in lacquer trees calculated by using Kimura-2 parameter model.

	Species	1	2	3	4	5	6	7	8	9	10	11	12	13	14	15	16	17	18	19	20	21	22	23
1	Aizu-L-1		0.004	0.004	0.004	0.004	**0.044a**	0.004	0.004	0.033	0.029	0.015	0.022	0.004	0.004	0.004	0.029	0.029	0.029	0.029	0.029	**0.114b**	0.026	0.004
2	Aizu-L-2	0.004		0.000	0.000	0.000	0.041	0.000	0.000	0.029	0.026	0.015	0.022	0.000	0.000	0.000	0.026	0.026	0.026	0.026	0.026	0.109	0.022	0.000
3	Aizu-L-3	0.000	0.004		0.000	0.000	0.041	0.000	0.000	0.029	0.026	0.015	0.022	0.000	0.000	0.000	0.026	0.026	0.026	0.026	0.026	0.109	0.022	0.000
4	Aizu-L-4	0.000	0.004	0.000		0.000	0.041	0.000	0.000	0.029	0.026	0.015	0.022	0.000	0.000	0.000	0.026	0.026	0.026	0.026	0.026	0.109	0.022	0.000
5	Aizu-L-5	0.004	0.008	0.004	0.004		0.041	0.000	0.000	0.029	0.026	0.015	0.022	0.000	0.000	0.000	0.026	0.026	0.026	0.026	0.026	0.109	0.022	0.000
6	Aizu-S-1	0.037	0.041	0.037	0.037	0.041		0.041	0.041	0.018	0.022	0.041	0.033	0.041	0.041	0.041	0.014	0.014	0.014	0.014	0.014	0.105	0.018	**0.041c**
7	Aizu-S-2	0.000	0.004	0.000	0.000	0.004	0.037		0.000	0.029	0.026	0.015	0.022	0.000	0.000	0.000	0.026	0.026	0.026	0.026	0.026	0.109	0.022	0.000
8	Aizu-S-3	0.000	0.004	0.000	0.000	0.004	0.037	0.000		0.029	0.026	0.015	0.022	0.000	0.000	0.000	0.026	0.026	0.026	0.026	0.026	0.109	0.022	0.000
9	Aizu-S-4	0.041	0.045	0.041	0.041	0.045	0.012	0.041	0.041		0.011	0.029	0.022	0.029	0.029	0.029	0.004	0.004	0.004	0.004	0.004	0.101	0.007	0.029
10	Aizu-S-5	0.033	0.037	0.033	0.033	0.037	0.012	0.033	0.033	0.016		0.026	0.018	0.026	0.026	0.026	0.007	0.007	0.007	0.007	0.007	0.096	0.004	0.026
11	Aizu-S-6	0.106	0.111	0.106	0.106	0.111	0.134	0.106	0.106	0.139	0.125		0.015	0.015	0.015	0.015	0.026	0.026	0.026	0.026	0.026	0.109	0.022	0.015
12	Aizu-S-7	0.125	0.130	0.125	0.125	0.130	0.102	0.125	0.125	0.116	0.106	0.102		0.022	0.022	0.022	0.018	0.018	0.018	0.018	0.018	0.100	0.014	0.022
13	Aizu-S-8	0.000	0.004	0.000	0.000	0.004	0.037	0.000	0.000	0.041	0.033	0.106	0.125		0.000	0.000	0.026	0.026	0.026	0.026	0.026	0.109	0.022	0.000
14	Aizu-S-9	0.000	0.004	0.000	0.000	0.004	0.037	0.000	0.000	0.041	0.033	0.106	0.125	0.000		0.000	0.026	0.026	0.026	0.026	0.026	0.109	0.022	0.000
15	Aizu-S-10	0.000	0.004	0.000	0.000	0.004	0.037	0.000	0.000	0.041	0.033	0.106	0.125	0.000	0.000		0.026	0.026	0.026	0.026	0.026	0.109	0.022	0.000
16	Aizu-K-1	0.041	0.045	0.041	0.041	0.045	0.012	0.041	0.041	0.016	0.016	**0.139a**	0.116	0.041	0.041	0.041		0.000	0.000	0.000	0.000	0.097	0.004	0.026
17	Aizu-k-2	0.033	0.037	0.033	0.033	0.037	0.004	0.033	0.033	0.008	0.008	0.130	0.106	0.033	0.033	0.033	0.008		0.000	0.000	0.000	0.097	0.004	0.026
18	Aizu-k-3	0.033	0.037	0.033	0.033	0.037	0.004	0.033	0.033	0.008	0.008	0.130	0.106	0.033	0.033	0.033	0.008	0.000		0.000	0.000	0.097	0.004	0.026
19	Aizu-k-4	0.033	0.037	0.033	0.033	0.037	0.004	0.033	0.033	0.008	0.008	0.130	0.106	0.033	0.033	0.033	0.008	0.000	0.000		0.000	0.097	0.004	0.026
20	Aizu-k-5	0.033	0.037	0.033	0.033	0.037	0.004	0.033	0.033	0.008	0.008	0.130	0.106	0.033	0.033	0.033	0.008	0.000	0.000	0.000		0.097	0.004	0.026
21	Iwate-Johoji	0.167	0.172	0.167	0.167	0.172	0.151	0.167	0.167	0.155	0.151	**0.278b**	0.245	0.167	0.167	0.167	0.161	0.151	0.151	0.151	0.151		0.092	0.109
22	AbashiriC5	0.041	0.045	0.041	0.041	0.045	0.020	0.041	0.041	0.024	0.008	0.134	0.116	0.041	0.041	0.041	0.024	0.016	0.016	0.016	0.016	0.142		0.022
23	AbashiriC0	0.008	0.012	0.008	0.008	0.012	0.045	0.008	0.008	0.049	0.041	0.116	**0.135c**	0.008	0.008	0.008	0.049	0.041	0.041	0.041	0.041	0.157	0.033	

Bold characters indicated the maxiumn divergences, a: Aizu-Aizu, b: Aizu-Iwate-johoji, c: Aizu-Abashiri-C

Table 3. Length and GC content of five DNA regions

Lacquer (*Rhus verniciflua*)	DNA region															
	Length (bp)								GC content (%)							
	ITS	(ITS1	5.8S	ITS2)	ETS	5S	*rbc*L	*mat*K	ITS	(ITS1	5.8S	ITS2)	ETS	5S	*rbc*L	*mat*K
Auzi S-1	729	286	161	282	341	266	1375	2160	62	67	54	62	62	46	44	34
Aizu S-2	732	287	161	284	341	266	1375	2160	63	68	54	63	62	46	44	34
Aizu S-3	732	287	161	284	341	266	1375	2160	63	68	54	63	62	46	44	34
Aizu S-4	729	286	161	282	341	266	1375	2160	62	66	54	62	62	46	44	34
Aizu S-5	729	286	161	282	341	266	1375	2160	62	66	54	62	62	46	44	34
Aizu S-6	731	287	161	283	343	266	1375	2160	63	69	54	62	62	46	44	34
Aizu S-7	732	287	161	284	343	266	1375	2160	63	69	54	62	62	48	44	34
Aizu S-8	732	287	161	284	343	266	1375	2160	63	68	54	63	62	48	44	34
Aizu S-9	732	287	161	284	342	266	1375	2160	63	68	54	63	62	48	44	34
Aizu S-10	732	287	161	284	342	266	1375	2160	63	68	54	63	62	48	44	34
Aizu L-1	732	287	161	284	341	266	1375	2160	63	68	54	63	62	48	44	34
Aizu L-2	732	287	161	284	341	266	1375	2160	63	68	54	63	62	48	44	34
Aizu L-3	732	287	161	284	341	266	1375	2160	63	68	54	63	62	46	44	34
Aizu L-4	732	287	161	284	341	266	1375	2160	63	68	54	63	62	46	44	34
Aizu L-5	732	287	161	284	341	266	1375	2160	63	68	54	63	62	46	44	34
Aizu K-1	730	286	161	282	341	266	1375	2160	62	66	54	62	61	46	44	34
Aizu K-2	729	286	161	282	341	266	1375	2160	62	66	54	62	61	48	44	34
Aizu K-3	729	286	161	282	341	266	1375	2160	62	66	54	62	62	48	44	34
Aizu K-4	729	286	161	282	341	266	1375	2160	62	66	54	62	62	48	44	34
Aizu K-5	729	286	161	282	341	266	1375	2160	62	66	54	62	61	46	44	34
Iwate-Johoji	695	255	161	279	341	266	1375	2160	55	55	54	55	62	46	44	34
Abashiri-C0	731	287	161	283	341	266	1375	2160	63	68	54	63	62	46	44	34
Abashiri-C5	728	286	161	281	341	266	1375	2160	62	66	54	61	62	46	44	34

Aizu-S: Syoku-san Area, Aizu-L: Sikki-danchi Area, Aizu-K: Kin-hori Area.

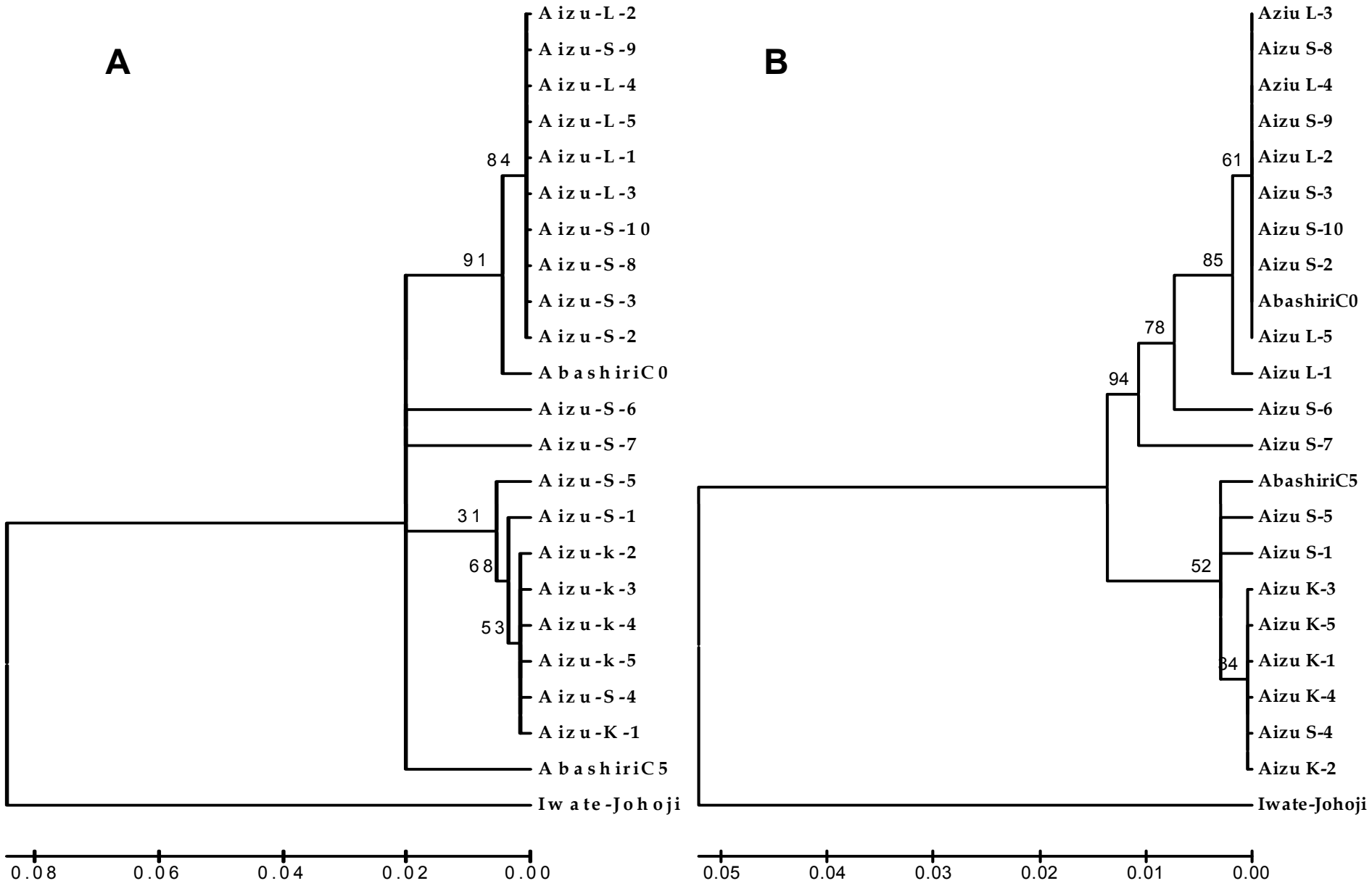

Fig.1 Phylogenetic trees of ITS1(A) and ITS2 (B) regions in Rhus verniciflua constructed by neighbor-joining method. Values showed above branches indicate bootstrap values for 100 replicates supporting the respective cluster. Both trees were similar each other, indicating high reliability.

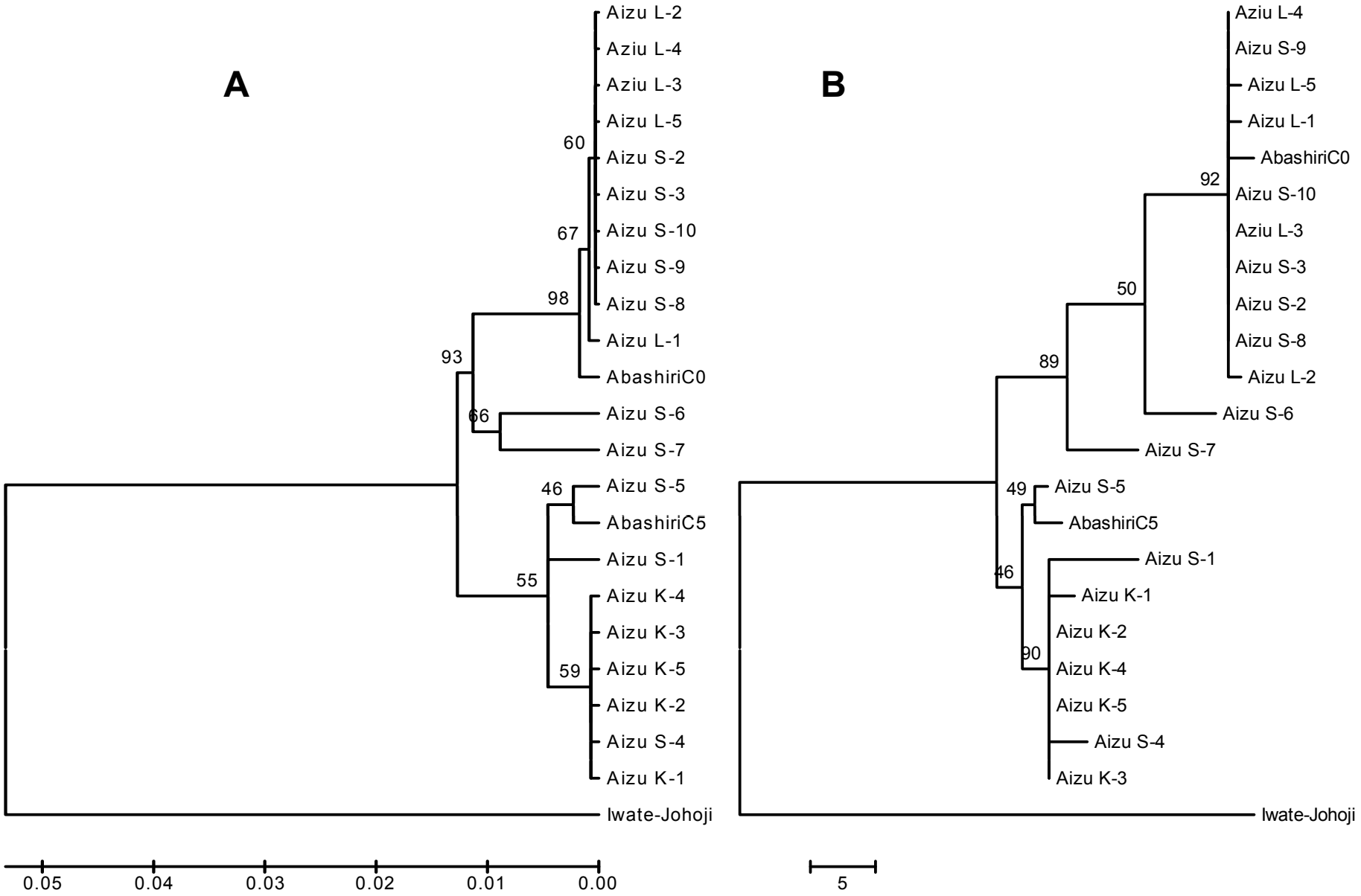

Figure 2. Phylogenetic tree of ITS region in Rhus verniciflua constructed by (A) neighbor-joining and (B)maximum parsimony methods, respectively. Values showed above branches indicate bootstrap values for 100 replicates supporting the respective cluster. Both trees were similar each other, indicating high reliability

Why such large divergence exists in ITS region?

Fig.1 The gene segment of eukaryotic rDNA contains 18S, 5.8S, and 28S tracts and forms a tandem repetitive cluster; the 5S rDNA is coded separately. **NTS**, nontranscribed spacer,**ETS**, external transcribed spacer, **ITS**, internal transcribed spacers 1 and 2, numbered from 5' end.

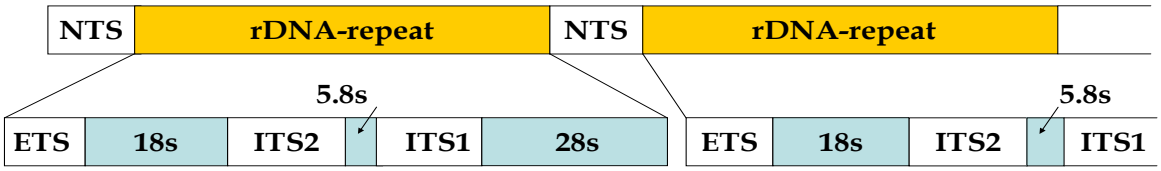

rDNA is consisted by a tandem repeat of a unit segment like above figure 1. In this rDNA tandem repeat process, we can predict a hypothesis that different sequences maybe repeated in ITS region, it is mean there maybe exist hetero-sequence in ITS region.

Fig.1　the PCR amplification of ITS region

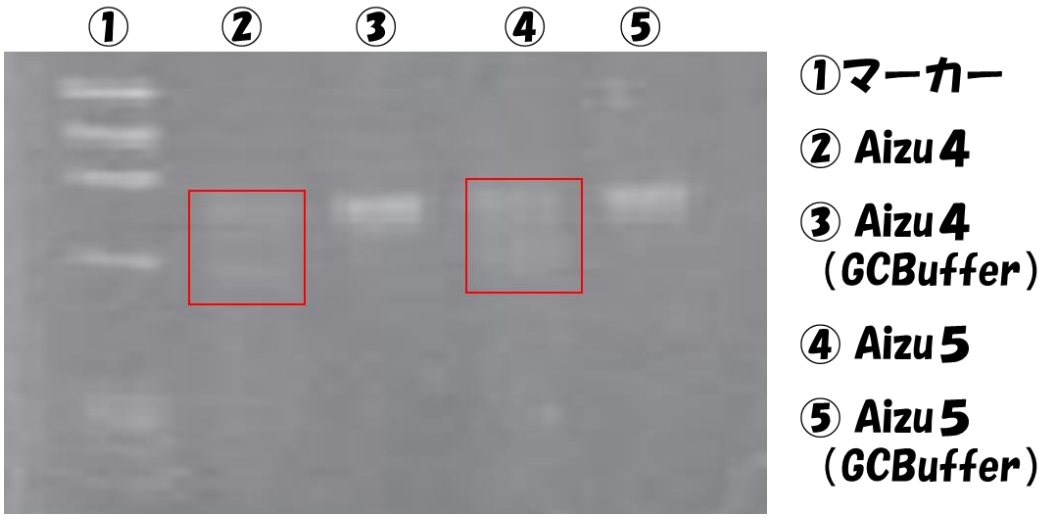

② and ④　were used　normal PCR buffer and ③ and ⑤　were

GC buffer for PCR amplification of ITS region in fig. 1. we found two bands (② of Aizu 4 and ④ of Aziu 5) were appeared in figure 2. It is mean there maybe exist hetero-sequence in ITS region. To verify this hypothesis, nested PCR amplification is required for ITS region.

The nested PCR amplification for ITS region

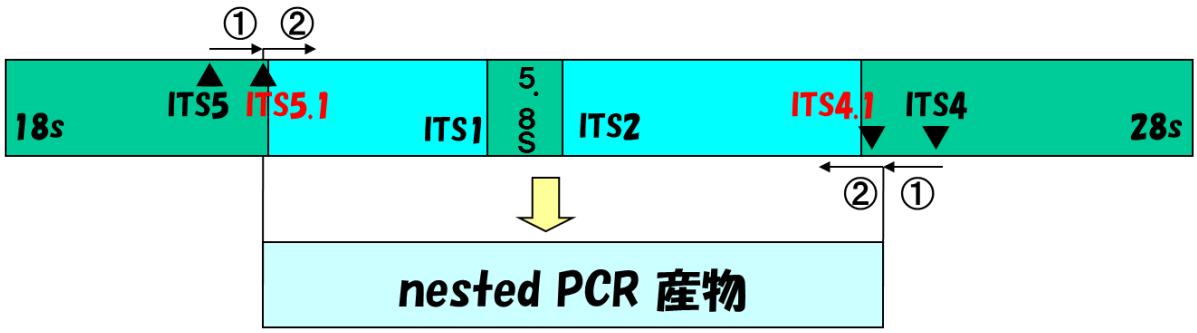

Fig.2 the 1st PCR amplification (in left) and nested PCR amplification (in right) of ITS region

① 1st PCR

Primes (ITS 5, ITS 4)

② nested PCR

Primes (ITS 5.1, ITS 4.1)

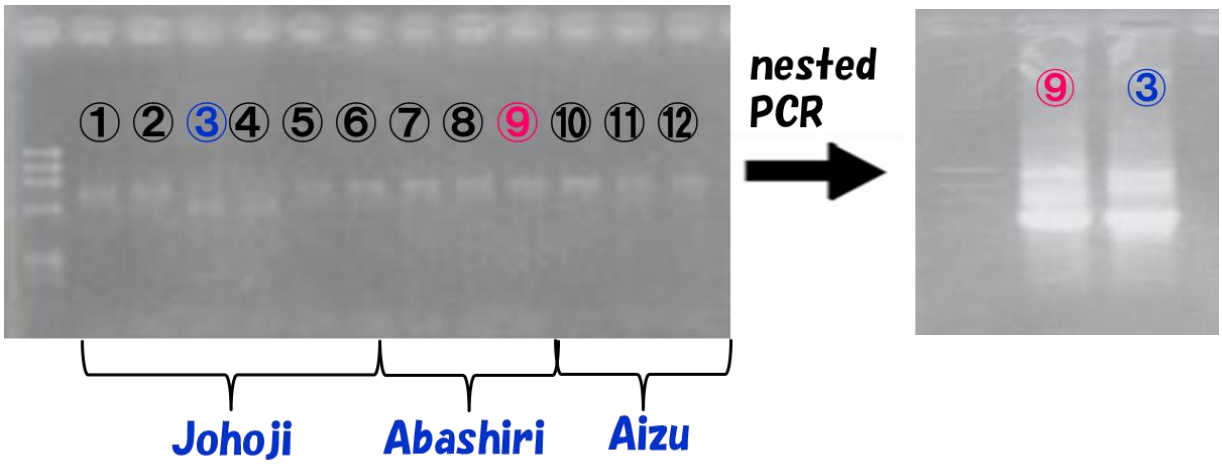

There are multi-bands appeared in nested PCR result in fig.2. It

means hetero-sequences are existed in ITS region. The next step is to elucidate the sequences of these multi-bands which should be separated to measure. The more highly homology of ITS phylogenetic trees are gotten using these sequences.

Chapter 4

Structural analysis and functional elucidation of laccase glycoprotein

---

ABSTRACT

Lacquer laccase is copper containing glycoprotein consisted of 533 amino acids and about 45% is carbohydrates. For the analysis of carbohydrate structure and glycosylation sites of Laccase glycoprotein, 1mg glycoprotein was digested with enzymes by trypsin and PNGase A and the digestion was analyzed by LC/MS/MS and MALDI-TOF/MS.

Laccase glycoprotein has fifteen potential sites of *N*-linked glycosylation. In this study, we utilized the LC-MS/MS to separate and analysis the glycopeptides and peptides digested by trypsin. From MS/MS, we found that twelve of the potential fifteen Asn-X-T/S were determined to be sites of *N*-linked glycosylation. Asn 5, 14, 28, 124, 180, 194, 233, 274, 284, 347, 381, and 398 were found to bind carbohydrates in this study.

Using carbohydrate marker ions such as HexNAc+ (204. 1) and Hex-HexNAc+ (366.2), we sorted out ms/ms product ion spectra of glycopeptides from the number of ms/ms spectra of peptides, and determined the amino sequences of glycopeptides, glycosylation

sites, and monosaccaride composition in single analysis.

4.1 Introduction

Laccase (*P*-diphenol: oxygen oxidoreductase, EC 1.10.3.2), a copper-containing oxidase was discovered as early as 1883 by Yoshida and was called diastatic matter [1]. A few years later, Bertrand analyzed the catalysis of diastatic matter and named it laccase [2]. Since then, laccase has been found in many plants and microorganisms and was found to play a variety of roles such as wound-healing, lignin biosysthesis and degradation, pigment formation, etc. [3].

The oriental lacquer is a natural polymer that has been valued for millennia for great durability and beauty. The lacquer is formed from a tree sap, obtained most commonly in China and Japan from the Rhus verniciflua stokes [4]. Raw lacquer is composed of 65-70% urushiol, 20-25% water, 10% gummy (polysaccharide) material, approximately 1% enzyme laccase and stellacyanin plus insoluble nitrogenous substances and trace metals e.g copper [5]. Oriental lacquer is a naturally occurring phenolic coating material and undergoes enzyme-catalyzed polymerization to give highly durable coating. Enzymic and aerobic oxidation of urushiol takes place in the lacquer making process. In the laccase-catalyzed polymerization Eny-Cu^{++} oxidizies urushiol to give semiquinone radicial and

Eny-Cu^{+}. The formed radicial undergoes C-C coupling reaction to give diphenyl and dibenzofuran dimmers of urushiol. And other hand, urushiol quinine formed through the disproportion reaction of radicial undergoes the H- abstraction from the triene side chain of urushiol and couples with the formed heptatrien cation to give ring-side bound dimer via 2nd order reaction. The reduced Eny-Cu^{+} return the activity by aero-oxidation reaction. Urushiol repeated this kind of enzymatic oxidation reaction called polymerization of Urushiol [6] [7].

The laccase from the lacquer tree has been widely studied enzymatically, spectroscopically and kinetically as prototype enzyme of multicopper oxidases such as fungal laccase, ascorbate oxidase, ceruloplasmin, Fet3, and bilirubin oxidase [8]. In 2002, the primary structure of laccase from Japanese lacquer tree was first published by kazutomo et.al. And they found the laccase consists of 533 amino acids with a molecular mass of 58981 Da excluding the four intrinsic Cu ions. The mature lacquer laccase is a glycoprotein, 45% of the molecular mass being carbonhydrate. They also indicated that laccase has fifteen potential sugar-binding motifs with the general formula Asn-X-Thr (Asn 5, 14, 28, 124, 180, 194, 233, 274, 284, 347, 364, 381, 398, 454, and 519) [9].

But the secondary structure of laccase isn't still cleared. In this study, we aim to the designing of HPLC and MS-based approach for

detailed structural investigation of lacquer laccase glycopreotein: detailed *N*-glycan structural analysis and their attachment sites with the laccase glycoprotein.

4.2 Material and methods

DTT:Dithiothreitol (sigma)
IAA: Iodoacetamide (Sigma)
Trypsin: from porcine pancreas (13,000-20,000 BAEE units/mg protein) (sigma)
PNGase A: N-Glycosidase A from almond (Roche)
PNGase F: peptide-N-Glycosidase F,recombinant (Roche)
2-PA: aminopyridine (Wako)
Dimethyamine-Borane (Wako)

4.2.1 Purification of laccase glycoprotein

The isolation and purification procedure of laccase glycoprotein obtained from acetone powder of lacquer tree Rhus verniciflua were described in Bengt 1970[10]. In briefly, the acetone powder (40g) was suspended 400ml water, and dialyzed overnight then filtered by glass ultra filter. The filtrate was turbid and has a greenish color and then concentrated to 100ml. Potassian phosphate buffers (pH 6.0) were used in all steps and cation-exchange chromatography method was used with the column of CM-Sephadex C-50 equilibrated with 0.01M buffer in purification procedure. In this step, the large amounts of yellow and turbid fractions were eluted and mainly components were urushi polyssacharides. When

increased the buffer concentration to 0.15M, the blue bond, which was found to be laccase appeared, then increased to 0.2M, the blue bond, laccase started to be eluted. The main fraction of laccase was further purified by the Anion-exchange chromatography method with a column of DECE-Sephadex A-50 equilibrated with 0.01M buffer. The eluted blue solution was laccase and freeze-dried in blue.

To remove the metal Cu, 100mg dried blue laccase was dissolved in 5ml water and add 12.5ml 20% trichloroacetic acid to be stirred 30min and dialyzed overnight, then freeze-dried to get white powder (87.2mg). Its purity and molecular mass were measured by GPC (Gel permeation chromatography) and SDS-PAGE (sodium dodecyl sulfate -polyaclylamide gel electrophoresis).

4.2.2 Digestion of the glycoprotein with trypsin

1mg purified laccase glycoprotein was resuspended in 50mM NH_4HCO_3 and reduced with 10mM DTT for 30min at 60℃, carbonamidomethylated with 20mM of IAA in the dark for 1h and then digested with 400unit of trypsin (Sigma) in the 50mM NH_4HCO_3 overnight at 37℃. Digested (glyco)-peptides were purified and desalted by the protea Tip ZIC-HILIC sample prep kit (10-200ul) according the protocol.

4.2.3 Release and purification of *N*-glycan

1mg purified laccase glycoprotein was resuspended in 50mM NH_4HCO_3 and reduced with 10mM DTT for 30min at 60℃, carbonamidomethylated with 20mM of IAA in the dark for 1h and then digested with 400unit of trypsin (Sigma) in the 50mM NH_4HCO_3 overnight at 37℃. The digestion with trypsin was dried down in Speed-Vac and resulting dried glycopeptides/peptides were resuspended in 60ul 20mM citrate/phosphate buffer at PH 5.0 and boiled at 95℃ to denature activity of trypsin. After cooled, the residual glycopeptides/peptides mixture was digested with 5mU PNGase A overnight at 37℃ for *N*-deglycoslation and then boiled at 95℃ for denaturation of the activities of PNGase A. After the enzymatic deglycosylation process, the N-glycan was captured and purified and then enriched with BlotGlyco beads (BlotGlyco kit, Sumitomo bakelife) by glycoblotting method [11]. Briefly, 50ul beads solution were loaded on the reaction chip and centrifuge, then 20uL digestion sample by PNGase A and 180ul 2% acetic acid/ acetonitrile solutions loaded on the reaction chip with beads was heated at 80℃ for 1h. After the bead dried by heating, washed the bead with the solvents to remove peptides.

4.2.4 Fluorophore Labeling of N-glycan

N-glycans were fluorescently labeled with 2-PA or 2-AB by

reductive amination method [12]. For 2-AB labeling, *N*-Glycans were dissolved in 50 μ L of 30%acetic acid/ DMSO containing 2-aminobenamide (2-AB, 350m M) and sodium cyanoborohydride (NaCNBH3 , 1 M, harmful) and incubated at 60℃for 2 h according to Bigge et al[13].

For PA labeling, N-glycans were dissolved in 30 μ L acetic acid containing 2-aminopyridine (29.4M) and incubated at 80℃ for 1h, Then adding 110ul acetic acid/water (8:5) solution containing dimethylaminoborane (26.1M) and incubate at 80℃ for 35min according to Kondo A. et al [14].

In order to eliminate the excess of fluorescent reagents, the mixture (sample: acetonitrile=5:95) was applied to solid extraction column (BlotGlyco kit, Sumitomo Bakelife) and wash with acetonitrile and then 95%acetonitrile/water three times respectively. Finally, N-glycans were eluted by 50ul milliQ water and stroed at -20℃ for analysis.

4.2.5 Normal-phase HPLC analysis of PA-labeled N-glycans

Normal phase HPLC (NP-HPLC) of the PA-labeled portion was performed using a TSK-Gel Amide-80 5 μ m 4.6*250 mm column (Tosoh Biosep, Japan) on a separation module (Merck-Hitachi, Japan) equipped with a fluorescence detector (RF-10A_{XL}, Shimadzu). Solvent A was formic acid 50 mM adjusted to pH 4.4 with ammonia

solution. Solvent B was acetonitrile. Labeled *N*-glycans were separated by a linear gradient of 20 up to 58% A, over 158 min at a flow rate of 0.4 mL/min. The fluorescence detection was carried out using an excitation wavelength of 320 nm and an emission wavelength of 400 nm and column temperature at 30℃[15]. For analysis, injection volume is 15 μ L.

4.2.6 LC/MS/MS analysis of tryptic digestion

The An AB SCIEX API 4000 Q TRAP LC/MS/MS system with Turbo spray source with electrospray Ionization (ESI) probe in positive polarity was used.

Gas and source parameters for Operating condition of the mass spectrometer were Curtain gas (CUR):20; collision gas (CAD): high; Ion spray voltage (IV): -4500; Temperature: 350; gas source 1(GS1): 50; gas source 2 (GS2): 80; Interface heater (IHE): on; Declustering Potential (DP): 40; Collision energy (CE): 5. EMS,EPI scan rate: 4000Da/s; ER scan rate: 250Da/s.

The (glyco)-peptides of tryptic digestion were subjected to the analysis by LC-ESI-MS/MS using LC system with C-18 reversed-phase column (ODS-80Ts, 5 μ m 4.6*150mm) and eluted with gradient of 0-60% acetonitrile: water (90:10) with 0.1%TFA (0-120min), washed and equilibrated with acetonitrile: water

(10:90) with 0.1% TFA (120-135 min) at the constant flow of 0.2ml/min (column oven at 30℃). Sample injection volume is 5 μ l.

4.2.7 MALDI-TOF MS analysis

The laccase glycoprotein digested by PNGase A enzyme is refined and reducing terminal labeled by Blotglyco glycan purification and labeling kit according to manual to get good sensitive N-glycans for MALDI-TOF MS messurement.

Labeled N-glycans were analyzed by DHB matrix 10mg/ml TA. The DHB matrix was prepared by 2, 5-dihydroxybenzoic acid in ACN/ 0.1M TFA (1:2 v/v). 1ul of the analyte and 3ul of the matrix were mixed and immediately spotted to the target plate (MTP 384 target ground steel TF) according to the "dried droplet" method.

Mass spectra were acquired using an Autoflex MALDI-TOF MS equipped with a nitrogen laser in positive ion mode and operated in reflector mode. An M/Z range of 500-3500 was measured. The instrument was calibrated using polyethylene glycol (PEG) 1000, 2000 and 3500. Laser power was adjusted to achieve a strong signal-to-noise ratio without oversaturation of the detector. Peaks were automated manually using flex analysis software.

4.3. Results and discussion

4.3.1 Purification of lacquer laccase glycoprotein

The lacquer laccase from Rhus verniciflua was sequence vertified to be in agreement with Genbank accession number BAB63411.2 shown in Figure 1.

Figure2 (A) shows the aqueous-phase GPC spectrum of purified laccase glycoprotein which the molecular weight was measured by gel permeation chromatography (GPC) and give $\overline{M}n=4.6 \times 10^4$ ($\overline{M}w/\overline{M}n = 1.87$). Figure2 (B) shows the SDS-PAGE, the first line is standard marker, and second line is purified laccase glycoprotein which appeared clearly one bond, and proposed molecular mass is around 100KDa.

The theoretical molecular weight of laccase is approximately 59.0kDa, while the observed Mw of purified laccase glycoprotein is 90~100kDa in SDS-PAGE gel and GPC analysis (figure 2), which suggests that the glycoform mass is approximately 31~41kDa.

4.3.2 LC/MS/MS analysis of tryptic analysis

The MASCOT reports of LC/MS/MS data of the tryptic digest of the glycoconjugates demonstrated the identification of laccase from the Toxicodendron verniciflum species. The laccase precursor (gi|23503483) was identified with the following sequence coverage: 15% (8 peptides identified). And 12 peptide residues were found in manual in shown in tab 3. The peptide sequence found coverage is 57.2% (N-glycan linked amino acid residues included)

The laccase glycoprotein contains fifteen possible glycosylation

sites: Asn5, Asn14, Asn28, Asn124, Asn180, Asn194, Asn233, Asn274, Asn284, Asn347, Asn364, Asn381, Asn398, Asn454, and Asn519 as shown in figure 1.

In this study Asn5, Asn14, Asn28, Asn124, Asn180, Asn194, Asn233, Asn274, Asn284, Asn347, Asn381, and Asn398 of lacquer laccase were found to bind carbohydrates as shown in red (figure 1) .

The MS/MS cleavage occurs preferentially between the two GlcNAc residues of the core chitobiose, resulting in a peptide fragment ion retaining one GlcNAc residue on the asparagines residue with high intensity [22].

N-acetylglucosamine with m/z 204.1 was used here as the carbohydrate marker ion since it can be easily generated from the MS^2 spectrum of N-linked glycans. As shown in the extracted ion chromatogram (XIC) of m/z 204.1 in fig.3 twenty one peaks were identified as glycopeptides as shown in figure 3.

We analyzed this peaks by manual and found they were derived from twelve different glycopeptides of laccase glycoprotein in table 1.An example is shown in figure 4, where the peak with elution time of 12.93min was chosen for detailed analysis. This fraction was dominated by peptide containing Asn284. Its precursor ion is the doubly charged ion at m/z 1381.2. The peak with elution time of 13.67 min is also derived from the same glycopeptides containing Asn284 which precursor ion is the doubly charged ion m/z 1126.1.

The most intense ion at m/z 568.4 is assigned to a peptide N*GSYK (284-288) (550.4 Da+ H_2O). Many Y series product ions generated by the cleavages of glycosidic linkages can be observed in this product ion spectrum. Such as, m/z 771.4 is peptide N*GSYK linked with one GlcNAc, m/z 975.5 with two GlcNAc, and m/z 1461.5 with $(GlcNAc)_2(Man)_3$. The m/z 917.5 is peptide N*GSYK linked with $(GlcNAc)_1(Fuc)_1$, and it indicate this Fucose is linked with core-GlcNAc residue. The m/z 1269.4 is peptide N*GSYK is linked with GlcNAc-GlcNAc-Man-Xyl. The molecular weight of the carbohydrate moiety can be calculated as 1700.2 Da and 2210.0 Da from by subtracting the theoretical mass of the peptide (568.4 Da) from the calculated glycopeptides mass 2250.4Da and 2760.4 Da. Consequently, the monosaccharide compositions can be estimated as $(HexNAc)_3(Hex)_4(dHex)_2(Pent)_1$ for 1700.2 Da and $(HexNAc)_4(Hex)_5(dHex)_3(Pent)_1$ for 2210.0 Da in the GlycoSuite database search as shown in table 1. In the product ion spectrum (figure 4), B ion corresponding to the $Hex_1HexNAc_1$, dHex1Hex1HexNAc1 and $Hex_2HexNAc_1$ were detected at m/z 366.2, 512.3 and 528.3, respectively.

Through the mass query search in GlycoSuite DB, we predict the glycan structures and found there have existed seven kinds of oligosaccharide structure (type A-G) in lacquer laccase glycoprotein in shown table 2. We found *N*-glycans linked with Asn14, Asn180,

Asn194, Asn233, Asn274, Asn284, Asn347, Asn381, and Asn398 have the similar calculated *N*-glycan mass 2209.4~2212.4 Da and 1697.9~ 1700.2 Da in tab.1. And these glycosylation sites are linked with the structures of E type Fuc(α1-6)[Gal(β1-4)]GlcNAc(β 1-2)Man(α1-3)[Man(α1-6)][Xyl(β1-2)]Man(β1-4)GlcNAc(β1-4)[Fuc(α 1-3)]GlcNAc with monoisotopic mass 1699.6 Da (entry No.1029-1021 in GlycoSuite DB) and F type Fuc(α 1-6)[Gal(β 1-4)]GlcNAc(β1-2)Man(α1-3)[Fuc(α1-6)[Gal(β1-4)]GlcNAc(β1-2)Man (α1-6)][Xyl(β1-2)]Man(β1-4)GlcNAc(β1-4)[Fuc(α1-3)]GlcNAc with monoiostopic mass 2210.8 Da (entry No.1033-1021in GlycoSuite DB) in Tab.2.

The E and F type of *N*-linked oligosaccharides have already reported that these structures had existed in laccase from sycamore cell and miraculin from miracle fruits [22].

And the other proposed ACD type structures are already existed in the plant system; however the proposed structure of B type and G type are from insect and mammlia, respectivly.

The structures of α-1, 3 Fucose linked with core GlcNAc were existed in all *N*-glycan linked Asparagines in laccase glycoprotein. The structure of β-1, 2 xylose linked with core Mannose were also appeared in all Asparagines which link with carbohydrate except Asn5,28,124 and 194 in laccase glycoprotein. These two kinds of structure are very popular in plant system.

4.3.3 NP-HPLC analysis of PA labeled N-glycans

We utilized BlotGlyco Glycan purification and labeling kit (Sumitomo bakelite) through purification the *N*-glycans from peptide mixtures and PA labeling to obtain the fluorescently labeled *N*-glycans easily and effectively.

We also used the peptide-N-glycosidase F (PNGase F) and fluorescent reagent 2-AB, but they didn't give the good results. It is because *N*-glycans of lacquer laccase glycoprotein mainly have the structure of core GlcNAc with α-1, 3 linked Fucose that is common in plants. However, PNGase F is enzyme used to deglycosylate mammalian protein, does not cleave oligosaccharides containing α-1, 3 linked Fucose from protein [23]. In contrast, Peptide-N-glycosidase A (PNGase A) is used to set free plant *N*-glycans from protein which treated with protease enzyme [24].

As shown in fig. 4, there appeared the large paeks in 8~20min, it is the excess of fluorescent reagents mainly aminopyridine (2-PA). There have seven peaks appeared between 20min~140min in fig.4. This result is identical to that of proposed *N*-glycan structures from LC-MS/MS analysis (Tab. 2).

4.3.4 MALDI-TOF MS analysis of labeled *N*-glycans

The reducing terminal of *N*-glycan was labeled by good-sensitive release reagent (aoWR, m/z 447.2) for MALDI-TOF

MS measurement. The accurate mass of *N*-glycans is obtained from the following formula: Mass of *N*-glycans = [mass of peak -447.2 (release reagent mass) +18.01-1.00].

From the ms spectrum, we found six kinds of *N*-glycans in figure 6. There are from A to F, respectively. In fact, the two most intense peaks were F and F type of *N*-glycans. This result is same with the LC/MS/MS and NP-HPLC analysis. But the G type N-glycan (m/z=3295.2) did not found in the spectrum, it may be the large mass and little amount of *N*-glycan is difficult to be detected in TOF-MS. No other N-glycan is found in this MS spectrum.

Conclusion

The lacquer laccase is relatively heavily glycosylated glycopreotein, and we found there have twelve glycosylation sites and elucidated each *N*-glycans composition and deduced the possible structure by LC-MS/MS spectrometry and MALDI-TOF/MS spectrometry. The calculated mass of *N*-glycans of laccase in this study is approximately 39.0KDa from table 1. This is very close to the maximum mass 41.0kDa we estimated. This means there maybe not existed so many *O*-glycans in lacquer laccase glycoprotein despite there have not a few *O*-glycosylation sites in amino sequences of laccase. Actually, we found two sites linked with short *O*-glycans in laccase amino acid sequences after treated with

PNGase A enzyme. They are amino acid sequences of TPGQTMD (240-246) linked with GalNAc-Gal and GHSTSASLN (356-363) linked with only one GalNAc.

Legend to figure and table

Figure1.Amino acid sequence of the lacquer laccase. N-X-T/S sites found to bind N-glycan were in red, no glycosylated sites were in blue, and the peptides found were in grey in this study.

Figure2. (A) Aqueous GPC Spectrum, $\overline{M}n$ = 4.6 x 104 ($\overline{M}w/\overline{M}n$ = 1.87), and (B) SDS-PAGE of purified lacquer laccase glycoprotein.

Figure3. Extracted ion chromatography (XIC) of carbohydrate marker ion protonated HexNAc+ (m/z 204.1) from total ion chromatography of tryptic digestion of laccase.

Figure4. Product ion spectrum (MS^2) of doubly charged glycopeptides precursor ion at m/z 1381.2. The glycopeptides Asn284~Lys288 is glycosylated with oligsaccharide, (HexNAc)4 (Hex)5(dHex)3(Pent)1 at Asn284.

Figure5. Normal-phase HPLC spectrum of PA labeled N-Glycan of laccase glycoprotein after PNGase A treatment.

Figure6. MALDI-TOF MS spectrum of labeled N-glycans of laccase glycoprotein after PNGase A treatment.

Table1. Glycosylation analysis of lacquer laccase glycoprotein.

Table2. Proposed structures of *N*-linked oligosaccharide obtained from the laccase glycoprotein.

Table3. Peptide tryptic digestion mapping of laccase glycoprotein

Acknowledgement

Reference

[1]Yoshida H., 1883, LXIII. Chemistry of lacquer (Urushi). Part I. Communication from the chemical society of Tokio. J. Chem. Soc. Trans., 43: 472-486

[2]Bertland G., Compt. Rend, 1894, Acad. Sci. T. 118: 1215.

[3]Messerschmidt A. (Ed.), 1997, Multi-Copper Oxidases, World scientific, Singapore.

[4]JAeschke H.F., 1992, Oriental lacquer: a natural polymer, polymers in conservation, 47-60.

[5] Oshima R., Kumanotani J., 1984, Structural studies of plant gum from sap of the lac tree, Rhus vernicifera, Carbohydr. Res., 127:43-57. (no PDF)

[6]Kumanotani J., 1988, Oriental (Japanese) Lacquer. A highly durable enzymatically catalyzed natural coating and its expansion to synthetic coatings, Congr. FATIPEC, 19:205-215

[7]Kumanotani J., 1995, 'Urushi (oriental lacquer) - a natural aesthetic durable and future-promising coating', Progress in Organic Coatings, 26:163-195.

[8] Catherine R., Patrice L., and Loic F., 1998, the protein N-glycosylation in plants, Journal of experimental botany, 49: 1463-1472.

[9] Altmann F., 1997, More than silk and honey—or, can insect cells serve in the production of therapeutic glycoproteins? Glycoconjugate Journal, 14: 643–6.

[10] Wuhrer M., Deelder A. M., Hokke C. H., 2005, Protein glycosylation analysis by liquid chromatography–mass spectrometry. J. Chromatogr. B Analyt. Technol. Biomed. Life Sci., 825: 124-133.

[11] Brooks S. A., 2009, Strategies for analysis of the glycosylation of proteins: current status and future perspectives. Mol. Biotechnol. 43: 76-88.

[12]Solomon E.T., U.M. Sundaram, T.E. machonkin, 1996, Multicopper oxidases and oxygenases. Chem. Rev., 96: 2563-2605.

[13]Nitta K., Kataoka K., Sakurai T., 2002, Primary structure of a

Japanese lacquer tree laccase as a prototype enzyme of multicopper oxidases. Journal of Inorganic Biochemistry, 91: 125-131.

[14]Bengt Reinhammar, 1969, purification and properties of laccase and stellacyanin from Rhus vernicifera, Biochimica Et Biophysica Acta., 205: 35-47.

[15] Laemmli U. K., 1970, Cleavage of structural proteins during the assembly of the head of bacteriophage T4, nature, 227: 680-685.

[16] Applied Biosystems, 2001, Information Dependent Acquisition—the next generation of data dependent experiments for LC/MS/MS analysis, product bulletin, 114PB07-01.

[17] Chales C. N., Danielle L. A., Hyeyyoung L., Larry A. L., Angela M. Z., J. Bruce German, and Carlito B. L, 2012, Comparision of the human and bovine milk N-glycome via high-performance microfluidic chip liquid chromatography and tandem mass spectrometry, Journal of proteome research, 11, 2912-2924.

[18]Bigge J.C., Patel T.P., Bruce J.A., Goulding P.N., Charles S.M., Parekh R.B., 1995, Nonselective and efficient fluorescent labeling of glycans using 2-aminobenzamide and anthranilic acid, Anal. Biochem. 230: 229–238.

[19]Kondo A., Suzuki J., Kuraya N., Hase S., Kato I., Ikenaka T., 1990, Improved method for fluorescence labeling of sugar

chains with sialic acid residues. Agric Biol Chem, 54:2169–2170.

[20]Guile G.R., Wong, S.Y., Dwek R.A., 1994, Analytical and preparative separation of anionic oligosaccharides by weak anion exchange high-performance liquid chromatography on an inert polymer column. Anal. Biochem., 222: 231–235.

[21]Masaki K., Takahiko M., Maho A., Jun-ichi F.,Yasuro S., Masato A., and Shin-Ichiro N., 2010, Sialic acid-focused quantitative mouse serum glycoproteomics by multiple reaction monitoring assay, Molecular & Cellular Proteomics 9.11, 2354-2368.

[22] Noriko T., Hiromu H, Hiroyuki H, Yoji A, and Yoshie K, 1990, Structural study of Asparagine-linked oligosaccharide moiety of taste-modifying protein, Miraculin, the Journal of Biological chemistry, 265 (14), 7793-7798.

[23]Tretter V., Altmann F., Ma¨rz L., (1991) Peptide-N4-(N-acetyl-b-glucosaminyl) asparagines amidase-F cannot release glycans with fucose attached a-1-3 to the asparaginelinked N-acetylglucosamine residue, Eur. J. Biochem., 199: 647–652.

[24] FRIEDRICH A., STEFAN S. and CHRISTOPH W., 1995, Kinetic comparison of peptide: N-glycosidases F and A reveals several differences in substrate specificity, Glycoconjugate Journal, 12:84-93.

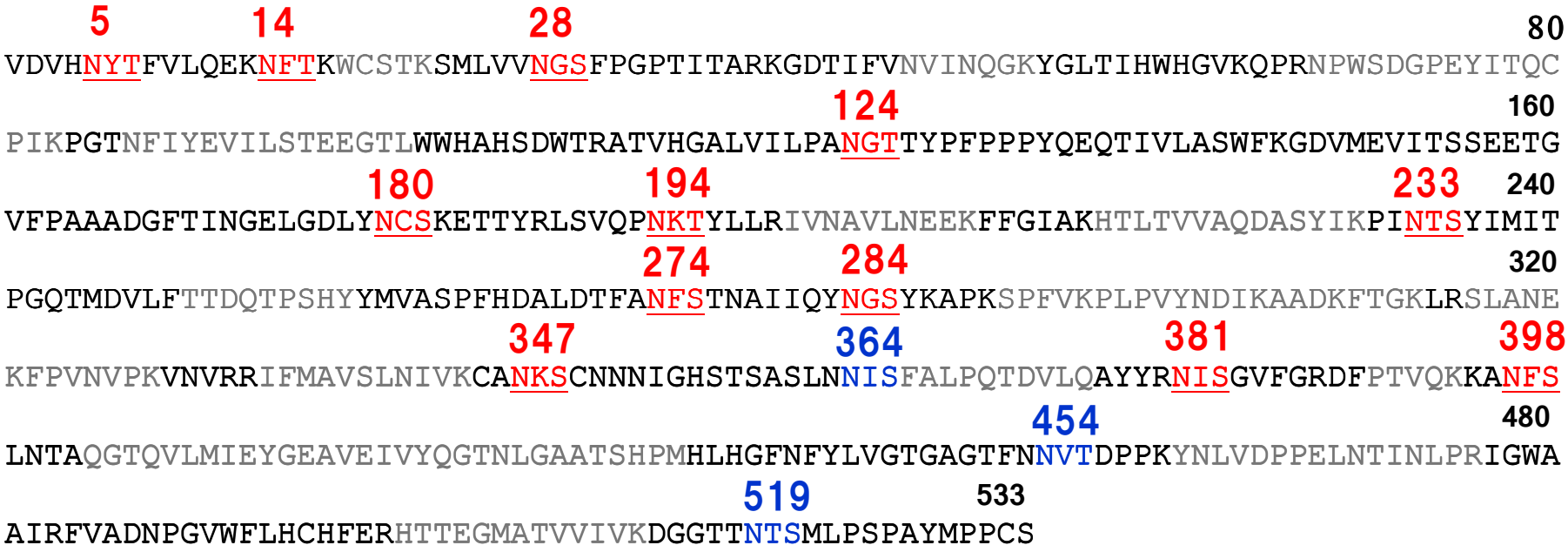

Figure1. Amino acid sequence of the lacquer laccase. N-X-T/S glycosylation sites found to bind *N*-glycan were in red, no glycosylated sites were in blue, and the peptides found in this study were in grey.

Figure 1

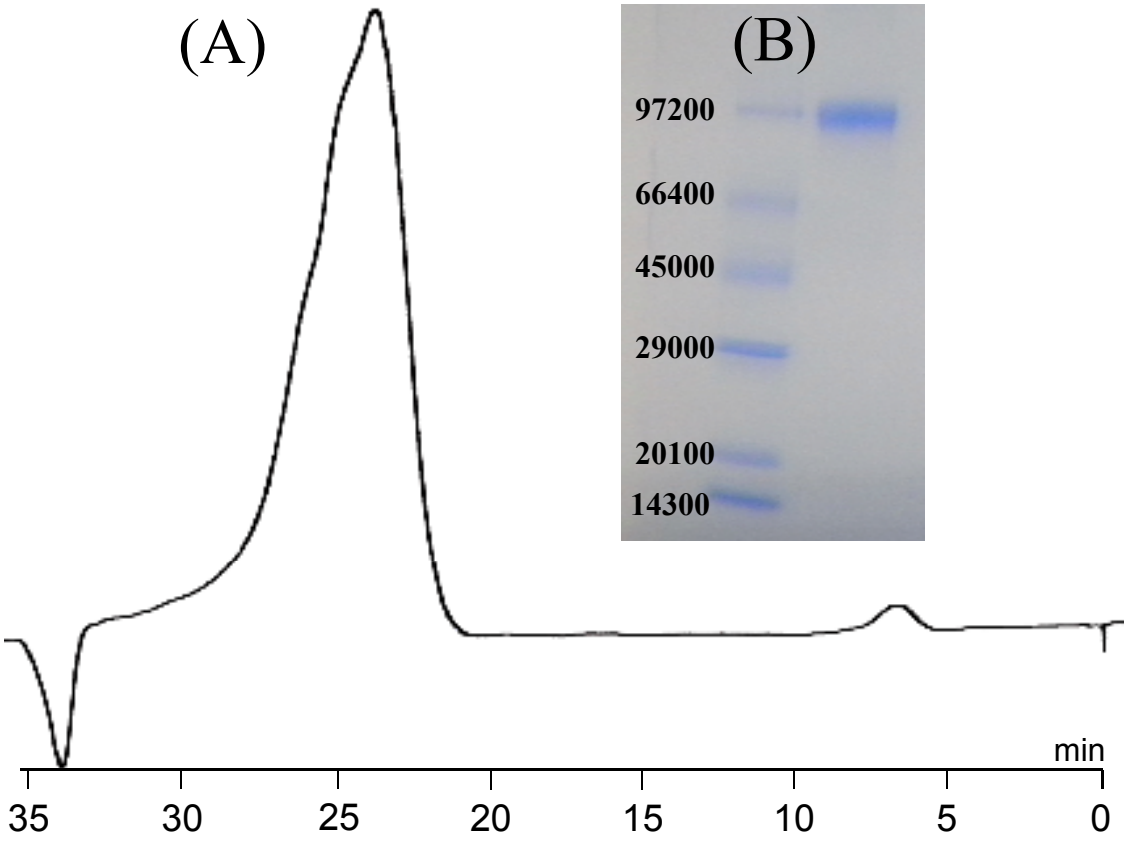

figure2. (A) Aqueous GPC Spectrum, Mn = 4.6 x 10^4 (M_w/M_n = 1.87), and (B) SDS-PAGE of purified lacquer laccase glycoprotein.

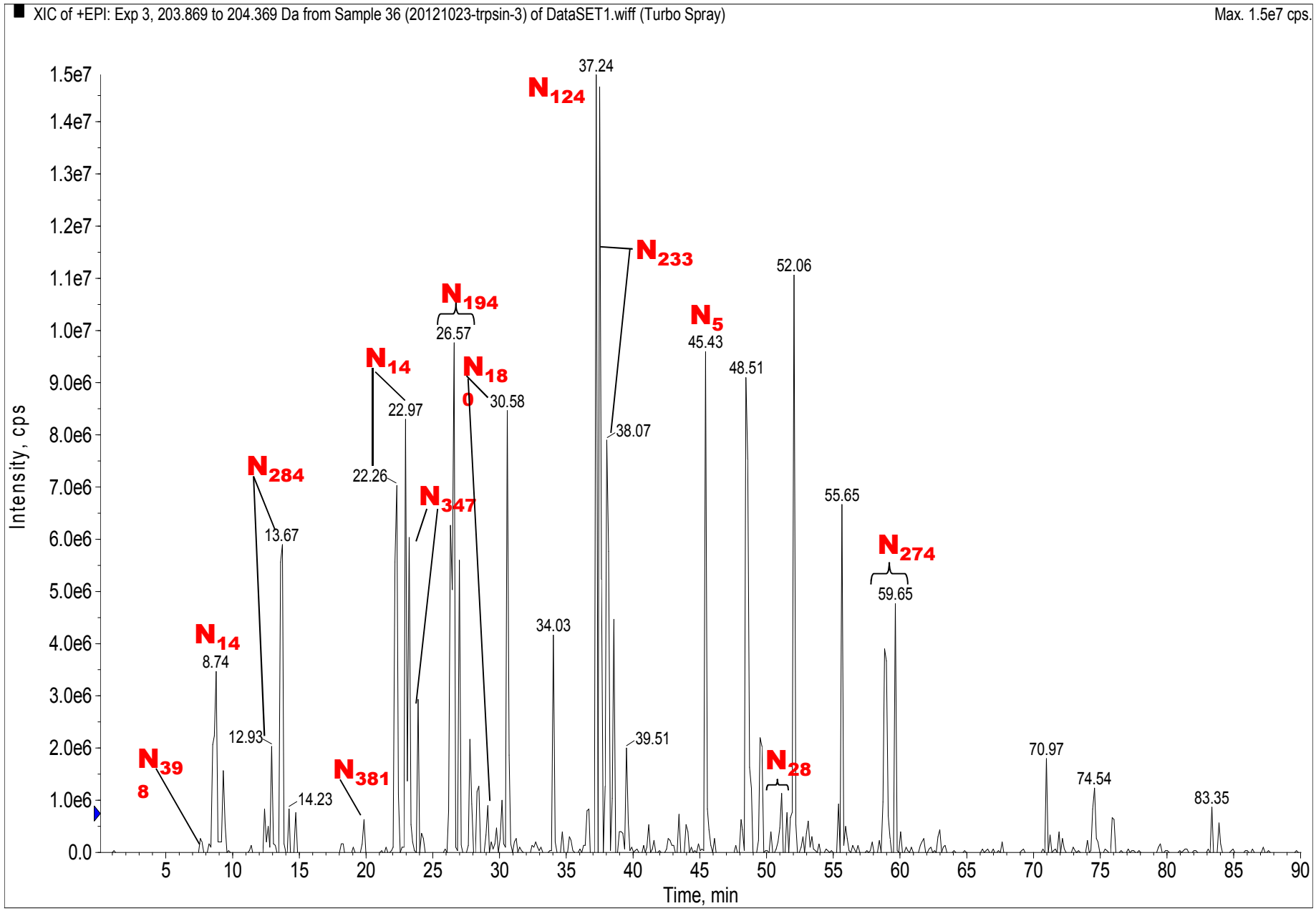

Figure 3. Extracted ion chromatography (XIC) of carbohydrate marker ion protonated HexNAc+ (m/z 204.1) from total ion chromatography of tryptic digestion of laccase.

Figure 3

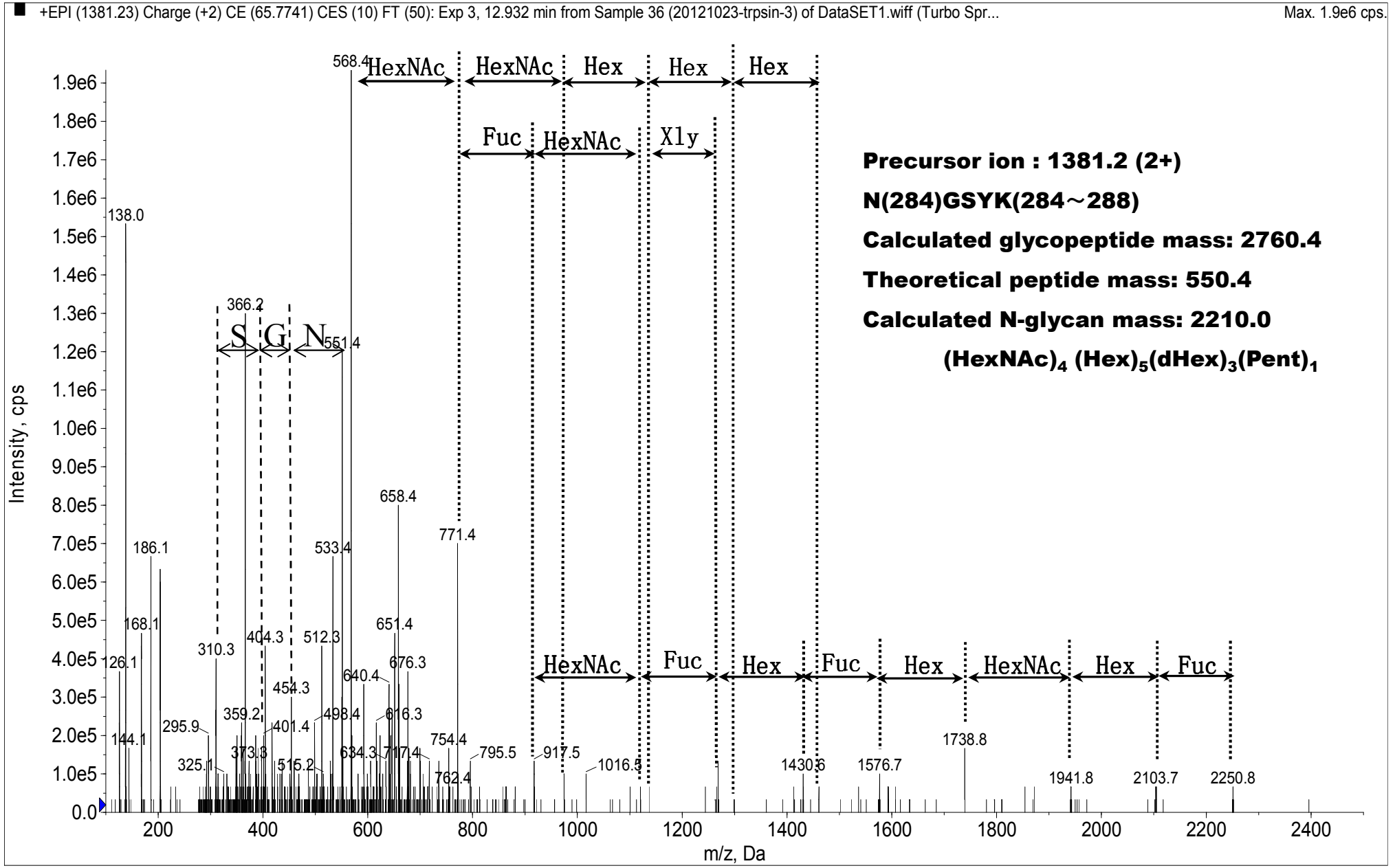

Fig 4. product ion spectrum (MS2) of doubly charged glycopeptides precursor ion at m/z 1381.2. The glycopeptides Asn284~Lys288 is glycosylated with oligsaccharide, $(HexNAc)_4$ $(Hex)_5(Fuc)_3$ $(Pent)_1$at Asn284.

Figure 4

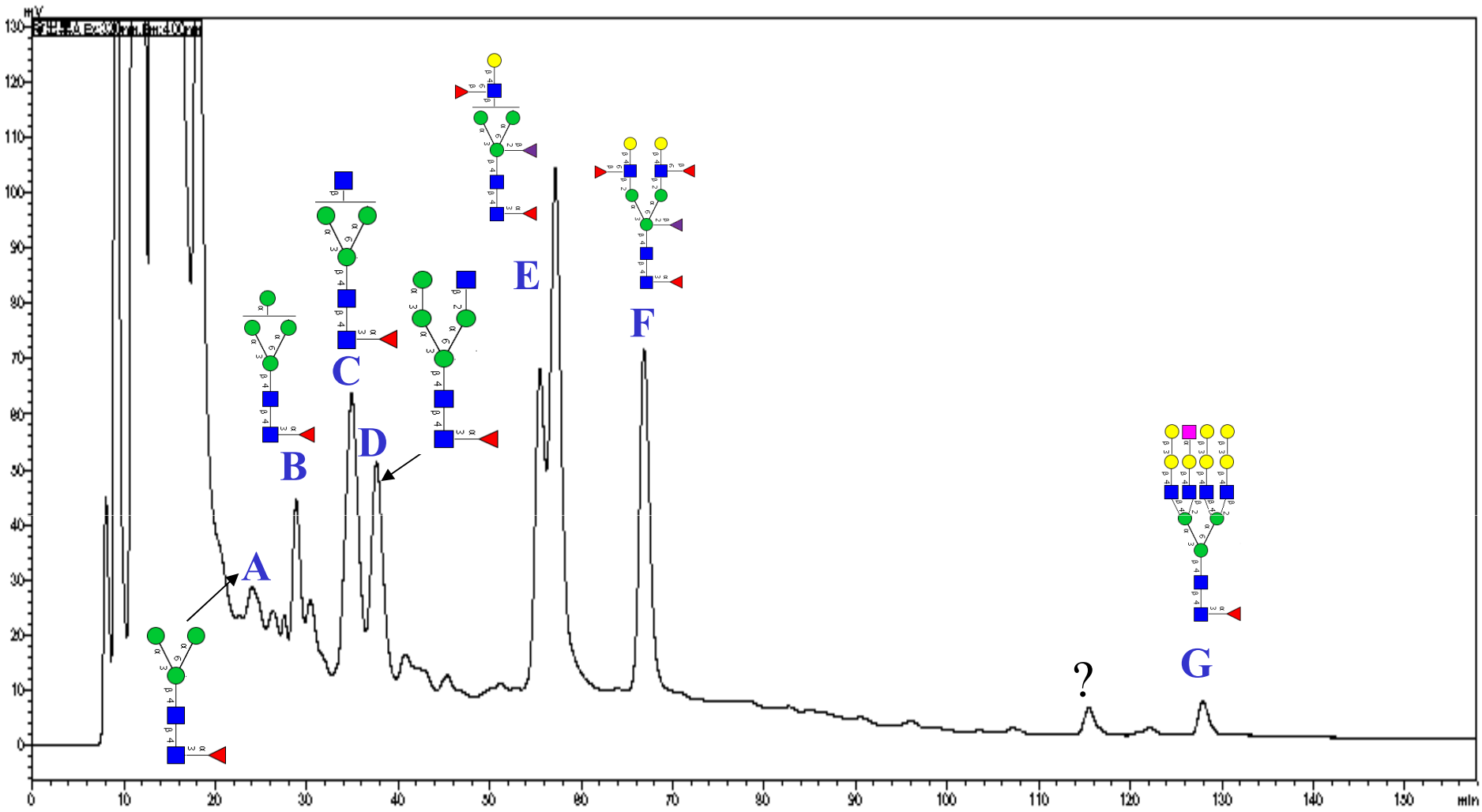

Figure 5 Normal Phase HPLC spectrum of PA labeled *N*-Glycan of lacquer laccase glycoprotein after PNGase A treatment.

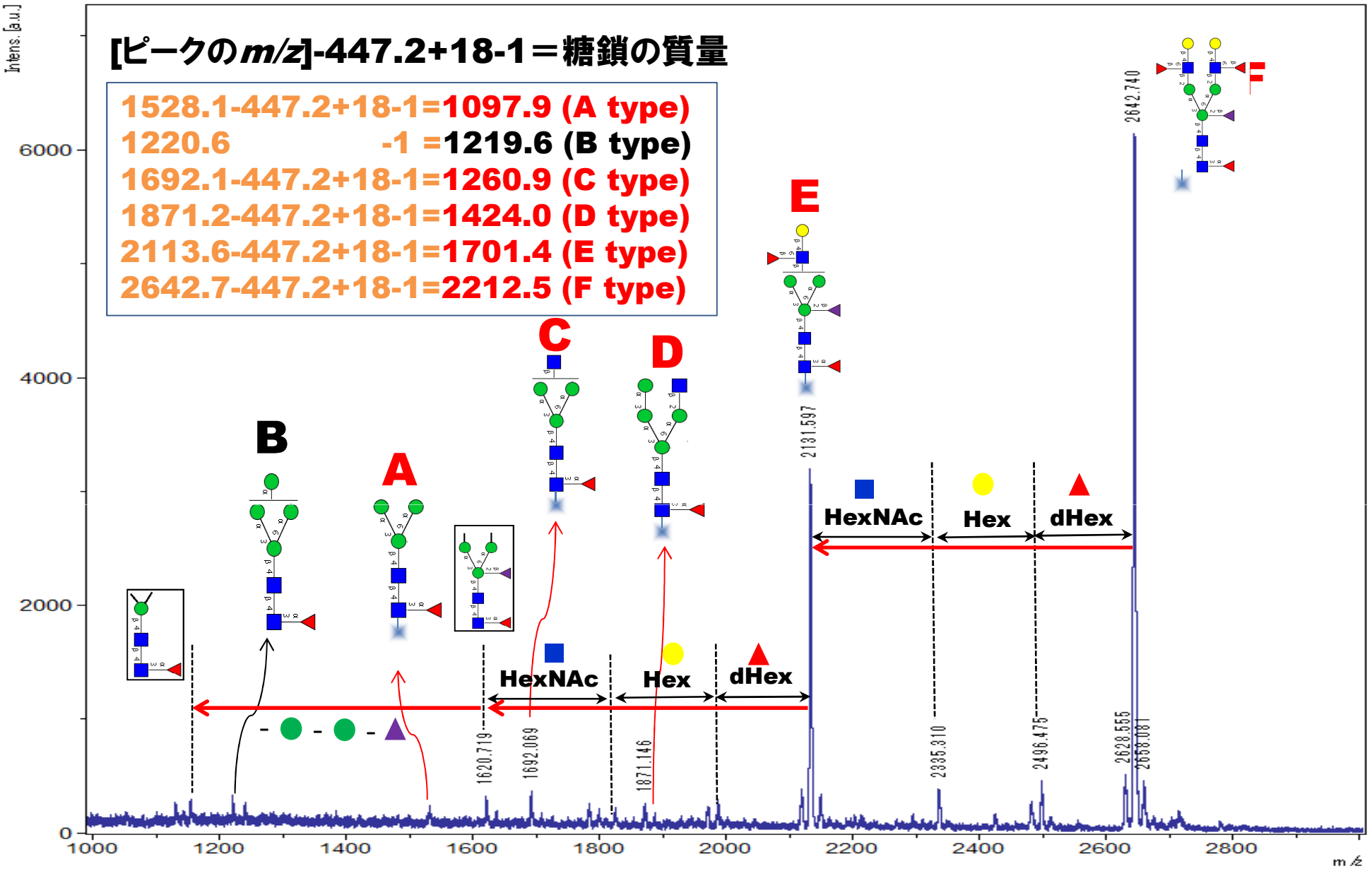

Fig.6 MALDI TOF-MS spectrum of labeled N-glycan of laccase glycoprotein after PNGase A digestion

Table 1 Glycosylation analysis of lacquer laccase glycoprotein

Glycosylation Site	Carbohydrate composition [a]					Theoretical Carbohydrate Mass [b]	Trypsin Digestion precursor ion			
	dHex	Hex	HexNAc	Pent	NeuAc		Observed *m/z*	Charge state	Amino acid Residue	Theoretical *m/z* [c]
Asn5	1 [d]	3	2	0	0	1097.4	1063.6	2	VDVHN*YTFV	(994.2)
Asn14	2[d]	4	3	1	0	1700.2	1096.1	2	N*FTK	490(509.3)
	3[d]	5	4	1	0	2212.4	1352.2	2	N*FTK	490(509.4)
Asn28	1[d]	3	3	0	0	1261.4	998.0	3	SMLVN*GSFPGPT-	1730(1747)
	1[d]	4	3	0	0	1423.4	1052.0	3	-ITAR	1730(1747)
Asn124	1[d]	10	6	0	1	3295.4	1082.3	4	VILPAN*GTTY	1029.8 (1049.8)
Asn180	2[d]	4	3	1	0	1699.3	1214.9	2	DLYN*CS	728.2 (746.4)
	3[d]	5	4	1	0	2210.9	1470.7	2	DLYN*CS	728.2 (746.5)
Asn194	1[d]	4	2	0	0	1219.3	993.9	2	LSVQPN*K	766.6 (785.6)
	2[d]	4	3	1	0	1699.6	1234.1	2	LSVQPN*K	766.6 (785.6)
	3[d]	5	4	1	0	2212.1	1490.3	2	LSVQPN*K	766.6 (785.6)
Asn233	3[d]	5	4	1	0	2209.4	1044.1	3	KPIN*TSYIM	919.6(935.6)
	2[d]	4	3	1	0	1697.8	1309.7	2	KPIN*TSYIM	919.6(935.6)
Asn274	2	4	3	1	0	1698.5	1417.1	2	HDALDTFAN*FS	1133.7(1150)
	3	5	4	1	0	2210.7	1673.3	2	HDALDTFAN*FS	1133.7(1150)
Asn284	2[d]	4	3	1	0	1700.2	1126.1	2	N*GSYK	550.4 (568.4)
	3[d]	5	4	1	0	2210.2	1381.2	2	N*GSYK	550.4 (568.4)
Asn347	2[d]	4	3	1	0	1697.9	1135.7	2	KCAN*K	571.5 (588.5)
	3[d]	5	4	1	0	2210.0	1391.7	2	KCAN*K	571.5 (588.5)
Asn381	2[d]	4	3	1	0	1697.9	1283.8	2	N*ISGVFG	867.7(884.5)
Asn398	2[d]	4	3	1	0	1699.2	1177.6	2	AN*FSLN	654.5

[a] dHex, deoxy-hexose; Hex, hexose ; HexNAc, *N*-acetylhexosamine; NeuAc, *N*-acetylneuramic acid and Pent, Xylose.
[b] Monoisotopic value.
[c] Observed peptide mass is indicated in parenthesis.
[d] one fucose is linked with core *N*-acetylglucoseamine.

Table.2 Proposed structures of *N*-linked oligosaccharides in laccase glycoprotein

Type	Mass/Da	GlycoSuite DB entry No.	Proposed structure of *N*-glycans
A	1097.		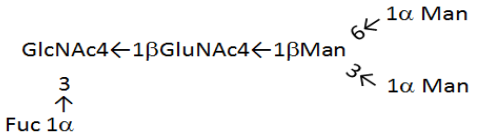
B	1218.4	5800-2540	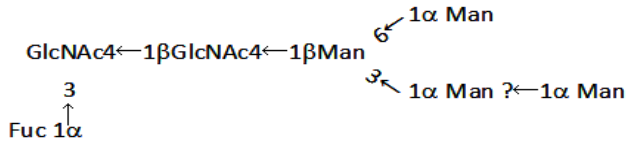
C	1261.4	7369-2976	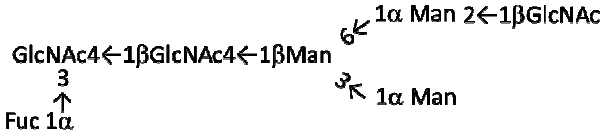
D	1423.4	2987-1392	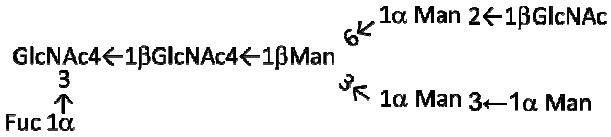
E	1699.7	1029-1021	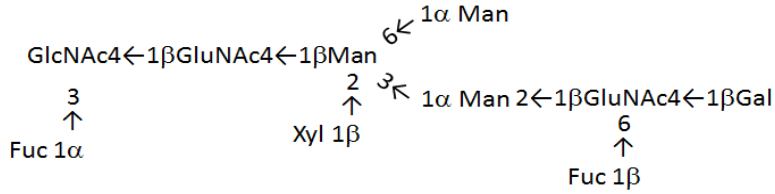
F	2210.8	1033-1021	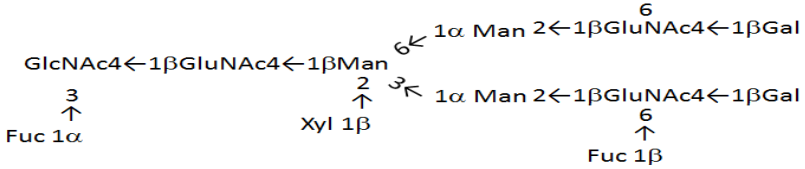
G	3294.2	7222-2938	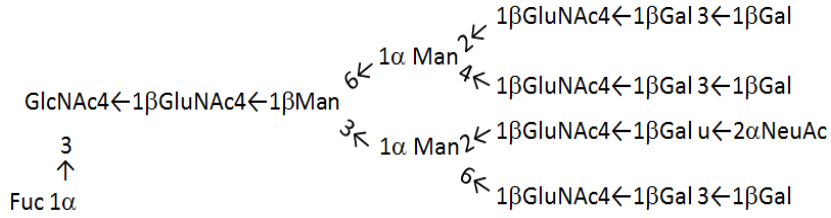

Table 3 Peptide tryptic digestion mapping of laccase glycoprotein

Residue	Amino acid sequence	The theoretical mass	The observed m/z	Charge state (+)	Search in
18-22	WCSTK	679.8	680.8	1	mascot
68-83	NPWSDGPEYITQCPIK	1904.3	953.2	2	mascot
201-210	IVNAVLNEEK	1129.1	565.6	2	mascot
289-294	SPFVK	575.9	576.9	1	mascot
322-328	FPVNVPK	799.4	400.7	2	mascot
334-344	IFMAVSLNIVK	1234.9	618.4	2	mascot
461-476	YNLVDPPELNTINLPR	1868.4	935.2	2	mascot
501-513	HTTEGMATVVIVK	1384.1	693.0	2	mascot
47-53	NVINQGK	770.2	436.1	2	manual
87-103	NFIYEVILSTEEGTLW	1904.4	953.2	2	manual
217-230	HTLTVVAQDASYIK	1302.6	653.3	2	manual
251-259	TTDQTPSHY	1048.8	525.4	2	manual
295-305	VKPLPVYNDIK	1270.2	636.1	2	manual
303-313	DIKAADKFTGK	1252.9	627.4	2	manual
316-321	SLANEK	644.5	661.4	1	manual
366-376	SFALPQTDVLQ	1282.3	642.1	2	manual
391-395	PTVQK	571.7	437.1	?	manual
405-411	QGTQVLM	774.1	475.1	?	manual
412-422	IEYGEAVEIVK	1415.2	708.2	2	manual
423-435	QGTNLGAATSHPM	1283.9	642.4	2	manual

Chapter 5

Sulfation and biological activities of konjac glucomannan

ABSTRACT

The synthesis and biological activities such as anti-HIV and blood anticoagulant activities of sulfated konjac glucomannans have been investigated. Konjac glucomannan is a naturally occurring polysaccharide and difficult to dissolve in water and DMSO because of having high molecular weights. Before sulfation, hydrolysis by diluted sulfuric acid was carried out to decrease molecular weights to $\overline{M}_n$ = 19.2 x 10^4 -0.2 x 10^4. Sulfation with piperidine-*N*-sulfonic acid or SO_3-pyridine complex gave sulfated konjac glucomannan with the molecular weights of $\overline{M}_n$ = 1.0 x 10^4-0.4 x 10^4 and degree of sulfation of DS = 1.3-1.4. It was found that the sulfated konjac glucomannans had potent anti-HIV activity of the 50% effective concentration of EC_{50} = 1.2-1.3 μg/ml, which activity was almost the same as that of an AIDS drug, ddC, EC_{50} = 3.2 μg/ml, and medium blood anticoagulant activity, AA =0.8-22.7 units/mg, which activities were almost the same activities as those of standard sulfated polysaccharides, curdlan (10 unit/mg) and dextran (22.7 unit/mg) sulfates. Structural analysis of sulfated konjac glucomannans was

performed by a high resolution NMR measurement and the interaction between polylysine as a model compound of proteins and peptides was calculated preliminary from a surface plasmon resonance (SPR) measurement, suggesting that sulfated konjac glucomannans had a high binding stability on poly-L-lysine as a model compound of proteins and peptides.

5.1 Introduction

Konjac glucomannan is abundant and easily-available heteropolysaccharides with high molecular weights in konjac plant tubers (Dave, 1997; Chua, 2010; Cescutti, 2002). Konjac glucomannan is water-soluble and a linear structure composed of 1, 4-β-linked D-glucopyranose and D-mannopyranose with a small amount of branches and partially acetylated hydroxyl groups in the sugar units. Konjac glucomannan has been used as foods (Albrecht, 2011), food additives (Iglesias-Otero, 2010), rapping films mixed with cellulose or curdlan (Lu, 2004; Wu, 2012), support of cation-exchange resin (Zhou, 2012), and water-absorbent polymers (Li, 2012). Although the researches on biological activities were little, biomaterials, supports of ion-exchange resin, and carrier of drug delivery system were reported for the application researches (Wang, 2010; Liu, 2012).

Fundamental researches of konjac glucomannan were mainly focused on the structural analysis and gelation mechanisms. Katsuraya and coworkers reported in detail the structural analysis

of konjac glucomannan by methylation analysis and NMR spectroscopic measurement, indicating that the small proportion of branches was existed at the C6 carbon of glucosyl main chain with 1, 6-β glucosyl branches. The ratio of glucose to mannose units of the main chain was about 2 and branches were about 8% (Katsuraya, 2003). Luo and coworkers described the gelation mechanism of konjac glucomannan in NaOH solution. Sodium hydroxide solution restrained the expansion of the molecular chain and promoted the gelation probably due to the obvious effects of deacetylation, self-aggregation, and entanglement (Luo, 2011). On the other hand, Liu and coworkers developed a carrier of pulsatile drug delivery system based on an impermeable capsule of konjac glucomannan (Liu, 2012). The plasma drug concentration was detected 5 h after oral administration of 5-aminosalicylic acid in the capsule. The pulsatile capsule may have therapeutic potential for colon-specific drug delivery system.

We have reported the synthesis, structural analysis, and biological activities of natural occurring and synthetic polysaccharides obtained by ring-opening polymerization of anhydro sugar monomers (Yoshida, 2001; 2005). Previously, we found that sulfated polysaccharides have high anti-HIV and blood anticoagulant activities. Especially, curdlan sulfate that was prepared by sulfation of curdlan produced by a strain, a natural

polysaccharide with linear 1, 3-β pyranosidic structure, completely inhibited the infection of HIV to MT-4 cell in the concentration as low as 3.3 μg/ml and low cytotoxicity as high as 1000 μg/ml (Yoshida, 1990). Therefore, an alkyl curdlan sulfate was prepared recently by an ionic interaction between a positive didodecyldimethyl ammonium bromide and a negative sulfate group of curdlan sulfate, and fixed on a membrane filter by a hydrophobic interaction with the long alkyl chain. Alkyl curdlan sulfate-coated membrane filters decreased hemagglutination to 1/4 to 1/32 on influenza A virus, suggesting that the membrane filter removed influenza A virus by the electrostatic interaction of negatively charged sulfate groups and positively charged envelope protein of the viruses (Tegshi, 2011).

Although there are many reports on the structure and applications of konjac glucomannan, a little report on the biological activities appeared. Sulfated polysaccharides are expected in the specific biological activities on antiviral and heparin-like activities (Lane, 1989). In this paper, we wish to report the sulfation of konjac glucomannan and its biological activities such as anti-HIV and blood anticoagulant activities. In addition, we describe the preliminary results on the interaction between sulfated konjac glucomannan and polylysine as a model compound of peptides and proteins by using a surface plasmon resonance (SPR) to elucidate the biological mechanisms.

5.2 Method and Material

5.2.1 Instruments and Chemicals

The ^{1}H NMR and ^{13}C NMR spectra were recorded with a JEOL ECM-400 spectrometer at 400 MHz and 100 MHz, respectively, in D_2O or 2.5% NaOH D2O solution at 50°C with 3-(trimethylsilyl)-1-propanesulfonic acid sodium salt (DSS) as an internal standard or in DMSO-d_6 at 60°C. Infrared spectra were measured in KBr pellet with a Perkin Elmer Spectrum One FT-IR spectrometer. The molecular weight of hydrolyzed konjac glucomannan was determined by an aqueous phase GPC (column; Tosoh TSK-gel G2500PW_{XL}, G3000PW_{XL}, and G4000PW_{XL}, 7.6 mm x 300 mm x 3 eluted with 66.7 mM of phosphate buffer, pH=6. 86) with a Tosoh RI detector using pullulan as a standard. Optical rotation was measured by using a JASCO DIP-140 digital polarimeter in 2.5% NaOH aqueous solution at 25°C in a water-jacketed 10 ml quartz cell. Elemental analysis was carried out with CE-440 elemental analyzer (System Engineering Inc). A surface plasmon resonance (SPR) spectrum was taken on a Biacore X100 instrument at 25°C using a CM5 sensor chip.

Konjac glucomannan was obtained from Chengdu Root Industry (China). Poly-L- lysine with $\overline{M}_w$ = 1000-5000 and anhydrous dimethyl sulfoxide were purchased from Sigma, Inc. Piperidine-*N*-sulfonic acid was prepared from piperidine and

chlorosulfonic acid according to the method of Nagazawa and Yoshidome (Nagasawa, 1969).

5.2.2 Hydrolysis of konjac glucomannan

Typical procedure for hydrolysis of konjac glucomannan is as follows. Konjac glucomannan (0.5 g) was added into 90 ml of deionized water and then stirred vigorously for 3 h at 70 °C. After sulfuric acid (25%, 10 ml) was dropwise added to the viscous konjac glucomannan solution (the final concentration of sulfuric acid in solution was 2.5 %), the mixture was further stirred for 2 h at 70 °C. After cooling to room temperature, the reaction mixture was neutralized by saturated $NaHCO_3$ solution, dialyzed against deionized water for 24 h, and then freeze-dried to give 0.41 g of low molecular weight konjac glucomannan ($\overline{M}_n$ = 3.7 x 10^4) after freeze-drying.

5.2.3 Sulfation of konjac glucomannan and their biological activities

Konjac glucomannan was sulfated by piperidine-*N*-sulfonic acid or SO3-pyridine complex. Typical methods are as follows.

For the sulfation by piperidine-*N*-sulfonic acid, konjac glucomannan (0.25 g, 1.5 mmol, $\overline{M}_n$ = 0.8 x 10^4) was dissolved in anhydrous DMSO (25 ml) solution at 85°C and then piperidine-*N*-sulfonic acid (1.0 g, 6.1 mmol) was added. The mixture

was stirred for 2 h at 85°C and then neutralized by 5% NaOH solution after cooling and the alkaline solution was dialyzed against deionized water for 2 days. The dialysate was freeze-dried to give 0.26 g of sulfated glucomannan with the number-average molecular weight of $\overline{M}_n$ = 0.7 x 10^4. Found for C; 19.7 %, H; 3.0 %, S; 14.7 %.

For the sulfation by SO_3-pyridine complex, konjac glucomannan (0.25 g, 1.5 mmol, $\overline{M}_n$= 5.6 x 10^4) was dissolved in anhydrous DMSO (25 ml) with stirring at 70 °C and then SO_3-pyridine complex (1.5 g, 9.4 mmol) was added. The mixture was stirred for further 45 min at 70 °C. After cooling to room temperature, the mixture was neutralized with saturated $NaHCO_3$ solution, dialyzed against deionized water for 2 days, and the dialysate was freeze-dried to give 0.5 g of sulfated glucomannan with the number-average molecular weight of $\overline{M}_n$ = 1.0 x 10^4. Found for C; 19.1 %, H; 2.9 %, S; 14.0 %.

5.2.4 Biological activities

The anti-HIV activity was assayed in vitro by the MTT method. (Pauwels, 1988) The activity was evaluated by the EC_{50} value, which is the 50% inhibitory concentration of HIV to avoid the infection into MT-4 cell. Cytotoxicity is determined by the CC_{50} value, which is the 50% cytotoxic concentration of sulfated glucomannans to MT-4 cell.

The blood anticoagulant activity was measured by using bovine

plasma according to the modified method of the US pharmacopeia (U. S. Pharmacopoeia National Formulary, 1985) and was calculated in comparison with the activity of a standard dextran sulfate (H-39), 22.7 units/mg.

5.2.5 Interaction of sulfated konjac glucomannan with polylysine by SPR

Interaction between sulfated glucomannan and polylysine was measured quantitatively by the Biacore X100 surface plasmon resonance (SPR) instrument at 25 °C. Poly-L-lysine was dissolved in the acetate buffer (10 mM sodium acetate, pH 5.5) to prepare ligand solution with concentration of 5000μg/ml. The poly-L-lysine solution was immobilized on the CM5 sensor chip by amine coupling reaction according to the method as described by the manufacturer. Final immobilized rate was 1839 RU. Sulfated glucomannans was dissolved in a HBS-EP running buffer (10 mmol HEPES, 0.15 M NaCl, 3.0 mmol EDTA, 0.05 % v/v Surfactant P20, pH7.4) and the solution was poured over the surface of the sensor chip at a flow rate of 30 μl/min for 120 s and followed by allowing the running buffer to flow at the same rate for 600 s. Ligands were regeneration with 50 mM NaOH. The association rate (k_a) and dissociation rate (k_d) constants were calculated from the Biacore-supplied software provided by GE Healthcare UK Ltd.

5.3 Results and Discussion

5.3.1 Decrease of molecular weights of konjac glucomannan

Konjac glucomannan has a natural occurring polysaccharide with almost linear structure and with high molecular weights more than 1 million. The constituted sugars are glucose and mannose with a 1, 4-β pyranosidic linkage similar to cellulose, so that it is difficult to dissolve in water and organic solvents. The aqueous solution in the low concentration gave viscous liquid. Therefore, konjac glucomannan was hydrolyzed by aqueous sulfuric acid to decrease molecular weights and then to dissolve in water and DMSO. Table 1 shows the results of hydrolysis of konjac glucomannan by diluted sulfuric acid. When 0.5% H_2SO_4 aqueous solution was used at 50°C for 4 h, the molecular weight decreased to $\overline{M}_n$ = 19.2 x 10^4, and the yield was 0.17 g from 0.5 g row material. It was found that the molecular weights decreased to $\overline{M}_n$ = 5.6 x 10^4 to 0.2 x 10^4 with increasing the concentration of sulfuric acid to 5%. With 5% H_2SO_4 at 70°C, the molecular weight decreased to $\overline{M}_n$ = 0.2 x 10^4, however, the yield was low, 0.05 g from 0.5 g of konjac glucomannan.

Figure 1 shows the GPC profiles of konjac glucomannan with low molecular weights. After hydrolysis, konjac glucomannan was dissolved in water to give viscous solution and the soluble part was measured the molecular weights by GPC, indicating that the

absorptions were delayed with decreasing molecular weights.

Figure 2B shows the ^{13}C NMR spectra of the hydrolyzed konjac glucomannan with the molecular weight of $\overline{M}_n$ = 8000 in 2.5% NaOH D_2O solution at 50°C. The C1 signals due to glucose and mannose units appeared at 103 and 106 ppm, respectively and it was found that the glucose and mannose units in the konjac glucomannan were almost the same proportion by their intensities. The carbon signal due to acetyl group appeared at 183 ppm.

5.3.2 Sulfation and biological activities of konjac glucomannan

The original and low molecular weight konjac glucomannans were sulfated with piperidine-*N*-sulfonic acid in DMSO or SO_3-pyridine complex in pyridine at high temperatures to give sulfated konjac glucomannan with the degree of sulfation (DS) of 1.3-1.4 (maximum, 3) as resulted in Table 2. The sulfated konjac glucomannans were soluble in water and the molecular weights were $\overline{M}_n$ = 0.2 x 10^4-1.0 x 10^4. Figure 2A shows the ^{13}C NMR spectrum of sulfated konjac glucomannan with the molecular weight of $\overline{M}_n$ = 8000 and degree of sulfation (DS) of 1.4 in D_2O solution at 50°C. After sulfation, the C_6 signals were sifted to downfiled to 70 ppm from 64ppm and broadened, suggesting that the sulfate group was introduced in the C_6 hydroxyl groups. The C_2 and C_3 signals were also shifted and broadened.

Table 2 also shows the results of anti-HIV and blood anticoagulant activity (AA) of sulfated konjac glucomannans compared to those of standard dextran and curdlan sulfates and AIDS drugs used clinically. The anti-HIV activity was measured by the MTT method and the 50% effective concentration and the cytotoxicity was denoted by the 50% cytotoxic concentration using MT-4 cell. It was found that sulfated konjac glucomannans showed anti-HIV activity as high as that of standard dextran sulfate and clinical used ddC of a HIV drug. The 50% cytotoxic concentration was also the same as that of standards. The blood anticoagulant activity was obtained by using bovine plasma compared to that of the standard polysaccharides in Table 2, indicating that the anticoagulant activity was low to medium, 8.0-22.7 unit/mg. These biological results suggest that sulfated konjac glucomannan is a candidate of an antiviral polysaccharide because of having high anti-HIV and low to medium blood anticoagulant activities.

5.3.3 Interaction of sulfated konjac glucomannan with polylysine.

The interaction of sulfated konjac glucomannan with polylysine was elucidated preliminary by a surface plasmon resonance (SPR) in water at 37 °C. Poly-L-lysine was used as a model compound of basic proteins and peptides on the surface of HIV and cells. Figure 3 shows the typical binding curves of sulfated konjac glucomannans

($\overline{M}_n$ = 0.2 x 10^4 and DS = 1.3) with different concentrations to immobilized poly-L-lysine. Sulfated konjac glucomannan was found to be bound strongly and concentration-dependently to poly-L-lysine. The dissociation rate was slow, suggesting that the binding between sulfated konjac glucomannan and polylysine was very strong. Table 3 shows the apparent kinetic results of sulfated konjac glucomannans with poly-L-lysine calculated from the two-state fitting model by the Biacore-supplied software. The kinetic results calculated from the two-state model that contains conformational change of the complex provided good fittings compared to those of the 1:1 binding model. We reported previously that sulfated polysaccharides with negatively-charged sulfate groups were interacted strongly with the positively charged glycoprotein gp120 on the surface of HIV and then the conformation of the complex was changed to avoid the infection of HIV to T cell. The binding of sulfated polysaccharides to HIV was expected to the conformational change of the glycoprotein. Therefore, the two-state fitting model was preferred to the 1:1 binding model. These results in Table 3 indicate that sulfated konjac glucomannans had a fast association rate and slow dissociation rate on poly-L-lysine, suggesting a high stability of the interaction.

5.4 Conclusion

Naturally occurring konjac glucomannan was sulfated to give

sulfated konjac glucomannans and the biological activities such as anti-HIV and blood anticoagulant activities were investigated for the first time. We found that sulfated konjac glucomannans had high anti-HIV activity of 1.4 μg/ml and the activity was almost the same activity as that of clinically used AIDS drug, ddC (1.2 μg/ml) and standard dextran sulfate (3.2 μg/ml). The interaction between sulfated konjac glucomannan with poly-L-lysine as a model compound of proteins and peptides was investigated preliminary by a SPR instrument, indicating that sulfated konjac glucomannan had a fast association rate and slow dissociation rate on poly-L-lysine, suggesting a high stability of the interaction. Details on the interactions are continuously investigated.

Acknowledgment

This research was partly supported by a Grant-in-Aid for Scientific Research (C) from Japan Society for the Promotion of Science 2009 - 2011 (no. 21550199), 2012-2014 (no. 24550129), and SVBL research program found of Kitami Institute of Technology 2009-2012.

Reference

Albrecht, S., van Mulswinkel, G. C. J., Xu, J., Schols, H., Voragen, A. A. G. J., & Gruppen, H. (2011).Enzymatic production and characterization of konjac glucomannan oligosaccharides: *J. Agr. Food Chem.*, *59*, 12658-12666.

Cescutti, P., Campa, C., Delben, F., & Rizzo, R. (2002). Structure of the oligomers obtained by enzymatic hydrolysis of the glucomannan produced by the plant Amorphophallus konjac: *Carbohydr Res.*, *337*, 2505-2511.

Chua, M., Baldwin, T. C., Hocking, T. J., & Chan, K. (2010). Traditional uses and potential health benefits on *Amorphophallus konjac* K. Koch ex N. E. Br.: *J. ethnopharmacol.*, *128*, 268-278.

Dave, V. & McCarthy, S. P. (1997). Review of konjac glucomannan: *J. Environ. Polym. degrade.*, *5*, 237-241.

Iglesias-Otero, M. A., Borderias, J., & Tovar, C. A. (2010). Use of konjac glucomannan as additive to reinforce the gels from low-quality squid surimi: *J. Food Engineer.*, *101*, 281-288.

Jeon, K. J., Katsuraya, K., Inazawa, K., Kaneko, Y., Mimura, T., & Uryu, T. (2000). NMR spectroscopy detection of interactions between a HIV protein sequence and a highly anti-HIV active curdlan sulfate", *J. Am. Chem.Soc.*, *122*, 12536 - 12541.

Kaneko, Y., Yoshida, O., Nakagawa, R., Yoshida, T., Date, M., Ogiwara, S., Shioya, S.,Matsuzawa, Y., Nagashima, N., Irie, Y., Mimura, Y., Shinkai, H., Yashuda, N., Matsuzaki, K., Uryu, T., & Yamamoto, N. (1990). Complete inhibition of HIV-1 infectivity with curdlan sulfate in vitro and suggested treatment for HIV patients",*Biochem. Pharmacol.*, *39*, 793 - 797.

Katsuraya, K., Okuyama, K., Hatanaka, K., Oshima, R., Sato, T., & Matsuzaki, K. (2003). Constitution of Konjac glucomannan: chemical analysis and ^{13}C NMR spectroscopy: *Carbohydr. Polym.*, *53*, 183-189.

Lane, D. A., & Lindahl, U., Ed. (1989). Heparin: Chemical and biological properties clinical applications: KABI, London, UK.Li, J., Ji, J., & Li, B. (2012). Preparation of konja glucomannan-based superabsorbent polymers by frontal polymerization: *Carbohydr. Polym.*, *87*, 757-763.

Liu, J., Zhang, L., Hu, W., Tian, R., Teng, Y., & Wang, C. (2012). Preparation of konjac glucomannan-based pulsatile capsule for colonic drug delivery system and its evaluation in vitro and in vivo: *Carbohydr. Polym.*, *87*, 377-382.

Lu, Y., Zhang, L., & Xiao, P. (2004). Structure, properties and biodegradability of water resistant regenerated cellulose films coated with polyurethane/benzyl konjac glucomannan semi-IPN coating: *Polym. Degrada. Stabil.*, *86*, 51-57.

Luo, X. Hu, P., & Lin, X. (2011). "The mechanism of sodium hydroxide solution promoting the gelation of Konjac glucomannan (KGM): *Food Hydrocol.*, *30*, 92-99.

Nagasawa, K., & Yoshidome, H. (1969). Solvent catalytic degradation of sulfamic acid and its *N*-substituted derivatives: *Chem. Pharmacol. Bull.*, *17*, 1316-1323.

Pauwels, R., Balzarini, J., Baba, M., Snoeck, R., Schols, D., Herdewijn. P., Desmyter, J., & DeCercq, E. (1988). Rapid and automated tetrazolium-based colorimetric assay for the detection of anti-HIV compounds: *J. Virolog. Methods*, *20*, 309–321.

Tegshi, M., Han, S., Kanamoto, T., Nakashima, H., & Yoshida, T. (2011). Synthesis and specific influenza A virus-adsorptive functionality of alkyl curdlan sulfate-coated membrane filter: *J. Polym. Sci., A: Polym. Chem.*, *49*, 3241 - 3247.

U. S. Pharmacopoeia National Formulary, USP XXI 1985, pp. 480 – 483.

Wang, K., Fan, J., Liu, Y., & He, Z. (2010). Konjac glucomannan and xanthan gum as compression coat for colonic drug delivery: experimental and theoretical evaluations: *Front. Chem. Engineer. China*, *4*, 102-108.

Wu, C., Peng, S., Wen, C., Wang, X., Fan, L., Deng, R., & Pang, J. (2012). Structural characterization and properties of konjac glucomannan/curdlan blend films: *Carbohydr. Polym.*, *89*, 497-503.

Yoshida, T., Hatanaka, K., Uryu, T., Kaneko, Y., Yasuda, N., Mimura, T., Yoshida, O., & Yamamoto, N. (1990). Synthesis and structural analysis of curdlan sulfate with potent anti-AIDS virus activity: *Macromolecules*, *23*, 3717 - 3722.

Yoshida, T. (2001). Synthesis of polysaccharides having specific biological activities: *Prog. Polym. Sci.*, *26*, 379-441.

Yoshida, T. (2005). Synthetic and natural polysaccharides having specific biological activities", in *Polysaccharides: Structural diversity and functional versatility*, 2nd Ed., Dumitriu, S., Ed., Marcel Dekker, Inc., New York.

Legend to Scheme and Figures

Scheme. Sulfation of konjac glucomannan.

Figure 1. Aqueous GPC profiles of hydrolyzed konjac glucomannans by diluted sulfuric acid. (A) $\overline{M}_n$ = 19.2 x 10^4 ($\overline{M}_w/\overline{M}_n$ = 1.82), (B) $\overline{M}_n$ = 5.6 x 10^4($\overline{M}_w/\overline{M}_n$ = 2.07), (C) $\overline{M}_n$ = 0.8 x 10^4 ($\overline{M}_w/\overline{M}_n$ = 2.39), (D) $\overline{M}_n$ = 0.2 x 10^4 ($\overline{M}_w/\overline{M}_n$ = 1.53).

Figure 2. 100MHz 13C NMR spectra of (A) sulfated konjac glucomannan with $\overline{M}_n$ = 0.8 x 10^4 and DS = 1.4 in D_2O at 50 °C and (B) konjac Glucomannan with $\overline{M}_n$ = 0.8 x 10^4 in 2.5% NaOH D_2O solution at 50 °C. The signals were assigned by 2D NMR measurements.

Figure 3. SPR binding affinity of sulfated konjac glucomannan ($\overline{M}_n$ = 1.0 x 10^4, DS = 1.3) to poly-L-lysine. Sulfated konjac glucomannan (60 □l) was injected for 120 sec at a flow rate of 30 □l/min of a HBS-EP running buffer at 25°C and then the running buffer was further flowed for 600 sec. Concentrations of sulfated konjac glucomannan were 5.0, 2.5, 1.25, 0.62, and 0.31 □g/ml, respectively.

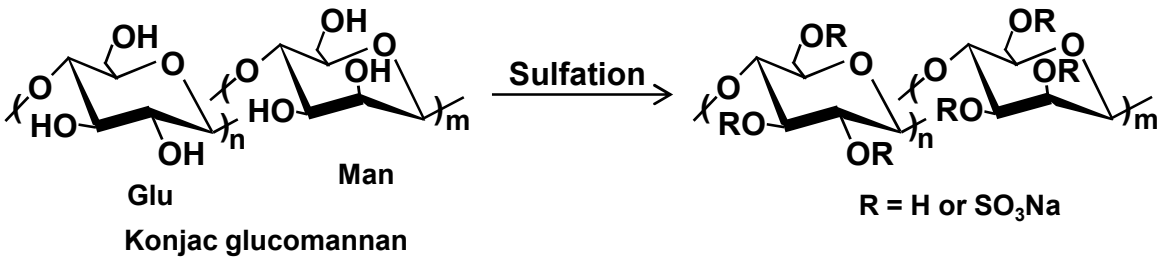

Scheme 1. Sulfation of konjac glucomannan

Scheme

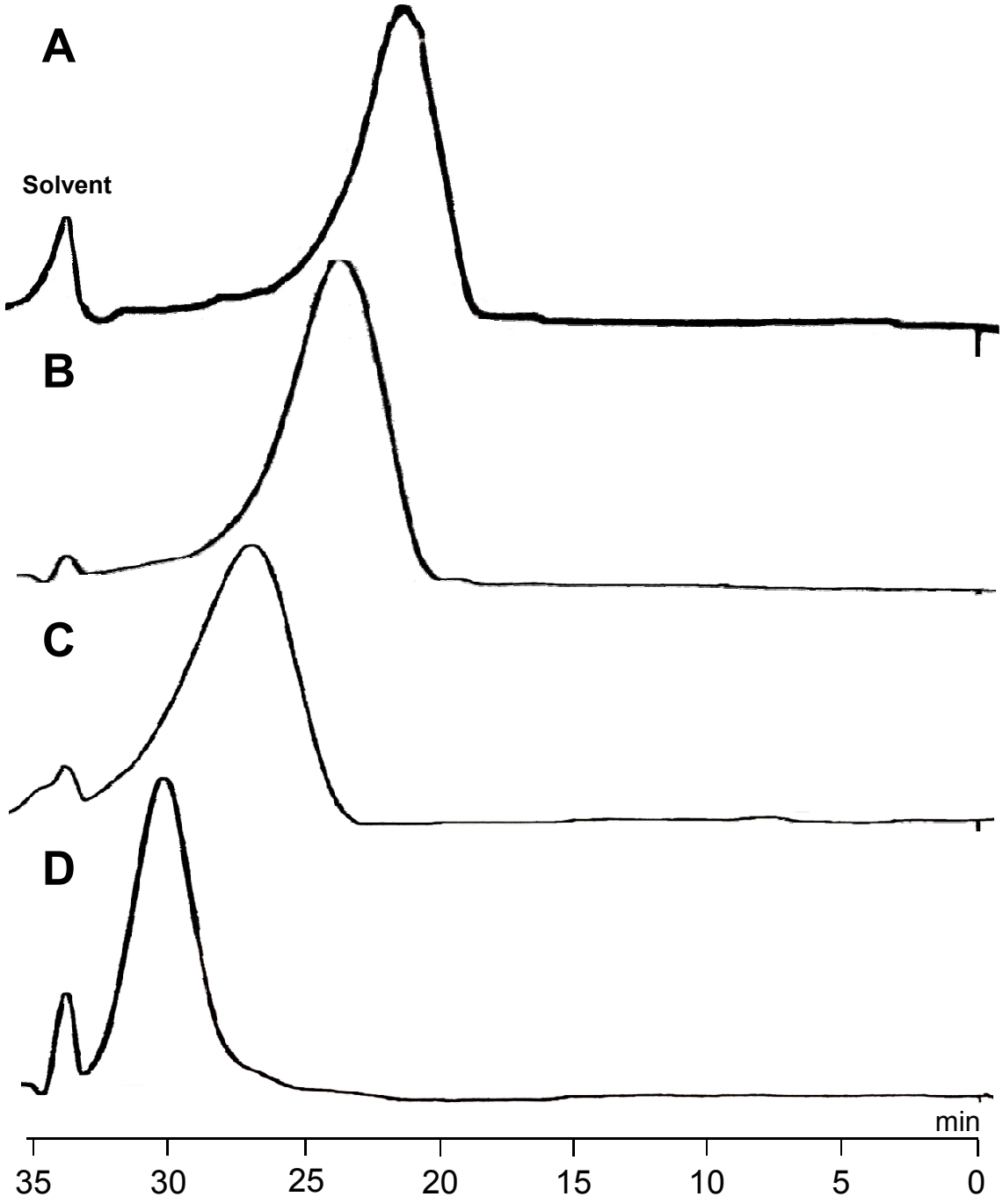

Figure 1. Aqueous GPC profiles of hydrolyzed konjac glucomannans by diluted sulfuric acid. (A) $\bar{M}_n$ = 19.2 x 10^4 ($\bar{M}_w/\bar{M}_n$ = 1.82), (B) $\bar{M}_n$ = 5.6 x 10^4 ($\bar{M}_w/\bar{M}_n$ = 2.07), (C) $\bar{M}_n$ = 0.8 x 10^4($\bar{M}_w/\bar{M}_n$ = 2.39), (D) $\bar{M}_n$ = 0.2 x 10^4 ($\bar{M}_w/\bar{M}_n$ = 1.53).

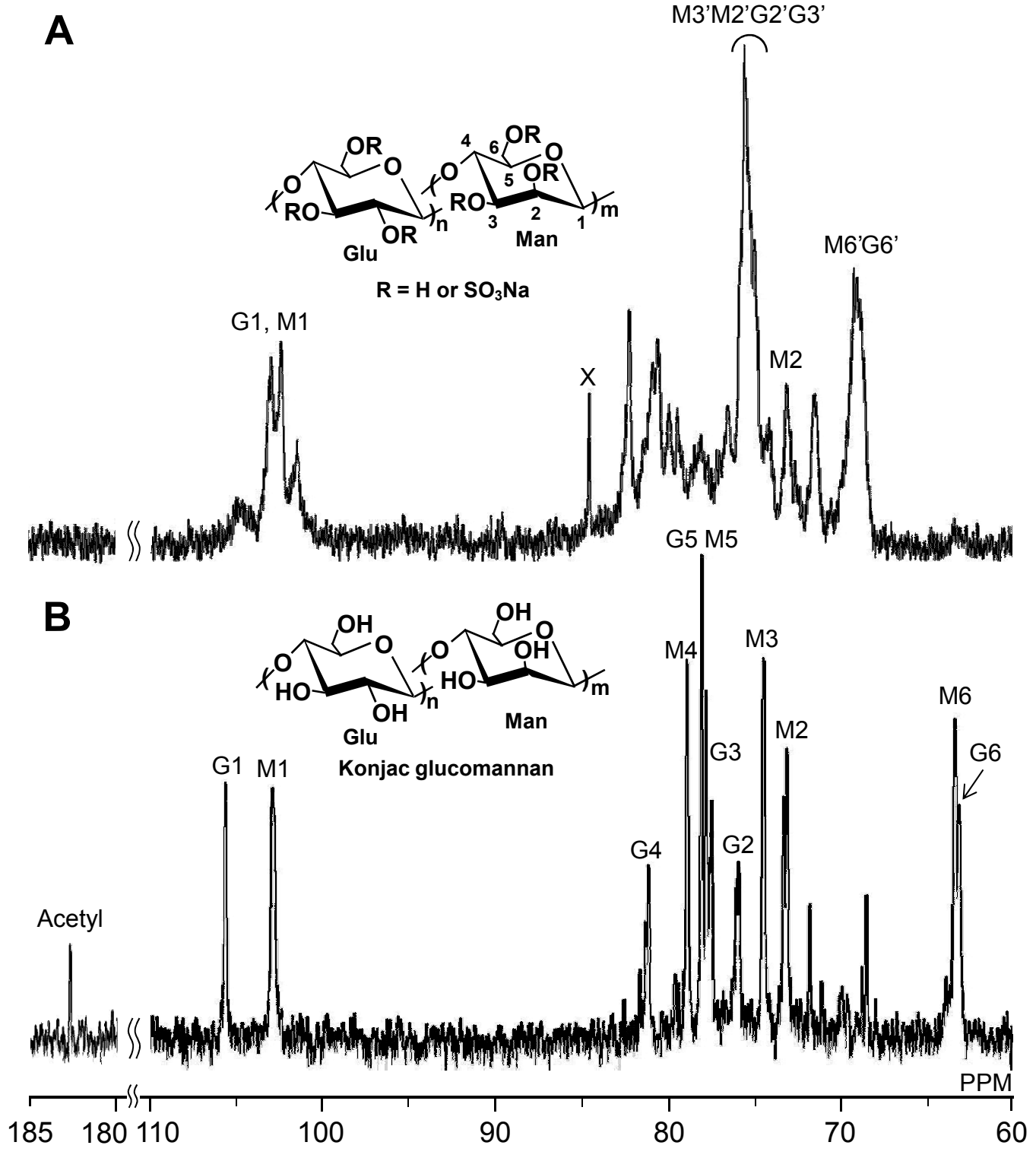

Figure 2. 100MHz ^{13}C NMR spectra of (A) sulfated konjac glucomannan with $\overline{M}_n$ = 0.8 x 10^4 and DS = 1.4 in D_2O at 50 ℃and (B) konjac glucomannan with $\overline{M}_n$ = 0.8 x 10^4 in 2.5% NaOH D_2O solution at 50 ℃.
The signals were assigned by 2D NMR measurements.

Figure 2

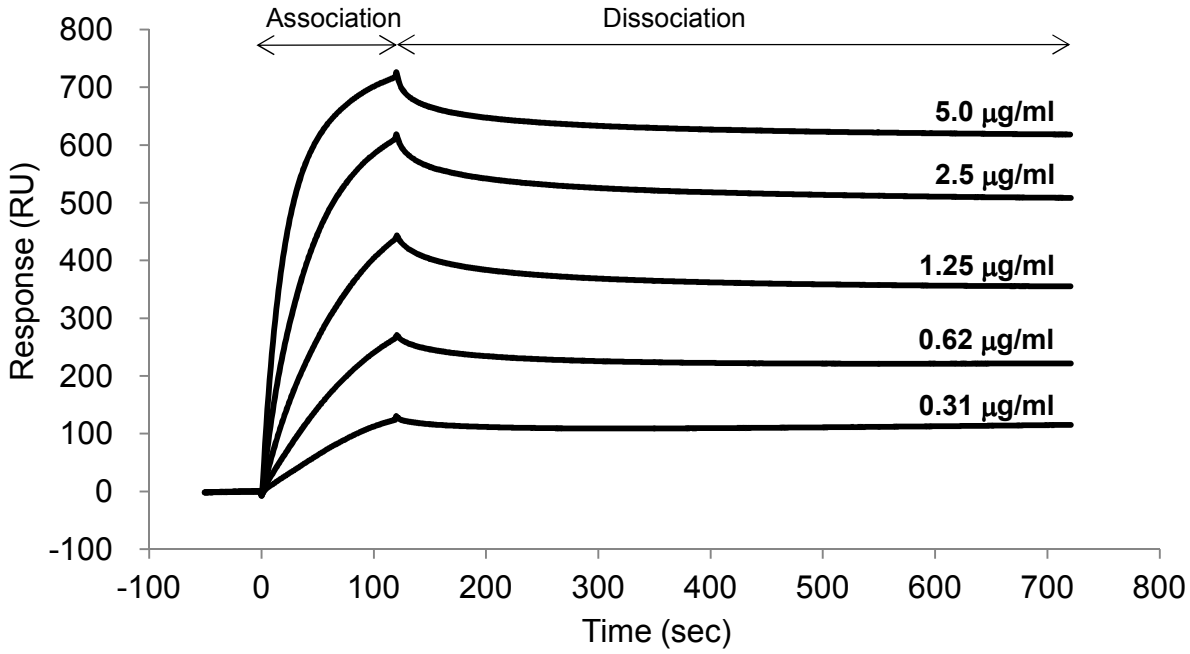

Figure 3. SPR binding affinity of sulfated konjac glucomannan ($\bar{M}_n$ = 1.0 x 10^4, DS = 1.3) to poly-L-lysine. Sulfated konjac glucomannan (60 μl) was injected for 120 sec at a flow rate of 30 μl/min of a HBS-EP running buffer at 25℃ and then the running buffer was further flowed for 600 sec. Concentration of sulfated konjac glucomannan were 5.0, 2.5, 1.25, 0.62, and 0.31 μg/ml, respectively.

Table 1. Hydrolysis of konjac glucomannan by diluted sulfuric acid[a]

	Konjac glucomannan				Hydrolyzed konjac glucomannan		
No		H_2SO_4	Temp	Time	Yield	$\overline{M}_n$[b]	$\overline{M}_w/\overline{M}_n$
	g	%	°C	h	g	x 10^4	
1	0.25	0.5	50	4	0.17	19.2	1.8
2	1.5	2.5	50	0.5	1.01	5.6	2.1
3	0.5	2.5	70	0.5	0.41	3.7	2.1
4	3.0	5	60	2	2.02	0.8	2.4
5	0.5	5	70	2	0.05	0.2	1.5

a) Before hydrolysis, glucomannan was stirred for 3 h in water at 70°C.

b) The molecular weights of soluble parts were measured by aqueous GPC using phosphate buffer as solvent.

Table 2. Sulfation and biological activities of konjac glucomannan[a]

No	Konjac glucomannan			Sulfated konjac glucomannan									
	$\overline{M}_n$	Temp	Time	Yield	$\overline{M}_n$[d]	$[\alpha]_D^{25}$[e]	Elemental analysis (%)			DS[f]	EC_{50}[g]	CC_{50}[h]	AA[i]
	x10^4	°C	min	g	x10^4	deg	C	H	S		μg/ml	μg/ml	unit/mg
1[b]	0.8	100	120	0.21	0.4	-12.2	21.6	3.2	14.2	1.3	1.4	62.6	8.0
2[b]	0.8	85	120	0.26	0.7	-14.1	19.7	3.0	14.7	1.4	1.3	331.8	13.8
3[c]	0.8	60	45	0.57	0.8	-16.3	17.2	2.9	17.3	1.9	1.6	680	n.d.
4[c]	5.6	rt	60	0.51	2.1	-18.4	18.4	3.0	15.7	1.6	0.7	649	n.d.
Dextran sulfate					0.9	+92.1			18.4	2.1	3.2	105.2	22.7
Curdlan sulfate					7.9	-0.3			14.1	1.4	0.1	518.2	10
AZT (μmol)											0.05	210.4	
ddC (μmol)											1.2	2216.5	

a) Konjac glucomannan (0.25g) was used.
Sulfation was carried out with piperidine-*N*-sulfonic acid (b) or sulfur trioxide pyridine complex (c).
d) Determined by GPC using phosphate buffer as solvent. e) Measured in H_2O (c 1%).
f) Degree of sulfation (maximum, 3.0). g) 50% Effective concentration of sulfated glucomannan on HIV.
h) 50% Cytotoxic concentration on MT-4 cell.
i) Anticoagulant activity compared to standard dextran sulfate H-039 with 22.7 unit/mg.

Table 3. Apparent association and dissociation rates of sulfated konjac glucomannan[a]

No	$\overline{M}_n$[b]	$[\alpha]_D^{25}$[c]	S	DS[d]	k_{a1}	k_{d1}	k_{a2}	k_{d2}	K_D
	x10^4	deg	%		x10^4 1/Ms	x10^{-2} 1/s	x10^{-2} 1/s	x10^{-4} 1/s	x10^{-9} M
1	2.0	-20.5	16.0	1.6	104.0	3.6	2.4	2.9	0.4
2	2.1	-18.1	15.7	1.6	61.1	2.0	2.1	3.2	0.5
3	0.8	-16.3	17.3	1.9	16.2	1.5	1.9	3.6	1.7
4	1.0	-13.8	14.0	1.3	8.6	0.7	1.3	4.0	2.6
5	2.8	-12.3	12.1	1.0	6.6	0.7	1.1	8.1	7.8
6	0.9	-15.4	9.5	0.7	4.9	1.2	1.3	6.7	11.9
7	0.7	-14.1	14.7	1.4	3.8	1.0	1.2	6.6	14.5
8	0.5	-9.0	13.9	1.3	3.7	1.0	1.3	5.3	10.3
9	0.4	-12.2	14.2	1.3	1.7	1.0	1.1	7.3	34.7

a) The apparent kinetic rates were calculated from the two-state model supplied by a Biacore software; k_a: association rate constant, k_d: dissociation rate constant, K_D: dissociation constant calculated by k_d/k_a.

b) Determined by GPC using phosphate buffer as solvent.

c) Measured in H_2O (c 1%). d) Degree of sulfation (maximum, 3).

Appendix1: protocol for the genomic DNA extraction

The fresh or the dried leaf was powdered under liquid nitrogen using a mortar and pestle, then stored in -80℃ freezer until extraction.Genomic DNA was extracted from powdered material (25~100mg) using DNeasy plant mini kits following the manufacturer's protocol (Qiagen,).

1. Place the powdered sample material (≤100mg wet weight or ≤20mg dried tissue) into t a 2ml microcentrifuge tube. Add 400ul lysis buffer AP1 (if having precipitate, warm to 65℃ to redissolve.) and vortex vigorously in 1 min and put it in room temperature one night.
2. Add 4ul RNase A to the tube, vortex strongly in 1 min.
3. Incubate the mixture for 1h at 65℃.Mix 5 or 6 times during incubation by inverting tube.(this step lyses the cells of the plant).
4. Add 130ul precipitation buffer AP2 to the lysate, mix, and incubation for 2h on ice. (This step precipitates detergent, protein and polysaccharides.)
5. Centrifuge the lysate for 5~7min at 20,000Xg.
6. Pipet the lysate into the QIAshredder Mini spin column placed into a 2ml collection tube, and centrifuge for 2min at 20,000Xg.
7. Transfer the flow-through fraction from the step 6 into the new

2ml tube without disturbing the cell-debris pellet.(typically 450ul of lysate is recovered)

8. Add the 1.5 volumes of binding buffer AP3/E to the cleared lysate, and mix by pipetting.
9. Pipet 650ul of the mixture from step 8 into the DNeasy Mini spin column placed in a 2ml collection tube. Centrifuge for 1min at 6000Xg, and discard the flow-through. Repeat this step with remaining sample; discard flow-through and collection tube.
10. Place the DNeasy Mini spin column into a new 2ml tube, add 500ul wash buffer AW, and centrifuge for 1min at 6000Xg, discard the flow-through. Then add 500ul wash buffer AW more one time into the column, and centrifuge for 5min at 20,000Xg for drying the membrane.
11. Discard the collection tube and open the cap of the column, dried for 30min at the room temperature.
12. Transfer the DNeasy Mini spin column to the 1.5ml microcentrifuge, and pipet 25ul Elution buffer AE directly into the Dneasy membrane. Incubate one night at 4℃ and centrifuge for 2min at 6000Xg to elute. The eluted solution is transfer into the new tube and is stored at 4℃ (-20℃ is recommended for the long storage).

Appendix2: Methods of purification of PCR product

2.1 Agencourt AMPure XP

1. Warm the Ampure beads to room temperature and mix thoroughly before use.
2. The 70% ethanol solution should be prepared fresh.
3. Add 36 μl of Ampure beads to 20ul sample, mix thoroughly and put for 5 minutes at room temperature for increasing the recovery.
4. Place samples on a magnetic separator for 5 min. When the beads have collected to the wall of the tube and the solution is clear, discard the clear solution and don't touch the bead part.
5. Add 200 μl of 70% ethanol. Remove and discard the ethanol.
6. Repeat steps 5 one more time.
7. Remove the tubes from the magnetic separator, quick spin the beads, place back on the magnet and remove any remaining liquid.
8. Add 20 μl of 1XTE buffer to the beads and vortex to mix thoroughly.
9. Place the samples on a magnetic separator, when the beads have collected to the wall of the tube and the solution is clear, transfer the liquid to a fresh tube. The liquid contains your purified library.

The following picture describes the process of purification by magnetic beads refereeing from the manufacture protocol of Agencourt AMPure XP.

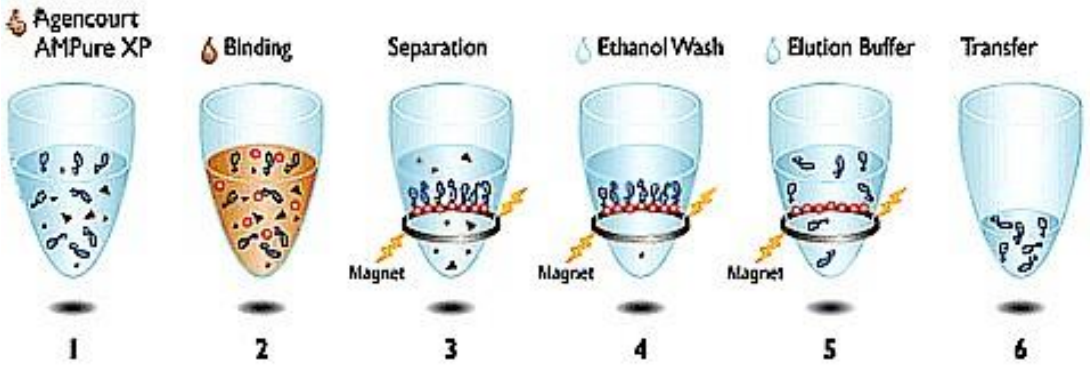

2.2 QIAEX Ⅱ Gel Extraction Kit

This protocol is designed for the extraction of 40-bp to 50-kb DNA fragments from 0.3–2% standard or low-melt agarose gels in TAE or TBE buffers.

1. Excise the DNA band from the agarose gel with a clean, sharp scalpel.
2. Weigh the gel slice in a colorless tube. Add 3 volumes of Buffer QX1 to 1 volume of gel for DNA fragments 100 bp – 4 kb; otherwise, follow the table below.
3. Resuspend QIAEX II by vortexing for 30 sec. Add QIAEX II to the sample according to the table below and mix.
4. Incubate at 50°C for 10 min to solubilize the agarose and bind the DNA. Mix by vortexing* every 2 min to keep QIAEX II in suspension. Check that the color of the mixture is yellow
5. Centrifuge the sample for 30 sec and carefully remove supernatant with a pipet.
6. Wash the pellet with 500 µl of Buffer QX1.
7. Wash the pellet twice with 500 µl of Buffer PE.

8. Air-dry the pellet for 10–15 min or until the pellet becomes white.

9. To elute DNA, add 20 µl of 10 mM Tris·Cl, pH 8.5 or H_2O and resuspend the pellet by vortexing*. Incubate according to the table below.

10. Centrifuge for 30 sec. carefully pipet the supernatant into a clean tube.

2.3 SUPEC-02 Cartridge (Takara)

SUPREC™-02 is a filter cartridge designed for rapid purification and/or concentration of DNA samples. It can also be used conveniently for buffer exchange. Possible applications are:

- Purification of DNA generated by PCR* (effectively eliminates Unused dNTPs and primers)
- Concentration of DNA
- Buffer exchange

1) Add 1XTE buffer to the PCR solution to make up a total volume of 400 µl.

2) Transfer the solution to the ultrafiltration cassette portion of SUPREC™-02.

3) Centrifuge at 1,500 x g, 8 minutes.

4) Discard filtrate. Add1X TE to the solution remaining in the ultrafiltration cassette

(Bring the total volume to 400 µl).

5) Centrifuge at 1,500 x g, 8 minutes.

6) Repeat steps 5) and 6), until the DNA solution reaches to a desired volume.

7) Analyze a small portion of the DNA solution by gel electrophoresis.

Appendix3 Programs for the construction of phylogenetic tree

Finally, briefly introduce some programs of construction for phylogenetic tree.

- MEGA (http://evolgen.biol.metro-u.ac.jp/MEGA/)
  – For MP method、Distance methods
- PHYLIP (http://evolution.genetics.washington.edu/phyli.html)
  –For ML method、MP method、Distance method
- PAUP* (http://paup.csit.fsu.edu)、Not free
  –For ML method、MP method、Distance method
- Molphy (http://www.ism.ac.jp/ismlib/softother_j.html)
  –For ML method
- PAML (http://abacus.gene.ucl.ac.uk/software/paml.html)
  – For ML method
- phyML （http://www.atgc-montpellier.fr/phyml/）
  – For ML method (rapid)
- MrBayes (http://mrbayes.csit.fsu.edu/index.php)

Acknowledgments

I would first and foremost like to thank my major professor, Dr Yoshida Takashi for supporting me as a student in his lab and teaching me a lot not only professional knowledge but also Japanese language and life during my doctoral three years in Japan. He has truly been my adviser in all aspects of Japanese lacquer plants project and continues to provide me with inspiration to further my endeavor to understand these beautiful and amazing plants.

I would like to thank two assistant teachers of our lab, Mr. Okimoto Mitsuhiro and Mr. Komata Masashi, to give me invaluable supports and get a lot encourage and self confidence from their smiles.

I also would like to thank my two friendly group members in Lacquer plants study, Miyazaki keita (M2) and Itou Nana (M1), to provide a lot of assistance for this study. And I am thankful to all kind-mind members of our lab for supporting me to accomplish my doctoral course.

I kindly would like to thank Professor *Dr* Miyakoshi Tetsuo (Meiji University) and Miyazato Masaco (the chief of Urasoe art meseum and a part-time professor at Okinawa prefectural University of Arts and Okinawa international University) for giving support to me in all lacquer samples collecting parts.

Finally, I'd like to thank for my family that has given me constant love and support since I began at Kitami, Hokkaido during these three years. Especially, I want to give deeply thanking to my husband, Muschin Tegshi, for his supports and love.